POP-UP HOOD PEDESTRIAN PROTECTION

Eva Ames
Peter Martin
National Highway Traffic Safety Administration
United States of America
Paper Number 15-0111

ABSTRACT

Objective: One means of protecting pedestrians is through vehicle safety systems that are built into a vehicle's front-end to protect pedestrians should a vehicle impact occur. These pedestrian protection systems include hood structures aimed at reducing pedestrian head injuries. Pop-up hoods function by increasing the head penetration space beneath the hood by quickly lifting upon vehicle contact with a pedestrian. This paper explores the prevalence of vehicles with pop-up hoods to show that their market penetration and performance benefits merit consideration in standardized pedestrian protection test protocols.
Methods: Euro NCAP test scores and the Parkers United Kingdom (UK) vehicle database were used to better understand the fleet performance and market penetration of vehicles with pop-up hoods. An analysis of Euro NCAP pedestrian test results and overall vehicle test scores was performed to compare the performance of vehicles equipped with pop-up hoods to those without, and the Parkers UK vehicle database was used to estimate historical vehicle prices and demonstrate that pop-up hoods are available on both high- and low-cost vehicles.
Results: There are many different types of systems that operate pop-up hoods, and their architectures vary widely from one vehicle to the next; however, they typically create an increase in the distance from the hood to rigid components in the engine bay, thus reducing the probability and/or severity of a head injury of a struck pedestrian. Compared to vehicles with non-deploying hoods, vehicles with pop-up hoods rated by Euro NCAP had better pedestrian protection scores on average. In the European Union (EU), pop-up hood systems, which have become more prevalent over time, were found on vehicles outside the oft-assumed market of only low-volume luxury models.
Discussion and Limitations: Pedestrian Protection is mandatory on all vehicles sold in the EU Conformity of pop-up hoods is based largely on headform impact tests conducted on a fully popped-up hood. During the Type Approval process, the determination of system reliability and consistency also must be demonstrated by the vehicle manufacturer, but the means and requirements to do so are not defined within the regulation itself. Because the operation of pop-up systems varies widely and they are generally unique to specific vehicle models, the demonstration of system functionality is agreed upon between the manufacturer and the Type Approval Authority. Euro NCAP operates in a similar manner.
Conclusions: Pop-up hoods generally perform better than non-deploying hoods in headform impact tests. As their development matures and vehicle styling progresses towards low, sleek, aerodynamic hood profiles, demand as well as variation in these systems may grow. To date there is not a published, fully prescriptive test protocol that tests the full functionality of such systems, including reliability and deployment thresholds, to objectively ensure that they function properly during an actual collision with a pedestrian.

INTRODUCTION

Fatal injuries to pedestrians from motor vehicles often result from the pedestrian's head striking either the vehicle or the ground. There are two primary means of protecting pedestrians through vehicle safety systems: one involves the use of crash avoidance safety systems, such as those for braking and lighting, to help the driver see the pedestrian and avoid a collision, and the other involves structural designs and mechanisms built into the vehicle front-end that reduce the injury potential to pedestrians should a crash occur. This paper will discuss pop-up hood systems, which increase the distance to rigid components in the engine bay, potentially reducing the head injury risk of a struck pedestrian [14], by quickly lifting the rear edge of the hood a few inches when triggered.

A sleek vehicle profile, and therefore a low hood profile, is often desirable by vehicle manufacturers for both styling purposes and aerodynamic performance. These low hood profiles are contrary to what is desired for good pedestrian head protection because they leave less space between the hood and underlying hard surface components, a clearance necessary for energy absorption during impact through free deformation of the hood. Though many manufacturers are able to provide the desired clearance through other means such as structural changes and component layout adjustments, some use pop-up hoods as an alternate strategy [5].

Pop-up hoods are particularly beneficial because they provide head penetration clearance near the hinges and at the rear edge of the hood along the cowl, where the windshield, hood, and firewall all intersect. It is in this area where pedestrian heads often strike. But it is also the area where non-deploying hoods are typically stiffest – even those

designed to conform to pedestrian safety standards. The beneficial qualities of pop-up hoods have been demonstrated in numerous studies [8][12][14].

Also, the addition of a pop-up hood to an existing vehicle designed for a market without pedestrian protection requirements may allow a vehicle manufacturer to sell vehicles in additional marketplaces while avoiding major structural and styling changes.

The basic premise behind pop-up hood deployment is that the vehicle is outfitted with a control unit which triggers hood deployment when the vehicle senses a pedestrian collision and is traveling within a predetermined threshold for which the control unit knows hood deployment will be effective. The control unit receives input from a contact sensor and/or pre-crash sensing technologies. Contact sensors in the bumper, in the form of accelerometers, pressure tubes, or resistive/capacitive sensors, detect that the vehicle has struck a pedestrian's leg (rather than a tree, pole, or other inanimate roadside object) through classification of the impact pulse. Some new vehicles are outfitted with pre-crash sensing technologies such as radar and LIDAR, which are able to influence the control unit's hood deployment algorithm through identification of a pedestrian prior to vehicle-pedestrian impact.

Deployment (lifting) technologies vary from springs and motors to pyrotechnic actuators using rapidly expanding gas to provide the necessary lift, similar to the devices used in air bag deployment. The lifting actuators are located at the rear corners of the hood at the hinge locations, and they lift the hood up as it pivots at the latch in the front [12]. The spring and motor method is considered to be desirable because the hood could be fully reset post-impact or after a false trigger, whereas the pyrotechnic method would require the replacement of certain components. Conversely the pyrotechnic method is desirable because of its ability to deploy the hood faster than the other option, and most research has focused in this area. Also, pyrotechnic components are generally smaller and weigh less. Minimizing the repair costs of a vehicle equipped with pop-up hood deployment also requires a hood that could be reused, which would depend upon a hood rigid enough to resist deformation from the impact of a head or torso. This may conflict with the ability of a hood to absorb energy when not deployed [11]. A newer pop-up hood system, first seen in mass production on the Volvo V40, is the pedestrian air bag [8]. Triggered with the same sensing methods as used for traditional pop-up hood actuation systems, an inflator fills the pedestrian air bag which then lifts the hood. This air bag is located at the base of the windshield, and it not only lifts the hood for additional clearance but also provides air bag coverage to the vehicle's A-pillars and lower windscreen, which are relatively very hard surfaces.

METHODS

The United States does not currently have pedestrian protection requirements applicable to vehicles, so vehicles in markets with pedestrian protection requirements were studied to examine trends regarding pop-up hood systems. Pedestrian safety systems such as pop-up hoods are not new to Europe. Euro NCAP, a non-regulatory consumer ratings group in Europe, supported by various European governments and motoring organizations, has been testing pedestrian protection for more than a decade. Additionally, many European countries are subject to pedestrian protection regulations.

In this paper, 498 Euro NCAP test reports from 2000-2014 were entered into a database. Next, the Parkers database of United Kingdom (UK) vehicle prices was consulted to assign new vehicle prices to each vehicle in the database. The Parkers information was consulted because it includes a wealth of historical vehicle pricing information, and the UK market was deemed large and varied enough to be an appropriate sample.

From these 498 database entries, 63 were excluded from the following calculations regarding test scores and price, leaving 435 unique vehicle entries with full Euro NCAP test scores and Parkers vehicle pricing information. Of the excluded entries, 33 were repeated entries, 1 was a Euro NCAP test report (the 2008 Mercedes Viano) that did not include pedestrian protection scores, and 29 were vehicles that lacked historical price information through Parkers.co.uk or were not offered for sale in the UK. The 33 Euro NCAP vehicle retests came from both the 2009 Euro NCAP test protocol change regarding rescoring and retesting and also from design changes stemming from poor initial Euro NCAP scores. In all of these cases, the most recent test report was kept. These repeat test vehicles had identical pedestrian scores except for the Mazda 6 retest in 2005, VW Passat retest in 2010, and Jaguar XF in 2011. The Passat and XF tests were redone specifically for pedestrian protection. The complete list of these

vehicles, as well as 12 additional European vehicles with pop-up hoods but not tested by Euro NCAP which were identified through various media outlets, is included in Appendix A.

Euro NCAP assigns an overall vehicle score on a five star scale, similar to the star assignment system used by NHTSA's own NCAP program. The number of overall stars is determined by the scores a vehicle receives in four main areas: Adult Occupant, Child Occupant, Pedestrian, and Safety Assist. For the year 2015, a vehicle must achieve 65 percent of the total possible points in the pedestrian test to qualify for a five star rating, and the pedestrian score comprises 20 percent of the overall score [1]. The pedestrian scores are compiled from three tests: headform, upper legform, and legform. The headform test is potentially 24 of the 36 total possible pedestrian points, and it tests for both child and adult impacts [3].

A vehicle equipped with a pop-up hood is tested with the pop-up hood only if the sales volume of vehicles with this feature is high enough according to the Euro NCAP sales volume specifications for that model year and if the vehicle manufacturer can work with the Euro NCAP Secretariat prior to testing to prove system functionality and reliability. Otherwise, it is tested without having its hood activated. In the Euro NCAP headform test, point values are assigned based on the HIC value from free motion headforms fired at the hood, targeting a grid of impact locations for both children and adults. This physical testing validates a simulation model provided by the vehicle manufacturer prior to the test [4].

RESULTS

Listed in Appendix B, there are 24 vehicles sold with pop-up hoods that Euro NCAP has tested, and they span the whole gamut of vehicle sizes and prices, going from the Fiat Freemont and Hyundai Santa Fe to the Mercedes M-Class, BMW 5-series and Jaguar XF. This is not to say that vehicles must have an pop-up hood to achieve a good head impact test score or that a pop-up hood guarantees a good head impact score – the 2012 Subaru Forester (without an pop-up hood) scored 20.3 of 24 potential points for head impact, and the 2011 Dodge Caravan (with an pop-up hood) scored only 11 points for head impact. Additionally, not all luxury vehicles have pop-up hoods – the Maserati Ghibli uses passive pedestrian protection without a pop-up hood. Inclusion of pop-up hoods in new vehicles has become more common over time.

As seen **Error! Reference source not found.** in Figure 1, the percentage of vehicles with pop-up hoods in the Euro NCAP test inventory has increased over time. Euro NCAP cannot test every vehicle so their inventory is not a census, but each year's vehicle selection is made in order to provide the broadest range of consumer information possible by collecting information about the most popular and interesting vehicle models [5]. Assuming the sample selection to be consistent over time, it can be posited that though pop-up hoods remain a small part of the vehicle fleet, they already have a high enough market penetration to have a tangible effect on overall pedestrian safety in the EU. However, we have no data on hood activations and pedestrian injury outcomes in real-world pedestrian crashes in the EU.
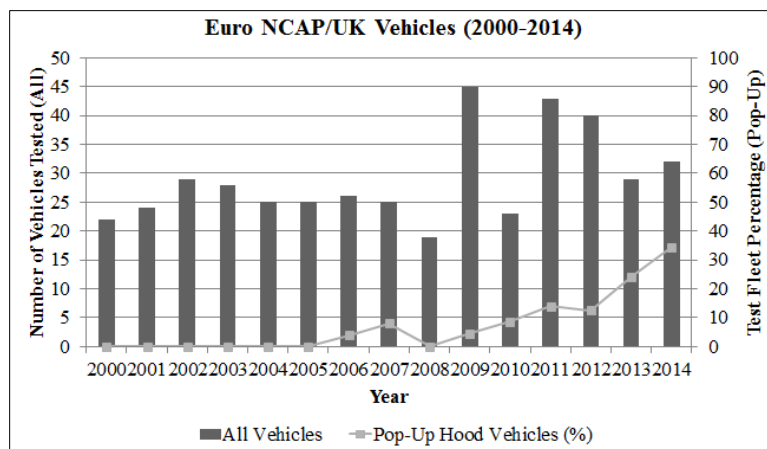

Figure 1. Pop-up Hood Market Penetration for 2000-2014 Euro NCAP/UK Vehicles Tested

Figure 2, below, shows the pedestrian protection scores for all vehicles. Those vehicles without pop-up hoods have increased their scores over time. Figure 3, below, shows that this trend is consistent with that for looking only at the scores from the headform test. Though the sample size is relatively small for vehicles with pop-up hoods, score gaps in both figures indicate that they yield higher scores than those without pop-up hoods.
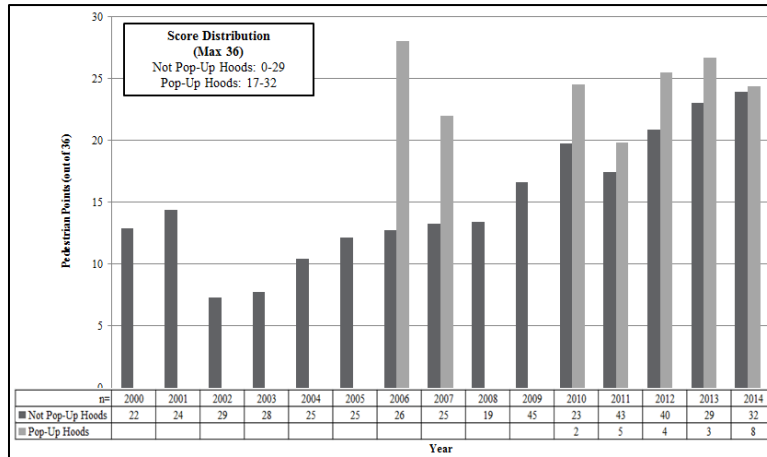
Figure 2. 2000-2014 Euro NCAP/UK Vehicle Overall Pedestrian Scores over Time
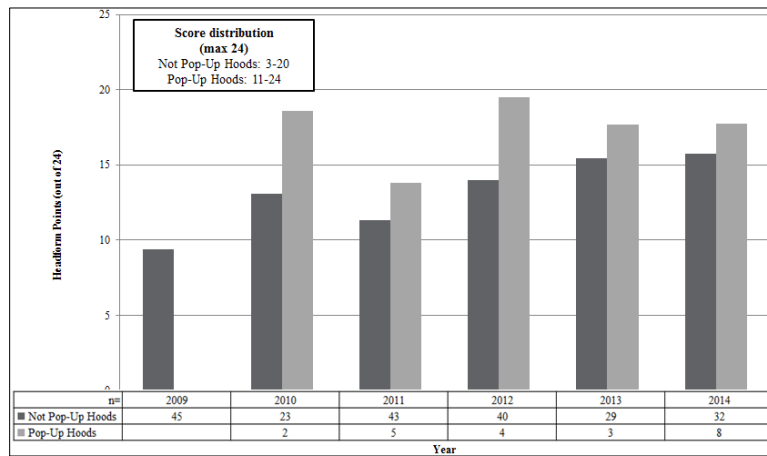
**Figure 3. 2000-2014 Euro NCAP/UK Vehicle Average Pedestrian Headform Scores**

To date, the 2012 Volvo V40 is the only vehicle in the Euro NCAP database to achieve a perfect 24 point score for the head impact testing. (The V40 is not sold in the U.S.) Note that prior to 2009, publically reported Euro NCAP pedestrian protection scores were given as overall scores and not broken into separate head, upper leg, and leg scores as they are currently. This result was achieved with a pedestrian air bag that deploys when the vehicle is moving at speeds between 20 and 50 km/h to not only lift the hood, but to also cushion the windshield wiper, windscreen, and A-pillar areas in case of a strike from a pedestrian head [6]. The 2010 BMW 5-series, equipped with a pop-up hood, also scored highly in both child and adult head impact tests, receiving 22 of 24 possible points. The 2006 Citroen C6 is also noteworthy because it is one of the earliest vehicles featuring a pop-up hood. Until 2009, Euro NCAP translated the overall pedestrian point score into a separate rating out of 4 stars. The 2006 Citroen C6 was the first vehicle to achieve that top 4 star pedestrian rating with a score of 28 of 36 points. This pre-2009 Euro NCAP pedestrian score was a single score with all of the three factors combined into a single score.

The effectiveness of the pop-up hood technology alone is seen with the 2013 Skoda Octavia and the 2010-2012 Jaguar XF. The 2013 Skoda Octavia's test results were updated in June 2013 because Skoda made the decision to remove the pop-up hood, which had previously been standard equipment on vehicles sold throughout the EU. The Euro NCAP test report states that the full pedestrian protection score, not specific to only head impact, was 30 points

with the pop-up hood technology or 24 without, out of a potential 36 points. Without the pop-up hood, the head impact score was only 16.5 out of a potential 24 points. Conversely the Jaguar XF was tested in 2010 without pop-up hood technology, where it scored 16 points out of a potential 24 for head impact testing. The 2010 XF was outfitted with pop-up hood technology, but was tested without it because the sensors in the bumper did not meet Euro NCAP standards. The XF was tested again in 2012 with the pop-up hood technology activated, which improved that score to 22 out of 24 points.

The historical pricing information from the Parkers database was used to characterize original, new vehicle sales prices for the vehicles in the database. The Parkers database provided a range of prices for the various option levels, and the median of this range was calculated for each vehicle and used to create Figure 4, below. Median new vehicle sales prices for vehicles with pop-up hoods are higher than those for vehicles without a pop-up hood, but as seen in Figure 4, not all vehicles with pop-up hoods are at the absolute top end of the price spectrum.
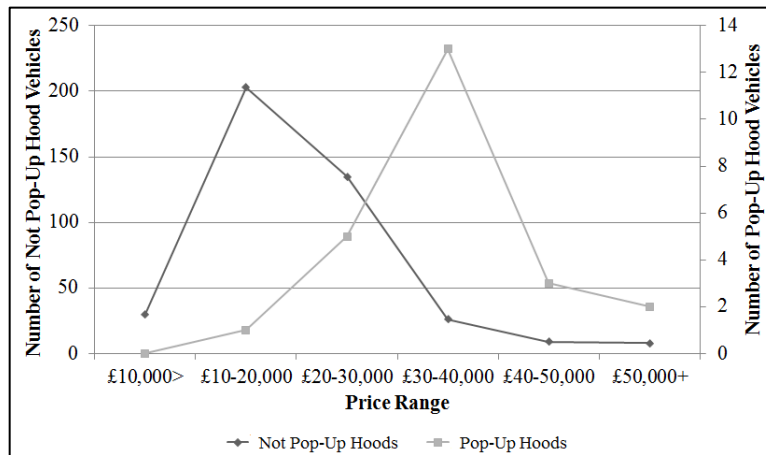
Figure 4. 2000-2014 Euro NCAP/UK Vehicle Median Price Distribution

The analysis of the vehicles in the database showed that while pop-up hoods can help to get a high pedestrian headform score in the Euro NCAP test, it was not essential to doing so. below, in Figure 5, it can be seen that the 2012 Subaru Forester, without a pop-up hood, scored 20.3 out of 24 headform points, while the comparably priced 2011 Dodge Caravan, with an pop-up hood, only scored 11 out of 24 headform points.
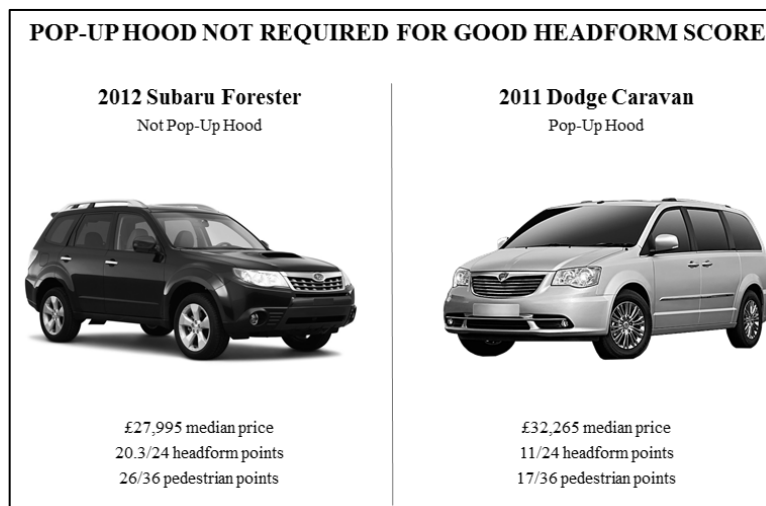
Figure 5. Pedestrian Protection Vehicle Comparison With and Without Pop-Up Hood

Market Penetration

We identified 40 vehicle models with pop-up hoods that have been marketed in Europe, as shown in Table 1 below. Only two of them are no longer produced: the Citroen C6 (ceased production in 2012) and the Acura RL (also ceased in 2012 but reintroduced in 2015). Of the current European models with pop-up hoods, most are versions of similar models sold in the U.S. without a deployment actuator.

One such vehicle is the Dodge Caravan, sold in the Europe as the Lancia Voyager. The Caravan is an example of a vehicle not originally designed for a market with pedestrian protection requirements (only 4,140 sales units in the EU vs. 272,191 in the U.S. for 2014). In light of these sales figures and its marginal headform score of 11.0 (lowest of all vehicles with pop-up hoods and below average for all), it would appear that the pop-up hood provided the manufacturer with a more economic option to allow an existing vehicle design entry into the European market. Otherwise, a costly redesign of the whole front end including hood under-components may have been required to achieve comparable pedestrian headform scores.

As seen in Table 1, about 8% of new cars sold in Europe have pop-up hoods and the U.S. market share of the North American versions is about the same. The market share of vehicles with pop-up hoods could increase further as the systems mature. Aside from the benefits to pedestrians discussed in the Introduction, a pop-up hood offers other advantages. From a vehicle styling viewpoint, a pop-up hood provides a means to achieve a desired appearance of a sleek vehicle with a low hood profile, which may provide better aerodynamic performance.

Table 1. European Passenger Cars with Pop-Up Hoods

Make	Model	United States version		European version		Euro NCAP head score /36	European name
		Sales 2014	Median Price	Sales 2014	Median Price		
Acura	RL	Discont.	$49,490	Discont.	£37,713	n/a	Honda Legend
Aston Martin	DB9	1,224	$191,200	285	£140,527	not tested	
Aston Martin	Vanquish		$279,995	325	£198,640	not tested	
Audi	A3	22,250	$29,060	199,537	£29,158	18	
BMW	2-Series	7,345	$33,000	26,215	£26,993	14.9	
BMW	6-Series	8,647	$53,253	7,902	£67,050	not tested	
BMW	5-Series	52,704	$50,950	98,519	£44,080	22	
Cadillac	ATS	29,890	$40,445	365	n/a[1]	not tested	
Cadillac	CTS	31,115	$63,215		n/a[1]	not tested	
Citroen	C6	not sold in U.S.		Discont.	£33,578	n/a[2]	
Chrysler	300	53,382	$33,745	487	£38,000	15.3	Lancia Thema
Dodge	Journey	93,572	$27,945	17,417	£20,970	12	Fiat Freemont
Dodge	Caravan	272,192	$34,710	4,140	£32,265	11	Lancia Voyager
Hyundai	Genesis	29,992	$42,125	247	n/a[3]	16.7[3]	
Hyundai	Santa Fe	107,906	$27,075	13,332	£30,363	18.6	
Infiniti	Q50	36,899	$41,200	2,426	£69,253	19.1	
Jaguar	F-type	4,112	$80,500	4,654	£69,253	not tested	
Jaguar	XF	5,880	$65,150	20,328	£40,670	16.2	
Jaguar	XK	1,452	$77,835	1,882	£81,965	not tested	
Kia	Sorento	102,520	$28,275	9,325	£31,900	18.3	
Land Rover	Discovery Sport	n/a	$41,320	n/a	£39,195	19.2	
Lexus	IS	51.358	$50,979	9,552	£33,643	16.9	
Mazda	MX-5/Miata	4,745	$26,485	5,787	£21,095	not tested	
Mercedes	A-Class	not sold in U.S.		121,321	£26,058	18	
Mercedes	CLA-Class	27.365	$38,675	38,423	£30,155	17	
Mercedes	GLA-class	6,884	$39,800	44,930	£30,218	18.4	

Make	Model	United States version		European version		Euro NCAP head score /36	European name
		Sales 2014	Median Price	Sales 2014	Median Price		
Mercedes	C-Class	75,065	$49,275	136,431	£32,580	21	
Mercedes	C-Class Coupe		$46,095		£33,725	14.6	
Mercedes	E-Class	66,400	$66,900	99,441	£37,563	15.2	
Mercedes	S-Class	25,276	$114,070	17,694	£74,900	not tested	
Mercedes	SL	5,030	$101,565	2,638	£78,190	not tested	
Mercedes	SLK	4,737	$51,150	11,107	£38,705	not tested	
Mercedes	M-Class	46,726	$71,990	23,710	£48,035	17.4	
Mini	Cooper	33,467	$22,900	94,909	£19,053	18.1	
Nissan	GT-R	1,436	$77,965	275	£81,610	not tested	
Peugeot	RCZ	not sold in U.S.		5,772	£27,050	not tested	
Porsche	Panamera	5,740	$111,200	5,647	£97,603	not tested	
Tesla	Model S	36,400	$81,650	8,841	£75,535	13.9	
Audi	TT	1,158	$40,795	9,786	£32,320	17.7	
Volvo	V40	not sold in U.S.		80,948	£25,388	24	
Total vehicles w/ pop-up hoods		1,174,225		1,043,650			
Total all light vehicles		16,531,070		12,939,046			

---

[1] Cadillac ATS and CTS not sold in U.K. Estimated price for the CTS in EU: 56,200 € (£40,800). No estimate for the ATS.
[2] Citroen C6: Separate headform score not reported.
[3] Hyundai Genesis not sold in U.K. Estimated price in EU: 65,000 € (£47,200). Headform score of 16.7 reported by Australia NCAP.

Standardized Test Protocols

Test protocols for pop-up hoods and associated requirements are discussed below. In addition to Euro NCAP's five star consumer ratings, which are consumer information ratings and not regulations, some countries also subscribe to various United Nations agreements and are therefore subject to United Nations regulations. United Nations Global Technical Regulation No. 9 (GTR No. 9), *Pedestrian Safety,* which applies to WP29 1998 Agreement signatory countries, includes a test protocol for evaluating the pedestrian friendliness of light duty vehicles. GTR No. 9 provides general guidance as to how testing of vehicles with pop-up hoods could be done.

GTR No. 9. GTR No. 9 [15] addresses pedestrian safety, targeting the energy absorption abilities of the bumper and hood areas in 40 km/h vehicle-to-pedestrian crashes. GTR No. 9 is broken into two main parts: Section A, the Statement of Technical Rationale and Justification, and Section B, the Text of the Regulation. The regulatory requirements are prescribed in Section B, where it is stated: "[a]ll devices designed to protect vulnerable road users when impacted by the vehicle shall be correctly activated before and/or be pop-up during the relevant test. It shall be the responsibility of the manufacturer to show that any devices will act as intended in a pedestrian impact." However, there are no specifics on how this demonstration is carried out. Pop-up hoods were still conceptual during the 1990s when the work of the ISO, IHRA, the EEVC, and NHTSA formed the building blocks of the GTR.

Section A, however, does provide informal guidance on pop-up hoods. It states that pop-up hoods "must not create a higher risk of injuries for the pedestrians." In conjunction with this point, working paper INF GR/PS/141, Certification Standard for Type Approval Testing of Active Deployable Systems of the Bonnet/Windscreen Area, is offered as a guideline for the certification of deployable devices by Contracting Parties looking to implement test procedures in their home countries, with previous working papers giving additional insight [1][16].

Another working paper provides a decision tree analysis for a Type Approval system of compliance in which the vehicle manufacturer and a type approval authority agree on the timing between a headform launch and a hood activation [17]. The guidelines serve mostly to specify terminology for defining the timing of a launch as provided by the manufacturer. They do not specify the timing itself, nor do they provide requirements for the triggering threshold or any requirements for hood activation.

Euro NCAP. Though not a regulatory body, Euro NCAP has had a pedestrian testing protocol in place for more than a decade, which covers headform, legform, and upper legform impact tests. The first vehicle tested with a pop-up hood in the Euro NCAP database of test results was the 2006 Citroen C6, followed by the 2007 Honda Legend and several others.

Since Version 5.2 (implemented in 2009), Section 2 in the Euro NCAP pedestrian testing protocol has been dedicated to the "assessment of vehicles with active bonnets," laying out detailed information for how Euro NCAP will assess not only the deployment but also the triggering and sensing capabilities of these pop-up systems. As the pop-up systems have matured, the Euro NCAP testing protocol has undergone periodic refinement to provide more objective assessment procedures.

Notwithstanding higher Euro NCAP scores, uncertainty remains over the true effectiveness of pop-up hoods. Absent a real-world analysis of pedestrian collisions, it is unknown whether higher headform scores for pop-up hoods have translated into reduced injury risk for pedestrians. Much of the uncertainty surrounds questions on how well pop-up hoods function in the real-world. The discussion below highlights these uncertainties and explains how they are treated under the current Euro NCAP protocol (Version 8.0, implemented in 2014).

DISCUSSION

Questions Regarding Real-World Effectiveness

The effectiveness of pop-up hoods has been questioned since the early stages of pedestrian safety standards development. The original uncertainties are perhaps best summarized in a 2006 feasibility report by Lawrence and Hardy [11]. The authors expressed low confidence for pop-up systems due to their complexity and the amount of tuning needed for them to work properly. The device must trigger and then physically push the bonnet upwards, before the pedestrian's head strikes, and the lifting mechanism must be strong enough for not only the initial lift but also to support the weight of the pedestrian's head and torso. The lift timing must be precise, and the sensors must be calibrated as to prevent false triggering. They must be able to differentiate between pedestrians about to be or having just been struck versus non-pedestrians, and a triggering threshold for a minimum vehicle collision speed must be established. The introduction of vehicles with active suspensions only serves to complicate the matter further.

In Euro NCAP, the functionality of the pop-up hood system is demonstrated through computer simulations carried out by the vehicle manufacturer. This exercise must adhere to a set of guidelines laid out in Section 2 of the Euro NCAP protocol and the integrity of the analysis must be approved by the Euro NCAP Secretariat. The protocol is not prescriptive of the system. Instead, Euro NCAP allows manufacturers to set their own sensing and triggering criteria and then performs a limited number of verification tests based on these provided criteria. System reliability and consistency is largely left to the discretion of the vehicle manufacturer. Some of the more prominent functionality concerns are discussed below.

Pedestrian sensing. All vehicles with pop-up hoods have some sort of pedestrian sensing mechanism to trigger the deployment of the hood. In Euro NCAP, this functionality is demonstrated by the manufacturer through computer simulations of knee-to-bumper interactions using full body models of pedestrians of various sizes. The simulations are run using models of various pedestrian sizes, but only for stances in which the pedestrian is walking perpendicular to the line of vehicle travel.

Hence, there is no physical test method for assuring that the sensors detect pedestrians in various gaits and stances and in a range of collision speeds, vehicle maneuvers (turning or braking) and environmental conditions (temperature, icy vs. dry). To verify sensing and deployment through a physical test, a special pedestrian manikin may be needed. Such a manikin would likely differ in form and function from the legform impactor used by Euro NCAP (and known as the Flex-PLI) to assess pedestrian leg injury risk.

There are also concerns that pedestrians will be left unprotected in a collision that is not initiated by leg-to-bumper contact so that the hood does not deploy. And since the sensors are located on the bumper, a criterion may be needed to assure that they do not become easily damaged. Also, it is also entirely possible that future systems would

use visual detection and not require actual contact, which would require even another manikin with considerations for environmental operating conditions (dirt, rain and snow, lighting).

Timing. In Euro NCAP, computer simulations are carried out by the manufacturer to demonstrate that the hood is fully deployed before landed upon by a pedestrian. However, it may be necessary to account for various pedestrian gaits and stances since they can influence the time lapse between the initial bumper-to-pedestrian contact and the subsequent head-to-hood impact. In Euro NCAP, there are no physical tests associated with this demonstration due in part to the absence of a standardized pedestrian test dummy.

Deployment threshold. In Euro NCAP, the manufacturer specifies the hood deployment thresholds (both at a speed below 40 km/h and at a speed of 50 km/h or higher), which are then verified through physical testing. Triggering thresholds generally differ from one vehicle to the next. The vehicle speed at which activation occurs may depend upon the protectiveness of the hood in its undeployed state, which is dependent on under-hood clearances and the size of the hood. Thus, a blanket requirement for a single threshold for all vehicles might not achieve all the potential benefits it could otherwise achieve if, for example, it did not deploy at a low enough speed. . However, a protocol may be needed to verify the thresholds are met under a variety of collision scenarios.

Head impacts below the deployment threshold. If a low-speed collision occurs below the hood activation threshold, a pedestrian may be placed in undue risk if the undeployed hood is overly stiff. In Euro NCAP, manufacturers are required to show that HIC values in actual headform impact tests on an undeployed hood are not exceedingly high (HIC values must be less than 1350) when the tests are run at the deployment threshold speed.

Width of bumper sensitivity. Relative to the width of the hood, the front-end vehicle width over which trigger sensors apply should be sufficiently wide. However, the legform test area specified by Euro NCAP (used in conjunction with the Flex-PLI to assess lower leg injuries) only extends to the edges of the bumper support structure. In the case of a vehicle with beveled front corners, the test area can be quite narrow (less than half the full width of some vehicles). Therefore, added assurance may be needed to verify that the hood deploys for any bumper-to-leg impact that could precede a head-to-hood impact.

Lifting device. The actuators used to raise the hood pose one of the greater risks to failure of the entire pop-up hood system. Test procedures may be needed to assure that the lifting linkages are strong enough for not only the initial lift but also to support the weight of the pedestrian's torso so that the hood does not collapse prior to or upon head-to-hood impact. In Euro NCAP, such assurances are provided by the manufacturer through computer simulations of vehicle-to-pedestrian collisions. For pyrotechnic devices, further requirements may be needed to assure that their performance does not degrade over time due to the harsh environmental conditions under a hood.

False deployments. Bumper sensors are tuned in some manner to differentiate between a human leg and an object of a similar shape. A test method for a pedestrian detection sensor may be needed to show that the trigger sensor is able to differentiate between a pedestrian and a common roadside object, such as a garbage can. False deployments are not explicitly covered by the Euro NCAP protocol. However, there could be visibility risks for occupants of a vehicle in motion whose pop-up hood deploys from a false-positive trigger event. Furthermore, deployed hoods have cost implications which require additional consideration. Not only is a pop-up hood system added cost to the vehicle at purchase, but it is also potentially an area for costly repairs. Will the driver be able to drive the vehicle with deployed hood to a repair shop, or will a tow truck be required? These are factors which need to be balanced when assessing false deployments. [11]

Overall objectivity. Standardized test methods with objective assessment criteria may be needed in order to fully assess the overall effectiveness of pop-up hood systems on real-world pedestrian safety. They may also be needed to assure conformity to given level of pedestrian safety by a third party. A performance requirement for a device that is reliant on a manufacturer to prescribe how it should be tested and assessed may lessen the ability of an independent evaluator to provide such assurances.

CONCLUSIONS

The range of vehicles in the Euro NCAP database shows that the early concerns about prohibitive cost and reliability of pop-up hoods did not appear to come to fruition. Our observations revealed the following:

• Since 2010, vehicles with pop-up hoods generally produced better Euro NCAP headform scores on average: 17.2 (out of a possible 24) for cars with pop-up hoods vs. 13.8 for cars with non-deploying hoods.

• From year-to-year, the Euro NCAP headform scores of cars with traditional, non-deploying hoods have been trending upwards. Nonetheless, in the latest year of our assessment (2014), the scores of cars with pop-up hoods were still higher.

• In 2014, there were 38 European new car models with pop-up hoods. The models tended to be in a higher price range (such as several Jaguar and Mercedes Benz models), but there are exceptions (examples: Hyundai Santa Fe, Mini Cooper).

• Cars with pop-up hoods comprise about 8% of all new light vehicles in Europe. These same vehicles comprise about 7% of new light vehicles sold in the U.S.

• Only one vehicle so far, the 2013 Skoda Octavia, has introduced pop-up hood technology as standard and later removed it.

• Pop-up hood technology is generally more costly than other passive strategies for protection pedestrians, but this examination of pop-up hood trends showed that sometimes a pop-up hood can lead to lower HIC values while enabling the vehicle to attain a better Euro NCAP score and still achieving a desired vehicle style.

• The Dodge Caravan exemplifies a situation where a pop-up hood provided an expedient means to achieve an acceptable pedestrian rating in a vehicle not originally designed for a market with pedestrian protection requirements. By fitting the sensing and lifting components to an existing design (rather than engaging in a lengthy and costly redesign of the vehicle front-end using a non-deploying hood), the vehicle was brought to the European market promptly.

• Notwithstanding the guidelines laid out in Section 2 of the Euro NCAP protocol, there is no standardized means to independently test and assess entire pop-up hood systems because of their unique and vehicle-specific operations. The basic technologies vary widely, and pop-up hoods activate within different speed ranges depending on the vehicle. These conditions make it difficult to develop a standardized test and criteria that is objective, uniform, and repeatable during testing across a fleet of vehicles with differing pop-up deployment designs.

Given the number of these systems in production today, it is clear that engineering has been able to overcome the initial technical challenges in a safe and reliable manner regardless of the remaining testing standardization challenges. Pop-up hoods are now yet another technical advance in the field of automotive engineering. The trends in the preceding analysis show that pop-up hoods are worthy of consideration for the development of new standardized test methods and assessment criteria.

REFERENCES

[1] CLEPA European Association of Automotive Suppliers (2004). *INF GR/PA/67 Pedestrian Protection Test method – Active hood/bonnet systems.* [Working Paper]

[2] Euro NCAP (July 2012). *European New Car Assessment Programme (Euro NCAP) Assessment Protocol – Overall Rating, Version 6.0.* [Test Protocol].

[3] Euro NCAP (June 2014). *European New Car Assessment Programme (Euro NCAP) Assessment Protocol – Pedestrian Protection, Version 8.0.* [Test Protocol].

[4] Euro NCAP (June 2014). *European New Car Assessment Programme (Euro NCAP) Pedestrian Testing Protocol, Version 8.0.* [Test Protocol].

[5] Euro NCAP (2015). *The Car Selection Explained | Euro NCAP – For Safer Cars Crash Test Safety Rating.* [Web]. Retrieved January 8, 2015 from http://euroncap.com/ourtests/selectionexplained.aspx.

[6] European Motor News. (2013, May 30). *THE ALL-NEW VOLVO V40 – PEDESTRIAN AIRBAG TECHNOLOGY* [Video File]. Retrieved from http://www.youtube.com/watch?v=NCjVS_-6hYs

[7] Evrard, Borg (2011). *Innovative Bonnet Active Actuator (B2A) For Pedestrian Protection*, Proceedings of the 22nd International Technical Conference on the Enhanced Safety of Vehicles, paper 11-0113, Washington, D.C.

[8] Fredriksson, R., Boström, O., Chang, L.Y., Yang, K., (2006). *Influence of pop-up hood systems on brain injuries for vulnerable road users*. In: 2006 International IRCOBI Conference on the Biomechanics of Impact, Madrid, Spain.

[9] Key, Edwin (2012). "Volvo S40 Comes with Pedestrian Airbag." *Ubergizmo*.

[10] Honeywill, Tristan. (2013, June 27). Skoda withdraws pedestrian-friendly pop-up hood on Octavia [Online Article]. *Car Safety Rules*. Retrieved August 28, 2013 from http://www.carsafetyrules.com/skoda-withdraws-pedestrian-protecting-hood-on-octavia/0627/.

[11] Lawrence, G J L, Hardy, B J, et al. (2006). *A study on the feasibility of measures relating to the protection of pedestrians and other vulnerable road users* [Project Report]. Berkshire, England, United Kingdom: Transportation Research Laboratory Limited (TRL), EC Contract No. UPR/VE/045/06 ENTR/05/17.01.

[12] Nagatomi K, Hanayama K, Ishizaki T, Sasaki A, Matsuda K (2005), *Development and full-scale dummy tests of a pop-up hood system for pedestrian protection,* Proceedings of the 19th International Technical Conference on the Enhanced Safety of Vehicles (ESV) - Washington D.C. June 6-9, 2005.

[13] *Road Safety Information: Pop Up Bonnet* [Pamphlet]. September 2005, Birmingham, England, United Kingdom: The Royal Society for the Prevention of Accidents (RoSPA).

[14] Takahashi, H, Miyazaki, H, et al. (2013). *Development of Pop-Up Hood System for Pedestrian Protection*, Proceedings of the 23rd International Technical Conference on the Enhanced Safety of Vehicles, paper 13-0126, Seoul, Korea.

[15] United Nations (18 November 2004). *Global technical regulation No. 9: Pedestrian Safety* [Addendum to GTR]. Geneva, Switzerland.

[16] United Nations (6 December 2003). *INF GR/PS/104 Minimum Standard for Type Approval Testing of Active Deployable Systems of the Bonnet/Windscreen Area.* [Working Paper]

[17] United Nations (6 December 2003). *INF GR/PS/141 Certification Standard for Type Approval Testing of Active Deployable Systems of the Bonnet Area.* [Working Paper]

APPENDIX A

Table 2, below, includes the processed list of vehicles described above in the Methods section. At the end of the list of vehicles used in the above calculations, 12 additional vehicles which were sold in Europe with pop-up hoods but not tested by Euro NCAP are listed. These 12 additional vehicles were identified through other media outlets.

Table 2. Vehicle Database

Yr	Make	Model	Ctgry	Pop Up ?	Overall Stars (/5)	Stars (/4)	Pts (/36)	Head (/24)	Pelvis (/6)	Leg (/6)	Yr	Make	Model	Ctgry	Pop Up ?	Overall Stars (/5)	Stars (/4)	Pts (/36)	Head (/24)	Pelvis (/6)	Leg (/6)
2000	Citroen	Saxo	3 door hatch	no	n/a	2	10	n/a	n/a	n/a	2000	VW	Beetle	2 door saloon	no	n/a	2	14	n/a	n/a	n/a
2000	Daewoo	Matiz	5 door hatch	no	n/a	2	15	n/a	n/a	n/a	2000	VW	Lupo	3 door hatch	no	n/a	2	13	n/a	n/a	n/a
2000	Daihatsu	Sirion	3 door hatch	no	n/a	3	19	n/a	n/a	n/a	2000	VW	Polo	3 door hatch	no	n/a	2	13	n/a	n/a	n/a
2000	Fiat	Seicento	3 door hatch	no	n/a	2	13	n/a	n/a	n/a	2001	Alfa Romeo	147	3 door hatch	no	n/a	2	17	n/a	n/a	n/a
2000	Ford	Fiesta	3 door hatch	no	n/a	1	8	n/a	n/a	n/a	2001	Audi	A4	4 door saloon	no	n/a	1	7	n/a	n/a	n/a
2000	Ford	Ka	3 door hatch	no	n/a	1	9	n/a	n/a	n/a	2001	BMW	3 Series	4 door saloon	no	n/a	1	8	n/a	n/a	n/a
2000	Honda	Accord	4 door saloon	no	n/a	2	16	n/a	n/a	n/a	2001	Citroen	C5	5 door hatch	no	n/a	2	16	n/a	n/a	n/a
2000	Honda	Logo	3 door hatch	no	n/a	2	14	n/a	n/a	n/a	2001	Citroen	Picasso	5 door MPV	no	n/a	2	12	n/a	n/a	n/a
2000	Lancia	Ypsilon	3 door hatch	no	n/a	2	12	n/a	n/a	n/a	2001	Fiat	Multipla	5 door MPV	no	n/a	2	13	n/a	n/a	n/a
2000	Nissan	Micra	3 door hatch	no	n/a	2	16	n/a	n/a	n/a	2001	Honda	Civic	5 door hatch	no	n/a	3	26	n/a	n/a	n/a
2000	Opel/Vauxhall	Corsa	3 door hatch	no	n/a	2	14	n/a	n/a	n/a	2001	Hyundai	Elantra	4 door saloon	no	n/a	2	16	n/a	n/a	n/a
2000	Peugeot	206	3 door hatch	no	n/a	2	11	n/a	n/a	n/a	2001	Mazda	Premacy	5 door MPV	no	n/a	3	19	n/a	n/a	n/a
2000	Renault	Clio	3 door hatch	no	n/a	2	13	n/a	n/a	n/a	2001	Mercedes	C-Class	4 door saloon	no	n/a	2	12	n/a	n/a	n/a
2000	Saab	9-3	5 door hatch	no	n/a	1	4	n/a	n/a	n/a	2001	Mitsubishi	Carisma	5 door hatch	no	n/a	2	16	n/a	n/a	n/a
2000	Seat	Ibiza	3 door hatch	no	n/a	2	17	n/a	n/a	n/a	2001	Mitsubishi	Space Star	5 door MPV	no	n/a	2	14	n/a	n/a	n/a
2000	Skoda	Fabia	5 door hatch	no	n/a	2	12	n/a	n/a	n/a	2001	Nissan	Almera	5 door hatch	no	n/a	2	16	n/a	n/a	n/a
2000	Smart	City Coupe	2 door saloon	no	n/a	2	14	n/a	n/a	n/a	2001	Nissan	Almera Tino	5 door MPV	no	n/a	2	16	n/a	n/a	n/a
2000	Toyota	Yaris	3 door hatch	no	n/a	2	13	n/a	n/a	n/a	2001	Opel/Vauxhall	Vectra	5 door hatch	no	n/a	2	14	n/a	n/a	n/a
2000	Volvo	S80	4 door saloon	no	n/a	2	14	n/a	n/a	n/a	2001	Opel/Vauxhall	Zafira	5 door MPV	no	n/a	2	13	n/a	n/a	n/a

		Vehicle Information			Euro NCAP Scores					
					Overall	Pedestrian Scores				
Yr	Make	Model	Ctgry	Pop Up?	Stars (/5)	Stars (/4)	Pts (/36)	Head (/24)	Pelvis (/6)	Leg (/6)
2001	Peugeot	307	5 door hatch	no	n/a	2	14	n/a	n/a	n/a
2001	Peugeot	406	4 door saloon	no	n/a	2	14	n/a	n/a	n/a
2001	Renault	Scenic	5 door MPV	no	n/a	2	10	n/a	n/a	n/a
2001	Rover	25	3 door hatch	no	n/a	2	18	n/a	n/a	n/a
2001	Rover	75	4 door saloon	no	n/a	2	13	n/a	n/a	n/a
2001	Skoda	Octavia	5 door hatch	no	n/a	2	14	n/a	n/a	n/a
2001	Volvo	S60	4 door saloon	no	n/a	2	14	n/a	n/a	n/a
2001	VW	Passat	4 door saloon	no	n/a	2	13	n/a	n/a	n/a
2002	Audi	A2	5 door hatch	no	n/a	1	5	n/a	n/a	n/a
2002	Chrysler	PT Cruiser	5 door MPV	no	n/a	1	3	n/a	n/a	n/a
2002	Citroen	C3	5 door hatch	no	n/a	2	11	n/a	n/a	n/a
2002	Ford	Fiesta	3 door hatch	no	n/a	2	14	n/a	n/a	n/a
2002	Ford	Mondeo	5 door hatch	no	n/a	2	13	n/a	n/a	n/a
2002	Honda	CR-V	5 door	no	n/a	3	19	n/a	n/a	n/a
2002	Hyundai	Santa Fe	off-roader	no	n/a	1	4	n/a	n/a	n/a
2002	Jaguar	X-Type	4 door saloon	no	n/a	1	2	n/a	n/a	n/a
2002	Land Rover	Freelander	off-roader	no	n/a	1	7	n/a	n/a	n/a
2002	Land Rover	Range Rover	Large Off-Road 4x4	no	n/a	1	2	n/a	n/a	n/a
2002	Mazda	MX-5	2-seater roadster	no	n/a	1	7	n/a	n/a	n/a
2002	Mercedes	E-Class	4 door saloon	no	n/a	1	4	n/a	n/a	n/a
2002	Mercedes	M-Class	off-roader	no	n/a	1	4	n/a	n/a	n/a
2002	Mercedes	SLK	2-seater roadster	no	n/a	1	8	n/a	n/a	n/a

		Vehicle Information			Euro NCAP Scores					
					Overall	Pedestrian Scores				
Yr	Make	Model	Ctgry	Pop Up?	Stars (/5)	Stars (/4)	Pts (/36)	Head (/24)	Pelvis (/6)	Leg (/6)
2002	Mercedes	Vaneo	5 door MPV	no	n/a	2	10	n/a	n/a	n/a
2002	MINI	One	3 door hatch	no	n/a	1	8	n/a	n/a	n/a
2002	Nissan	Primera	5 door hatch	no	n/a	1	9	n/a	n/a	n/a
2002	Nissan	X Trail	5 door	no	n/a	2	10	n/a	n/a	n/a
2002	Opel/Vauxhall	Corsa	3 door hatch	no	n/a	1	9	n/a	n/a	n/a
2002	Opel/Vauxhall	Frontera	5 door	no	n/a	1	2	n/a	n/a	n/a
2002	Opel/Vauxhall	Vectra	4 door saloon	no	n/a	1	5	n/a	n/a	n/a
2002	Peugeot	607	4 door saloon	no	n/a	1	3	n/a	n/a	n/a
2002	Proton	Impian	4 door saloon	no	n/a	1	4	n/a	n/a	n/a
2002	Renault	Megane	5 door hatch	no	n/a	2	11	n/a	n/a	n/a
2002	Saab	9-3	4 door saloon	no	n/a	1	7	n/a	n/a	n/a
2002	Seat	Ibiza	5 door hatch	no	n/a	2	14	n/a	n/a	n/a
2002	Suzuki	Grand Vitara	off-roader	no	n/a	0	0	n/a	n/a	n/a
2002	Toyota	Corolla	5 door hatch	no	n/a	2	11	n/a	n/a	n/a
2002	VW	Polo	5 door hatch	no	n/a	1	6	n/a	n/a	n/a
2003	Audi	A3	Small Family	no	n/a	1	8	n/a	n/a	n/a
2003	Audi	TT	2-seater roadster	no	n/a	0	0	n/a	n/a	n/a
2003	BMW	X5	5 door	no	n/a	1	2	n/a	n/a	n/a
2003	Citroen	C2	Super mini	no	n/a	2	12	n/a	n/a	n/a
2003	Citroen	C3 Pluriel	Super mini	no	n/a	2	13	n/a	n/a	n/a
2003	Ford	Focus C-MAX	Small MPV	no	n/a	2	14	n/a	n/a	n/a
2003	Ford	Fusion	Small MPV	no	n/a	2	11	n/a	n/a	n/a
2003	Honda	Accord	4 door saloon	no	n/a	2	16	n/a	n/a	n/a
2003	Hyundai	Trajet	MPV	no	n/a	1	9	n/a	n/a	n/a

Ames 13

Vehicle Information / Euro NCAP Scores

Yr	Make	Model	Ctgry	Pop Up?	Overall Stars (/5)	Stars (/4)	Pts (/36)	Head (/24)	Pelvis (/6)	Leg (/6)
2003	Jeep	Cherokee	Small Off-Road 4x4	no	n/a	1	3	n/a	n/a	n/a
2003	Kia	Carnival/Sedona	MPV	no	n/a	1	4	n/a	n/a	n/a
2003	Kia	Sorento	Large Off-Road 4x4	no	n/a	1	3	n/a	n/a	n/a
2003	Mitsubishi	Pajero Pinin	off-roader	no	n/a	1	1	n/a	n/a	n/a
2003	Nissan	Micra	Super mini	no	n/a	2	12	n/a	n/a	n/a
2003	Opel/Vauxhall	Meriva	Small MPV	no	n/a	1	3	n/a	n/a	n/a
2003	Opel/Vauxhall	Signum	5 door hatch	no	n/a	1	1	n/a	n/a	n/a
2003	Peugeot	807	MPV	no	n/a	1	6	n/a	n/a	n/a
2003	Peugeot	307CC	Cabriolet	no	n/a	2	10	n/a	n/a	n/a
2003	Renault	Espace	MPV	no	n/a	2	10	n/a	n/a	n/a
2003	Renault	Kangoo	Small MPV	no	n/a	1	2	n/a	n/a	n/a
2003	Renault	Laguna	5 door hatch	no	n/a	2	12	n/a	n/a	n/a
2003	Renault	Scenic	Small MPV	no	n/a	2	11	n/a	n/a	n/a
2003	Saab	9-5	4 door saloon	no	n/a	2	12	n/a	n/a	n/a
2003	Skoda	Superb	4 door saloon	no	n/a	0	0	n/a	n/a	n/a
2003	Toyota	Avensis	4 door saloon	no	n/a	1	8	n/a	n/a	n/a
2003	Toyota	Previa	MPV	no	n/a	1	5	n/a	n/a	n/a
2003	Volvo	XC90	Large Off-Road 4x4	no	n/a	2	10	n/a	n/a	n/a
2003	VW	Touran	Small MPV	no	n/a	3	19	n/a	n/a	n/a
2004	Audi	A6	4 door saloon	no	n/a	1	3	n/a	n/a	n/a
2004	BMW	1 Series	5 door hatch	no	n/a	1	2	n/a	n/a	n/a
2004	BMW	5 Series	Executive	no	n/a	1	2	n/a	n/a	n/a
2004	BMW	Z4	2-seater roadster	no	n/a	2	13	n/a	n/a	n/a
2004	Citroen	C4	Small Family	no	n/a	3	22	n/a	n/a	n/a
2004	Citroen	C5	Large Family	no	n/a	1	8	n/a	n/a	n/a
2004	Fiat	Doblo	Small MPV	no	n/a	1	1	n/a	n/a	n/a
2004	Fiat	Panda	Super mini	no	n/a	1	6	n/a	n/a	n/a
2004	Ford	Focus	5 door hatch	no	n/a	2	15	n/a	n/a	n/a
2004	Honda	Jazz	Super mini	no	n/a	3	19	n/a	n/a	n/a
2004	Hyundai	Getz	Super mini	no	n/a	1	5	n/a	n/a	n/a
2004	Kia	Picanto	Super mini	no	n/a	1	6	n/a	n/a	n/a
2004	Mazda	2	Super mini	no	n/a	2	10	n/a	n/a	n/a
2004	Opel/Vauxhall	Astra	5 door hatch	no	n/a	1	3	n/a	n/a	n/a
2004	Opel/Vauxhall	Tigra	2-seater roadster	no	n/a	2	10	n/a	n/a	n/a
2004	Peugeot	407	4 door saloon	no	n/a	2	15	n/a	n/a	n/a
2004	Renault	Megane CC	Cabriolet	no	n/a	2	11	n/a	n/a	n/a
2004	Renault	Modus	Super mini	no	n/a	1	6	n/a	n/a	n/a
2004	Saab	9-3 Convertible	Convertible	no	n/a	1	7	n/a	n/a	n/a
2004	Seat	Altea	Small MPV	no	n/a	3	22	n/a	n/a	n/a
2004	Skoda	Octavia	Family Saloon	no	n/a	2	17	n/a	n/a	n/a
2004	Toyota	Prius	4 door	no	n/a	2	13	n/a	n/a	n/a
2004	Volvo	S40	Family Saloon	no	n/a	2	18	n/a	n/a	n/a
2004	VW	Golf	5 door hatch	no	n/a	3	19	n/a	n/a	n/a
2004	VW	Touareg	Large Off-Road 4x4	no	n/a	1	7	n/a	n/a	n/a

| | Vehicle Information | | | | Euro NCAP Scores | | | | | |
| | | | | | Overall | Pedestrian Scores | | | | |
Yr	Make	Model	Ctgry	Pop Up?	Stars (/5)	Stars (/4)	Pts (/36)	Head (/24)	Pelvis (/6)	Leg (/6)
2005	BMW	3 Series	Large Family	no	n/a	1	4	n/a	n/a	n/a
2005	Chevrolet	Matiz	5 door hatch	no	n/a	2	13	n/a	n/a	n/a
2005	Citroen	C1	Super mini	no	n/a	2	14	n/a	n/a	n/a
2005	Daihatsu	Sirion	5 door hatch	no	n/a	2	15	n/a	n/a	n/a
2005	Fiat	Croma	Large Family	no	n/a	1	6	n/a	n/a	n/a
2005	Fiat	Grande Punto	3 door hatch	no	n/a	3	19	n/a	n/a	n/a
2005	Fiat	Stilo	Small Family	no	n/a	1	8	n/a	n/a	n/a
2005	Honda	FR-V	Small MPV	no	n/a	3	20	n/a	n/a	n/a
2005	Jeep	Grand Cherokee	Large Off-Road 4x4	no	n/a	0	0	n/a	n/a	n/a
2005	Kia	Rio	5 door hatch	no	n/a	2	13	n/a	n/a	n/a
2005	Lexus	GS	Executive	no	n/a	2	18	n/a	n/a	n/a
2005	Mazda	5	Small MPV	no	n/a	2	12	n/a	n/a	n/a
2005	Mazda	6	5 door hatch	no	n/a	1	5	n/a	n/a	n/a
2005	Mercedes	A-Class	Small Family	no	n/a	2	17	n/a	n/a	n/a
2005	Mitsubishi	Colt	5 door hatch	no	n/a	1	7	n/a	n/a	n/a
2005	Opel/Vauxhall	Zafira	Small MPV	no	n/a	2	16	n/a	n/a	n/a
2005	Peugeot	1007	3 door hatch	no	n/a	2	10	n/a	n/a	n/a
2005	Peugeot	407 Coupe		no	n/a	2	15	n/a	n/a	n/a
2005	Renault	Clio	Super mini	no	n/a	1	9	n/a	n/a	n/a
2005	Renault	Vel Satis	4 door saloon	no	n/a	1	2	n/a	n/a	n/a
2005	Seat	Leon	5 door hatch	no	n/a	3	24	n/a	n/a	n/a
2005	Smart	forfour	Super mini	no	n/a	1	7	n/a	n/a	n/a
2005	Suzuki	Swift	Super mini	no	n/a	3	20	n/a	n/a	n/a
2005	Toyota	Yaris	5 door hatch	no	n/a	2	18	n/a	n/a	n/a

| | Vehicle Information | | | | Euro NCAP Scores | | | | | |
| | | | | | Overall | Pedestrian Scores | | | | |
Yr	Make	Model	Ctgry	Pop Up?	Stars (/5)	Stars (/4)	Pts (/36)	Head (/24)	Pelvis (/6)	Leg (/6)
2005	VW	Fox	3 door hatch	no	n/a	2	12	n/a	n/a	n/a
2006	Alfa Romeo	159	4 door saloon	no	n/a	1	9	n/a	n/a	n/a
2006	Audi	Q7	5 door SUV	no	n/a	2	15	n/a	n/a	n/a
2006	Chevrolet	Aveo	4 door saloon	no	n/a	3	19	n/a	n/a	n/a
2006	Chevrolet	Kalos	5 door hatch	no	n/a	2	11	n/a	n/a	n/a
2006	Citroen	C6	4 door saloon	yes	n/a	4	28	n/a	n/a	n/a
2006	Fiat	Idea	5 door MPV	no	n/a	1	8	n/a	n/a	n/a
2006	Ford	Galaxy	5 door MPV	no	n/a	2	15	n/a	n/a	n/a
2006	Ford	S-MAX	5 door MPV	no	n/a	2	13	n/a	n/a	n/a
2006	Hyundai	Santa Fe	off-roader	no	n/a	0	0	n/a	n/a	n/a
2006	Hyundai	Sonata	5 door sedan	no	n/a	2	12	n/a	n/a	n/a
2006	Hyundai	Tucson	5 door	no	n/a	1	4	n/a	n/a	n/a
2006	Kia	Carnival/Sedona	5 door MPV	no	n/a	1	3	n/a	n/a	n/a
2006	Kia	Cerato	5 door hatch	no	n/a	1	8	n/a	n/a	n/a
2006	Kia	Magentis	4 door saloon	no	n/a	1	3	n/a	n/a	n/a
2006	Land Rover	Discovery	Large Off-Road 4x4	no	n/a	1	8	n/a	n/a	n/a
2006	Lexus	IS	5 door saloon	no	n/a	2	15	n/a	n/a	n/a
2006	Mazda	3	5 door hatch	no	n/a	2	15	n/a	n/a	n/a
2006	Mercedes	B-Class	5 door MPV	no	n/a	2	12	n/a	n/a	n/a
2006	Nissan	Note	5 door hatch	no	n/a	2	15	n/a	n/a	n/a
2006	Nissan	Pathfinder	5 door	no	n/a	2	18	n/a	n/a	n/a
2006	Opel/Vauxhall	Corsa	3 door hatch	no	n/a	3	19	n/a	n/a	n/a
2006	Peugeot	207	5 door hatch	no	n/a	3	19	n/a	n/a	n/a
2006	Skoda	Roomster	5 door MPV	no	n/a	2	14	n/a	n/a	n/a

Vehicle Information | Euro NCAP Scores

Yr	Make	Model	Ctgry	Pop Up?	Overall Stars (/5)	Stars (/4)	Pts (/36)	Head (/24)	Pelvis (/6)	Leg (/6)
2006	Suzuki	SX4	5 door hatch	no	n/a	3	22	n/a	n/a	n/a
2006	Toyota	Auris	5 door hatch	no	n/a	3	21	n/a	n/a	n/a
2006	Toyota	RAV4	5 door SUV	no	n/a	3	21	n/a	n/a	n/a
2007	Chrysler	Voyager	5 door MPV	no	n/a	0	0	n/a	n/a	n/a
2007	Daihatsu	Materia	5 door hatch	no	n/a	2	16	n/a	n/a	n/a
2007	Dodge	Caliber	5 door hatch	no	n/a	1	5	n/a	n/a	n/a
2007	Fiat	500	3 door hatch	no	n/a	2	14	n/a	n/a	n/a
2007	Fiat	Bravo	5 door hatch	no	n/a	2	16	n/a	n/a	n/a
2007	Ford	Mondeo	5 door hatch	no	n/a	2	18	n/a	n/a	n/a
2007	Honda	Civic Hybrid	4 door sedan	no	n/a	3	21	n/a	n/a	n/a
2007	Honda	CR-V	5 door SUV	no	n/a	2	13	n/a	n/a	n/a
2007	Honda	Legend	4 door saloon	yes	n/a	3	n/a	n/a	n/a	n/a
2007	Kia	Carens	5 door MPV	no	n/a	1	9	n/a	n/a	n/a
2007	Kia	Cee'd	5 door hatch	no	n/a	2	11	n/a	n/a	n/a
2007	Land Rover	Freelander	5 door SUV	no	n/a	1	7	n/a	n/a	n/a
2007	Mazda	2	5 door hatch	no	n/a	2	18	n/a	n/a	n/a
2007	MINI	Cooper	3 door hatch	no	n/a	2	14	n/a	n/a	n/a
2007	Mitsubishi	Outlander	5 door SUV	no	n/a	2	17	n/a	n/a	n/a
2007	Nissan	Qashqai	5 door	no	n/a	2	18	n/a	n/a	n/a
2007	Nissan	X Trail	5 door SUV	no	n/a	2	12	n/a	n/a	n/a
2007	Peugeot	207CC	2-seater roadster	no	n/a	2	16	n/a	n/a	n/a
2007	Renault	Laguna	5 door hatch	no	n/a	2	10	n/a	n/a	n/a
2007	Renault	Twingo	3 door hatch	no	n/a	2	11	n/a	n/a	n/a
2007	Skoda	Fabia	5 door hatch	no	n/a	2	17	n/a	n/a	n/a

Vehicle Information | Euro NCAP Scores

Yr	Make	Model	Ctgry	Pop Up?	Overall Stars (/5)	Stars (/4)	Pts (/36)	Head (/24)	Pelvis (/6)	Leg (/6)
2007	Smart	fortwo	2 door	no	n/a	2	10	n/a	n/a	n/a
2007	Suzuki	Grand Vitara	5 door SUV	no	n/a	3	19	n/a	n/a	n/a
2007	VW	Caddy	5 door MPV	no	n/a	2	13	n/a	n/a	n/a
2007	VW	Eos	2 door cabriolet	no	n/a	2	13	n/a	n/a	n/a
2008	Alfa Romeo	MiTo	3 door hatch	no	n/a	2	18	n/a	n/a	n/a
2008	BMW	X3	5 door SUV	no	n/a	1	5	n/a	n/a	n/a
2008	Citroen	Berlingo	5 door MPV	no	n/a	2	10	n/a	n/a	n/a
2008	Daihatsu	Terios	5 door SUV	no	n/a	3	19	n/a	n/a	n/a
2008	Ford	Fiesta	5 door hatch	no	n/a	3	20	n/a	n/a	n/a
2008	Ford	Ka	3 door hatch	no	n/a	2	11	n/a	n/a	n/a
2008	Ford	Kuga	5 door SUV	no	n/a	3	20	n/a	n/a	n/a
2008	Hyundai	i10	5 door hatch	no	n/a	3	21	n/a	n/a	n/a
2008	Hyundai	i30	5 door hatch	no	n/a	2	14	n/a	n/a	n/a
2008	Lancia	Delta	4 door saloon	no	n/a	2	15	n/a	n/a	n/a
2008	Mercedes	M-Class	Large Off-Road 4x4	no	n/a	1	6	n/a	n/a	n/a
2008	Mitsubishi	L200	4 door pickup	no	n/a	1	2	n/a	n/a	n/a
2008	Nissan	Navara	4 door pickup	no	n/a	2	14	n/a	n/a	n/a
2008	Renault	Kangoo	5 door MPV	no	n/a	2	14	n/a	n/a	n/a
2008	Renault	Koleos	Small Off-Road 4x4	no	n/a	2	14	n/a	n/a	n/a
2008	Renault	Megane	5 door hatch	no	n/a	2	11	n/a	n/a	n/a
2008	Seat	Ibiza	5 door hatch	no	n/a	3	19	n/a	n/a	n/a
2008	Suzuki	Splash	5 door hatch	no	n/a	3	19	n/a	n/a	n/a
2008	VW	T5	MPV	no	n/a	1	3	n/a	n/a	n/a

Ames 16

| | Vehicle Information | | | | Euro NCAP Scores | | | | | |
| | | | | | Overall | Pedestrian Scores | | | | |
Yr	Make	Model	Ctgry	Pop Up?	Stars (/5)	Stars (/4)	Pts (/36)	Head (/24)	Pelvis (/6)	Leg (/6)
2009	Audi	A4	Large Family	no	5	n/a	14	7.9	0.0	6.0
2009	Audi	Q5	Small Off-Road 4x4	no	5	n/a	12	5.5	0.0	6.0
2009	Chevrolet	Cruze	Small Family	no	5	n/a	12	6.2	0.0	6.0
2009	Chevrolet	Spark	Super mini	no	4	n/a	16	9.6	0.0	6.0
2009	Citroen	C3	Super mini	no	4	n/a	12	5.8	0.0	6.0
2009	Citroen	C3 Picasso	Small MPV	no	4	n/a	16	5.6	4.0	6.0
2009	Citroen	C4 Picasso	Small MPV	no	5	n/a	16	8.0	2.4	6.0
2009	Citroen	C5	Large Family	no	5	n/a	11	5.4	0.0	6.0
2009	Citroen	DS3	Super mini	no	5	n/a	13	6.3	0.3	5.9
2009	Honda	Accord	Large Family	no	5	n/a	19	13.3	0.0	6.0
2009	Honda	Civic	Small Family	no	5	n/a	24	12.2	6.0	6.0
2009	Honda	Insight Hybrid	Small Family	no	5	n/a	27	15.4	6.0	6.0
2009	Honda	Jazz	Super mini	no	5	n/a	22	10.4	5.2	6.0
2009	Hyundai	i20	Super mini	no	5	n/a	23	12.0	5.2	5.8
2009	Infiniti	FX	Large Off-Road 4x4	no	5	n/a	16	10.2	1.6	4.2
2009	Kia	Sorento	Large Off-Road 4x4	no	5	n/a	16	10.2	0.0	5.7
2009	Kia	Soul	Small MPV	no	5	n/a	14	8.0	0.0	5.9
2009	Mazda	3	Small Family	no	5	n/a	18	10.2	2.0	6.0
2009	Mazda	6	Large Family	no	5	n/a	18	10.1	1.5	6.0
2009	Mercedes	C-Class	Large Family	no	5	n/a	11	3.7	1.5	5.6
2009	Mitsubishi	Lancer	Small Family	no	5	n/a	12	7.5	0.0	4.7
2009	Opel/Vauxhall	Astra	Small Family	no	5	n/a	16	10.4	0.0	6.0
2009	Opel/Vauxhall	Insignia	Large Family	no	5	n/a	14	8.3	0.0	6.0
2009	Peugeot	308	Small Family	no	5	n/a	19	7.7	5.3	6.0
2009	Peugeot	3008	Small Family	no	5	n/a	11	3.0	2.1	6.0
2009	Peugeot	5008	Small MPV	no	5	n/a	13	7.4	0.0	6.0
2009	Peugeot	308CC	Small Family	no	5	n/a	12	4.9	0.8	6.0
2009	Renault	Grand Scenic	Small MPV	no	5	n/a	15	6.8	2.3	6.0
2009	Saab	9-5	4 door saloon	no	5	n/a	16	9.9	0.0	6.0
2009	Skoda	Superb	5 door saloon	no	5	n/a	18	12.0	0.0	6.0
2009	Skoda	Yeti	5 door SUV	no	5	n/a	17	10.7	0.0	6.0
2009	Subaru	Impreza	5 door hatch	no	4	n/a	26	16.2	3.6	6.0
2009	Subaru	Legacy	5 door	no	5	n/a	21	15.1	0.0	5.8
2009	Suzuki	Alto	Super mini	no	3	n/a	13	9.5	0.0	3.3
2009	Toyota	Avensis	Large Family	no	5	n/a	19	12.6	0.5	6.0
2009	Toyota	iQ	Super mini	no	5	n/a	19	11.8	1.7	6.0
2009	Toyota	Prius	Large Family	no	5	n/a	24	14.9	4.3	5.2
2009	Toyota	Urban Cruiser	Small MPV	no	3	n/a	19	13.1	0.0	5.9
2009	Volvo	C30	Small Family	no	5	n/a	9	5.2	0.0	4.0
2009	Volvo	V70	Large Family	no	5	n/a	16	9.6	0.0	6.0
2009	Volvo	XC60	Small Off-Road 4x4	no	5	n/a	17	11.3	0.0	6.0
2009	VW	Golf	Small Family	no	5	n/a	22	12.0	3.9	6.0
2009	VW	Polo	Super mini	no	5	n/a	15	8.5	2.4	4.0
2009	VW	Scirocco	Small Family	no	5	n/a	19	7.1	6.0	6.0
2009	VW	Tiguan	Small Off-Road 4x4	no	5	n/a	17	11.2	0.0	6.0

Ames 17

| | Vehicle Information | | | | Euro NCAP Scores | | | | | |
| | | | | | Overall | Pedestrian Scores | | | | |
Yr	Make	Model	Ctgry	Pop Up ?	Stars (/5)	Stars (/4)	Pts (/36)	Head (/24)	Pelvis (/6)	Leg (/6)
2010	Alfa Romeo	Giulietta	Small Family	no	5	n/a	23	13.5	3.1	6.0
2010	Audi	A1	Super mini	no	5	n/a	18	11.6	0.2	6.0
2010	BMW	5 Series	Executive	yes	5	n/a	28	22.0	0.0	6.0
2010	Citroen	C4	Small Family	no	5	n/a	15	7.9	4.5	6.0
2010	Citroen	Nemo	Small MPV	no	3	n/a	20	9.0	4.8	6.0
2010	Ford	C-MAX	Small MPV	no	5	n/a	18	13.0	0.9	4.0
2010	Ford	Grand C-MAX	Small MPV	no	5	n/a	18	13.0	0.9	4.0
2010	Honda	CR-Z	Super mini	no	5	n/a	25	15.5	6.0	4.0
2010	Hyundai	ix35	Small Off-Road 4x4	no	5	n/a	20	14.0	0.0	5.6
2010	Kia	Sportage	Small Off-Road 4x4	no	5	n/a	18	11.6	1.2	4.9
2010	Kia	Venga	Small Off-Road 4x4	no	5	n/a	23	12.8	4.2	6.0
2010	Mazda	CX-7	Small Off-Road 4x4	no	4	n/a	16	6.5	3.1	6.0
2010	Mercedes	E-Class	Executive	yes	5	n/a	21	15.2	0.0	6.0
2010	MINI	Countryman	Small MPV	no	5	n/a	23	15.3	1.5	6.0
2010	Nissan	Cube	Small MPV	no	4	n/a	20	14.0	0.3	6.0
2010	Nissan	Micra	Super mini	no	4	n/a	21	13.4	1.6	6.0
2010	Opel/Vauxhall	Meriva	Small MPV	no	5	n/a	20	15.0	0.9	4.0
2010	Seat	Alhambra	Large MPV	no	5	n/a	16	12.4	0.0	4.0
2010	Seat	Exeo	4 door saloon	no	4	n/a	18	12.2	0.0	5.9
2010	Suzuki	Swift	5 door hatch	no	5	n/a	22	18.4	0.0	4.0
2010	Toyota	Verso	Small MPV	no	5	n/a	25	18.8	0.0	6.0

| | Vehicle Information | | | | Euro NCAP Scores | | | | | |
| | | | | | Overall | Pedestrian Scores | | | | |
Yr	Make	Model	Ctgry	Pop Up ?	Stars (/5)	Stars (/4)	Pts (/36)	Head (/24)	Pelvis (/6)	Leg (/6)
2010	VW	Passat	Large Family	no	5	n/a	19	14.0	0.0	5.3
2010	VW	Sharan	Large MPV	no	5	n/a	16	12.4	0.0	4.0
2011	Audi	A6	Executive	no	5	n/a	15	8.7	0.0	6.0
2011	Audi	Q3	Small Off-Road 4x4	no	5	n/a	19	12.8	0.0	6.0
2011	BMW	X3	Small Off-Road 4x4	no	5	n/a	19	13.1	0.0	6.0
2011	Chevrolet	Aveo	Super mini	no	5	n/a	19	13.7	0.2	5.3
2011	Chevrolet	Captiva	Small Off-Road 4x4	no	5	n/a	17	14.0	0.0	3.3
2011	Chevrolet	Orlando	Small MPV	no	5	n/a	18	13.1	0.0	4.5
2011	Chevrolet	Volt	Small Family	no	5	n/a	15	8.9	0.0	6.0
2011	Citroen	C-Zero	Super mini	no	4	n/a	17	11.2	0.0	6.0
2011	Citroen	DS4	Small Family	no	5	n/a	15	7.5	2.0	6.0
2011	Citroen	DS5	Large Family	no	5	n/a	15	6.3	2.2	6.0
2011	Dacia	Duster	Small Off-Road 4x4	no	3	n/a	10	10.0	0.0	0.0
2011	Fiat	Freemont	Large MPV	yes	5	n/a	18	12.0	0.0	6.0
2011	Fiat	Panda	Super mini	no	4	n/a	18	10.7	0.8	6.0
2011	Hyundai	i40	Large Family	no	5	n/a	16	8.1	1.5	6.0
2011	Hyundai	ix20	Small MPV	no	5	n/a	23	12.8	4.2	6.0
2011	Hyundai	Veloster	Small Family	no	5	n/a	18	7.3	4.4	6.0
2011	Jaguar	XF	Executive	yes	4	n/a	22	16.2	0.0	6.0
2011	Jeep	Grand Cherokee	Large Off-Road 4x4	no	4	n/a	16	10.1	0.0	6.0

	Vehicle Information				Euro NCAP Scores					
					Overall	Pedestrian Scores				
Yr	Make	Model	Ctgry	Pop Up?	Stars (/5)	Stars (/4)	Pts (/36)	Head (/24)	Pelvis (/6)	Leg (/6)
2011	Kia	Picanto	Super mini	no	4	n/a	17	9.2	1.5	6.0
2011	Kia	Rio	Super mini	no	5	n/a	17	11.3	0.0	5.4
2011	Lancia	Thema	Executive	yes	5	n/a	21	15.3	0.0	6.0
2011	Lancia	Voyager	Large MPV	yes	4	n/a	17	11.0	0.0	6.0
2011	Land Rover	Range Rover Evoque	Small Off-Road 4x4	no	5	n/a	15	8.8	0.0	6.0
2011	Lexus	CT200h	Small Family	no	5	n/a	20	13.5	0.2	6.0
2011	Mercedes	B-Class	Small MPV	no	5	n/a	20	14.1	0.0	6.0
2011	Mercedes	C-Class Coupe	Small Family	yes	5	n/a	21	14.6	0.0	6.0
2011	Mitsubishi	ASX	Small Family	no	5	n/a	22	17.6	0.0	4.0
2011	Mitsubishi	i-MiEV	Super mini	no	4	n/a	17	11.2	0.0	6.0
2011	Nissan	Juke	Super mini	no	5	n/a	15	9.5	0.8	4.4
2011	Opel/Vauxhall	Ampera	Small Family	no	5	n/a	15	8.9	0.0	6.0
2011	Opel/Vauxhall	Astra GTC	Small Family	no	5	n/a	18	12.0	0.0	6.0
2011	Opel/Vauxhall	Zafira Tourer	Small MPV	no	5	n/a	19	14.0	0.0	4.9
2011	Peugeot	508	Large Family	no	5	n/a	15	9.1	1.5	4.0
2011	Peugeot	iOn	Super mini	no	4	n/a	17	11.2	0.0	6.0
2011	Renault	Fluence ZE	Small Family	no	4	n/a	13	7.2	0.1	6.0
2011	Seat	Ibiza	Super mini	no	5	n/a	21	15.3	0.0	6.0
2011	Seat	Mii	Super mini	no	5	n/a	17	11.7	0.0	4.9
2011	Skoda	Citigo	3 door hatch	no	5	n/a	17	11.7	0.0	4.9
2011	Toyota	Yaris	Super mini	no	5	n/a	21	15.3	0.1	6.0
2011	VW	Beetle	Small Family	no	5	n/a	19	15.0	0.0	4.0
2011	VW	Golf Cabriolet	Small Family	no	5	n/a	19	11.3	3.9	3.8

	Vehicle Information				Euro NCAP Scores					
					Overall	Pedestrian Scores				
Yr	Make	Model	Ctgry	Pop Up?	Stars (/5)	Stars (/4)	Pts (/36)	Head (/24)	Pelvis (/6)	Leg (/6)
2011	VW	Jetta	Small Family	no	5	n/a	20	11.7	2.5	6.0
2011	VW	up!	Super mini	no	5	n/a	17	11.7	0.0	4.9
2012	Audi	A3	Small Family	no	5	n/a	27	19.6	1.0	6.0
2012	BMW	1 Series	Small Family	no	5	n/a	23	16.6	0.0	6.0
2012	BMW	3 Series	Large Family	no	5	n/a	28	15.9	6.0	6.0
2012	BMW	X1	Small Off-Road 4x4	no	5	n/a	23	16.9	0.0	6.0
2012	Citroen	C1	Super mini	no	3	n/a	19	13.2	0.0	6.0
2012	Citroen	Jumpy	Van-based people carrier	no	3	n/a	8	7.8	n/a	0.0
2012	Fiat	500L	Small MPV	no	5	n/a	23	15.0	2.5	6.0
2012	Fiat	Scudo	Van-based people carrier	no	3	n/a	8	7.8	0.0	0.0
2012	Ford	B-MAX	Small MPV	no	5	n/a	24	15.0	3.0	6.0
2012	Ford	Fiesta	Super mini	no	5	n/a	23	12.2	5.1	6.0
2012	Ford	Focus	Small Family	no	5	n/a	26	16.0	6.0	4.0
2012	Ford	Kuga	Small Off-Road 4x4	no	5	n/a	25	15.4	3.7	6.0
2012	Honda	Civic	Small Family	no	5	n/a	25	12.9	6.0	6.0
2012	Hyundai	H-1	Van-based people carrier	no	3	n/a	10	4.2	n/a	6.0
2012	Hyundai	i30	Small Family	no	5	n/a	24	14.3	4.0	6.0
2012	Hyundai	Santa Fe	Large Off-Road 4x4	yes	5	n/a	25	18.6	0.9	6.0
2012	Isuzu	D-Max	4 door pickup	no	4	n/a	18	12.4	0.0	6.0

| | Vehicle Information | | | | Euro NCAP Scores | | | | | |
| | | | | | Overall | Pedestrian Scores | | | | |
Yr	Make	Model	Ctgry	Pop Up ?	Stars (/5)	Stars (/4)	Pts (/36)	Head (/24)	Pelvis (/6)	Leg (/6)
2012	Jeep	Compass	Small Off-Road 4x4	no	2	n/a	8	8.4	0.0	0.0
2012	Kia	Cee'd	Small Family	no	5	n/a	22	12.6	3.6	5.8
2012	Land Rover	Range Rover	Large Off-Road 4x4	no	5	n/a	23	16.6	0.0	6.0
2012	Mazda	CX-5	Small Off-Road 4x4	no	5	n/a	23	17.0	0.2	6.0
2012	Mercedes	A-Class	Small Family	yes	5	n/a	24	18.0	0.0	6.0
2012	Mercedes	M-Class	Large Off-Road 4x4	yes	5	n/a	21	17.4	0.0	4.0
2012	Mitsubishi	Outlander	Small Off-Road 4x4	no	5	n/a	23	16.9	0.0	6.0
2012	Nissan	Leaf	Small Family	no	5	n/a	23	15.2	3.0	5.1
2012	Opel/Vauxhall	Mokka	Small Family	no	5	n/a	24	18.0	0.0	6.0
2012	Peugeot	107	Super mini	no	3	n/a	19	13.2	0.0	6.0
2012	Peugeot	208	Super mini	no	5	n/a	22	12.5	3.5	6.0
2012	Peugeot	Expert	Van-based people carrier	no	3	n/a	8	7.8	n/a	0.0
2012	Renault	Clio	Super mini	no	5	n/a	24	11.8	5.9	6.0
2012	Renault	Trafic	Passenger Van	no	2	n/a	8	8.5	n/a	0.0
2012	Seat	Leon	5 door hatch	no	5	n/a	25	16.9	2.2	6.0
2012	Seat	Toledo	5 door hatch	no	5	n/a	25	16.6	2.1	6.0
2012	Skoda	Rapid	5 door hatch	no	5	n/a	25	16.6	2.1	6.0
2012	Subaru	Forester	5 door SUV	no	5	n/a	26	20.3	0.0	6.0

| | Vehicle Information | | | | Euro NCAP Scores | | | | | |
| | | | | | Overall | Pedestrian Scores | | | | |
Yr	Make	Model	Ctgry	Pop Up ?	Stars (/5)	Stars (/4)	Pts (/36)	Head (/24)	Pelvis (/6)	Leg (/6)
2012	Subaru	XV	5 door hatch	no	5	n/a	23	16.9	0.0	6.0
2012	Toyota	Aygo	Super mini	no	3	n/a	19	13.2	0.0	6.0
2012	Volvo	V40	Small Family	yes	5	n/a	32	24.0	2.0	5.8
2012	Volvo	V60	Large Family	no	5	n/a	23	14.7	2.8	5.7
2012	VW	Golf	Small Family	no	5	n/a	24	14.8	2.8	6.0
2013	BMW	i3	Small Family	no	4	n/a	21	14.8	0.0	6.0
2013	Chevrolet	Trax	Small Family	no	5	n/a	23	17.1	0.0	6.0
2013	Citroen	C4 Picasso	Small MPV	no	5	n/a	25	15.3	3.3	6.0
2013	Dacia	Sandero	Super mini	no	4	n/a	21	14.8	0.0	6.0
2013	Ford	EcoSport	Small Family	no	4	n/a	21	14.7	0.4	6.0
2013	Ford	Tourneo Connect	Small MPV	no	5	n/a	22	16.2	0.3	6.0
2013	Honda	CR-V	Small Off-Road 4x4	no	5	n/a	25	15.8	2.9	6.0
2013	Infiniti	Q50	Executive	yes	5	n/a	24	19.1	0.0	5.1
2013	Jeep	Cherokee	Small Off-Road 4x4	no	5	n/a	24	16.9	1.6	6.0
2013	Kia	Carens	Small MPV	no	5	n/a	23	15.4	1.7	6.0
2013	Lexus	IS 300h	Large Family	yes	5	n/a	29	16.9	6.0	6.0
2013	Maserati	Ghibli	Executive	no	5	n/a	27	14.8	6.0	6.0
2013	Mazda	3	Small Family	no	5	n/a	24	17.1	0.5	6.0
2013	Mazda	6	Large Family	no	5	n/a	24	17.8	0.0	6.0
2013	Mercedes	CITAN Kombi	Small MPV	no	4	n/a	20	14.0	0.5	5.9
2013	Mercedes	CLA-Class	Small Family	yes	5	n/a	27	17.0	4.0	6.0
2013	Mitsubishi	Space Star/Mirage	Super mini	no	4	n/a	26	16.5	3.8	6.0

		Vehicle Information			Euro NCAP Scores					
					Overall	Pedestrian Scores				
Yr	Make	Model	Ctgry	Pop Up?	Stars (/5)	Stars (/4)	Pts (/36)	Head (/24)	Pelvis (/6)	Leg (/6)
2013	Nissan	Evalia	Small MPV	no	3	n/a	24	14.4	5.0	4.8
2013	Nissan	Note	Super mini	no	4	n/a	21	15.0	0.0	6.0
2013	Opel/Vauxhall	Adam	Super mini	no	4	n/a	24	13.6	4.0	6.0
2013	Peugeot	308	Small Family	no	5	n/a	23	12.2	5.2	6.0
2013	Peugeot	2008	Super mini	no	5	n/a	26	16.0	4.2	6.0
2013	Renault	CAPTUR	Super mini	no	5	n/a	22	13.4	2.7	6.0
2013	Renault	ZOE	Super mini	no	5	n/a	24	14.2	3.9	6.0
2013	Skoda	Octavia	5 door hatch	no*	5	n/a	24	16.5	1.6	6.0
2013	Suzuki	SX4	Small Family	no	5	n/a	26	20.2	0.0	6.0
2013	Toyota	Auris	Small Family	no	5	n/a	25	16.8	2.0	6.0
2013	Toyota	RAV4	Small Off-Road 4x4	no	5	n/a	24	18.0	0.0	6.0
2013	VW	T5	Business and family van	no	4	n/a	10	9.8	0.0	0.0
2014	Audi	A3 Saloon	Small Family	yes	5	n/a	24	18.0	0.1	6.0
2014	BMW	2 Series Active Tourer	Small Family	yes	5	n/a	22	14.9	2.0	4.9
2014	Citroen	Berlingo	Small MPV	no	3	n/a	23	13.3	3.5	6.0
2014	Citroen	C4 Cactus	Small Family	no	4	n/a	29	17.1	6.0	6.0
2014	Dacia	Logan MCV	Small MPV	no	3	n/a	20	14.8	0.0	5.2
2014	Ford	Mondeo	Large Family	no	5	n/a	24	17.9	0.0	6.0
2014	Ford	Tourneo Courier	Super mini	no	4	n/a	27	16.3	4.6	6.0
2014	Hyundai	i10	Super mini	no	4	n/a	26	16.0	3.7	6.0
2014	Kia	Sorento	Large Off-Road 4x4	yes	5	n/a	24	18.3	0.0	5.9
2014	Kia	Soul	Small MPV	no	4	n/a	21	15.3	0.0	6.0
2014	Kia	Soul EV	Small MPV	no	4	n/a	21	15.3	0.0	6.0
2014	Land Rover	Discovery Sport	Small Off-Road 4x4	yes	5	n/a	25	19.2	0.0	5.9
2014	Lexus	NX	Small Off-Road 4x4	no	5	n/a	25	18.8	0.1	6.0
2014	Mercedes	C-Class	Large Family	yes	5	n/a	28	21.0	0.8	5.9
2014	Mercedes	GLA-class	Small Off-Road 4x4	yes	5	n/a	24	18.4	0.0	6.0
2014	MG Motor	MG 3	Super mini	no	3	n/a	21	16.4	0.0	5.1
2014	Mini	Cooper (F56)	Super mini	yes	4	n/a	24	18.1	0.0	6.0
2014	Nissan	Pulsar	Small Family	no	5	n/a	27	15.8	5.5	6.0
2014	Nissan	Qashqai	Small Family	no	5	n/a	25	15.8	3.1	6.0
2014	Nissan	X Trail	Small Off-Road 4x4	no	5	n/a	27	15.4	5.8	6.0
2014	Opel/Vauxhall	Corsa	Super mini	no	4	n/a	26	14.3	5.3	6.0
2014	Porsche	Macan	Small Off-Road 4x4	no	5	n/a	22	15.6	0.0	6.0
2014	Renault	Megane Hatch	Small Family	no	4	n/a	22	14.2	1.6	6.0
2014	Renault	Twingo	Super mini	no	4	n/a	25	15.3	3.2	6.0
2014	Skoda	Fabia	Super mini	no	5	n/a	25	14.6	4.4	6.0
2014	Smart	forfour	Super mini	no	4	n/a	24	15.2	2.4	6.0
2014	Smart	fortwo	Super mini	no	4	n/a	20	13.3	1.2	6.0
2014	Subaru	Outback	Large Family	no	5	n/a	25	18.9	0.4	6.0
2014	Tesla	Model S	Executive	yes	5	n/a	24	13.9	4.1	5.8

Yr	Make	Model	Ctgry	Pop Up?	Stars (/5)	Stars (/4)	Pts (/36)	Head (/24)	Pelvis (/6)	Leg (/6)
					Overall	**Pedestrian Scores**				
2014	Toyota	Aygo	Super mini	no	4	n/a	23	16.3	0.2	6.0
2014	VW	Golf Sportsvan	Small MPV	no	5	n/a	22	16.4	0.0	6.0
2014	VW	Passat	Large Family	no	5	n/a	24	15.3	2.6	6.0
2007	Jaguar	XK		yes						
2009	Nissan	GT-R		yes						
2009	Porsche	Panamera		yes						
2011	Peugeot	RCZ		yes						
2012	BMW	6-Series Coupe		yes						

Yr	Make	Model	Ctgry	Pop Up?	Stars (/5)	Stars (/4)	Pts (/36)	Head (/24)	Pelvis (/6)	Leg (/6)
					Overall	**Pedestrian Scores**				
2013	Cadillac	ATS		yes						
2013	Cadillac	CTS		yes						
2013	Fiat	Punto		yes						
2013	Mazda	MX-5 Roadster (Miata)		yes						
2014	Aston Martin	DB9		yes						
2014	Aston Martin	Vanquish		yes						
2014	Jaguar	F-type		yes						

*The Skoda Octavia was originally to be sold with a pop-up hood as standard equipment and was tested by Euro NCAP as such. Later, Skoda announced the pop-up hood would no longer be included as standard, so Euro NCAP retested the vehicle without the pop-up hood. The scores on the report for this vehicle are for the test without the pop-up hood deployment [10].

APPENDIX B

Table 3. Vehicles With Pop-up Hoods and Euro NCAP Scores

Year	Make	Model
2006	Citroen	C6
2007	Honda	Legend
2010	BMW	5-series
2010	Mercedes	E-class
2011	Fiat	Freemont
2011	Lancia	Thema
2011	Lancia	Voyager
2011	Mercedes	C-Class Coupe
2012	Hyundai	Santa Fe
2012	Jaguar	XF
2012	Mercedes	M-Class
2012	Volvo	V40
2013	Infiniti	Q50
2013	Lexus	IS 300h
2013	Mercedes	A-Class
2013	Mercedes	CLA-Class
2014	Audi	A3 Saloon
2014	BMW	2 Series Active Tourer
2014	Kia	Sorento
2014	Land Rover	Discovery Sport
2014	Mercedes	C-Class
2014	Mercedes	GLA-Class
2014	Mini	Cooper (F56)
2014	Tesla	Model S

CYCLIST-CAR ACCIDENTS – THEIR CONSEQUENCES FOR CYCLISTS AND TYPICAL ACCIDENT SCENARIOS

Matthias Kuehn
Thomas Hummel
Antje Lang
German Insurers Accident Research
Germany

ABSTRACT

The structure of the official German statistics does not permit in-depth analyses to be carried out, so the UDV built up a set of representative case material in order to examine accidents between cars and cyclists in more detail and derive effective measures to improve the safety of cyclists. This material was formed from accidents with personal injury from the years 2002 to 2010 that were covered by motor third-party insurance and involved injury and damage costs of 15,000 euros or more. The cyclist accident material consists of a total of 407 accidents between cars and cyclists. This paper describes how and under what circumstances cyclist-car accidents occur, the maximum levels of injury severity sustained by the cyclists and the impact constellations that occur particularly frequently. In 84% of the cases, the impact between the bicycle and the car occurred at the front part of the vehicle (the front of the car plus the left- and right-hand front wings). In 42% of these cases, the bicycle was coming from the right (as seen by the driver), and in 34% of the cases from the left. Moreover, the analysis of the cyclist-car accidents revealed that the average speed of the cars was a relatively low 24 km/h. The speed of the cyclists often could not be ascertained from the available documents. However, it is known from the UDV's measurements of the speeds of 20,000 cyclists that they travel at an average speed of 18.6 km/h. Three typical scenarios were obtained from the accident material that together account for 42% of all cyclist-car accidents. These three scenarios are "car traveling straight ahead, cyclist coming from the right" (15%), "car turning right, cyclist coming from the right" (15%) and "car traveling straight ahead, cyclist coming from the left" (12%). Another key finding is that the collisions in these three scenarios often (in 47% to 85% of the cases) took place at the entries to or exits from properties or parking lots and at junctions. The findings described make it possible both to work out the requirements that have to be met by future systems for preventing cyclist-car accidents and to design effective test procedures.

INTRODUCTION

In the last 10 years, the number of people killed on the roads has fallen significantly. That is true not just in Germany but also in the European Union as a whole [1]. However, the picture for cyclists is not quite as positive. In Germany in 2013, for example, 43% fewer road users were killed than in 2004. Fatalities among car occupants fell by as much as 51%, whereas those among cyclists fell by only 25%. The improvement in cyclists' safety thus has not kept pace with the general trend. However, future technical systems in cars (such as emergency brake assist systems with cyclist detection) will have a positive effect on the accident statistics of cyclists. Before such systems can be designed, however, it is essential to have detailed information on how cyclist-car accidents happen and the course they take. The purpose of this paper is to add to this information.

DATABASE OF THE UDV

The UDV (German Insurers Accident Research) is a department of the GDV (the Gesamtverband der Deutschen Versicherungswirtschaft e.V. or German Insurance Association). It has access to all of the third-party vehicle insurance claims reported to the GDV. In 2013, for example, there were 3.9 million of these claims [2]. For the purposes of accident research, the UDV has created a database (the UDB) that contains a representative cross-section of the data (from the years 2002 to 2010) in this large pool. The data collected is conditioned for interdisciplinary purposes to facilitate research in the fields of vehicle safety, transportation infrastructure and behavior on the roads. The UDB is based on the contents of insurers' claim files. Around 700 to 1,000 new cases are added to the UDB each year. Only accidents with personal injury and a total claim value of 15,000 euros or more are added to the UDB.

DESCRIPTION OF THE CYCLIST ACCIDENT MATERIAL

Areas of impact on the car

In 356 of the total of 407 cyclist-car accidents it was possible to ascertain what part of the car was involved in the impact with the bicycle. The distribution of the areas of impact was as follows:

- Front of the car: 218 cases (61%)
- Left-hand side of the car: 55 cases (15%)
- Right-hand side of the car: 69 cases (20%)
- Rear of the car: 14 cases (4%)

Areas of impact on the car and the cyclist's maximum level of injury severity

If we group together all of the impacts between the bicycle and the front part of the car (the front of the car plus the left- and right-hand front wings), we get the following picture:

- Front part of the car: 299 cases (84%)
- Passenger compartment plus left-hand rear wing: 23 cases (6%)
- Passenger compartment plus right-hand rear wing: 20 cases (6%)
- Rear: 14 cases (4%)

Figure 1 indicates how seriously the cyclists were injured in collisions involving each of these areas of impact. Figure 1 clearly shows that measures to improve the safety of cyclists need to be focused primarily on the front of the car. This is true in relation to both the frequency of the impacts and cyclists' maximum level of injury severity [3].

100% (n=356)

6% (n=23)
4% (n=14)
84% (n=299)
6% (n=20)

MAIS	No.	%
0	0	0
1	7	30.4
2	12	52.2
3	4	17.4
4	0	0
5	0	0
6	0	0
Total	23	100%
Not clear	0	
9*	0	

MAIS	No.	%
0	0	0
1	4	28.6
2	5	35.7
3	3	21.4
4	2	14.3
5	0	0
6	0	0
Total	14	100%
Not clear	0	
9*	0	

MAIS	No.	%
0	0	0
1	2	11.1
2	13	72.2
3	2	11.1
4	0	0
5	1	5.6
6	0	0
Total	18	100%
Not clear	0	
9*	2	

MAIS	No.	%
0	0	0
1	50	16.8
2	159	53.5
3	63	21.2
4	19	6.4
5	4	1.4
6	2	0.7
Total	297	100%
Not clear	2	
9*	0	

9* = fatally injured, MAIS unknown
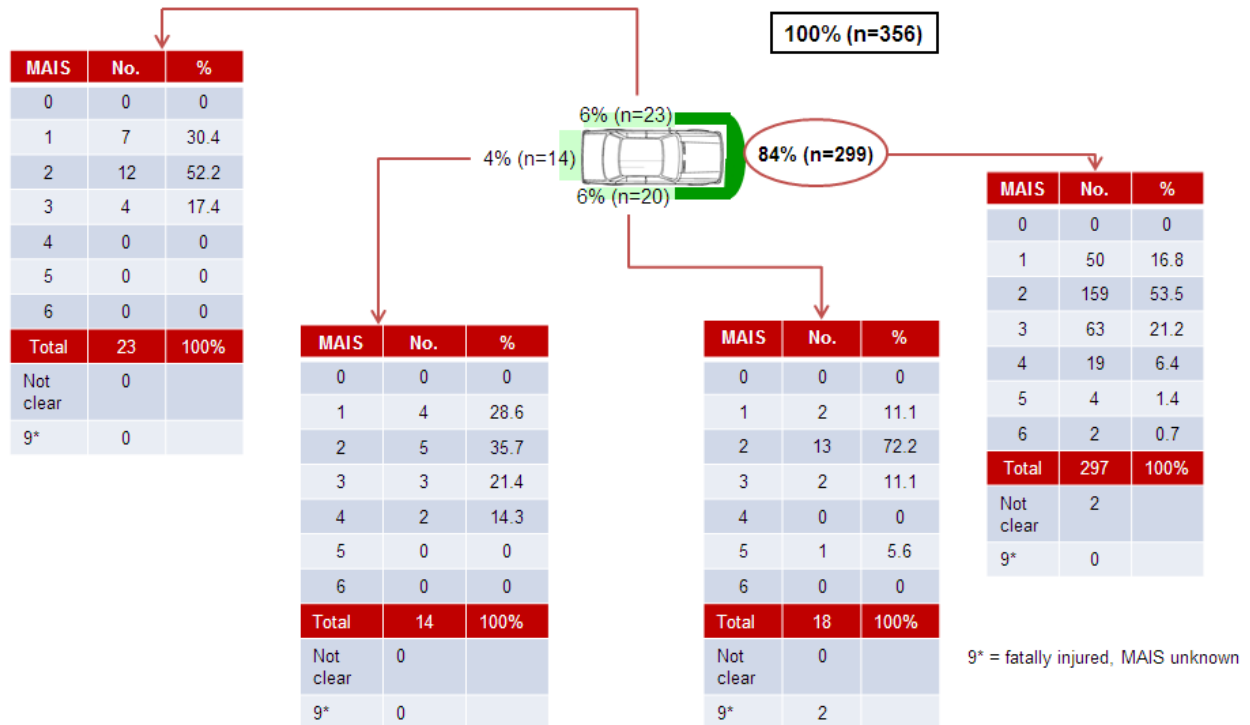
Figure 1.   Maximum levels of injury severity (MAIS) in the cyclists by area of impact on the car

TYPICAL ACCIDENT SCENARIOS IN CYCLIST-CAR ACCIDENTS

Figure 1 illustrates that most collisions between bicycles and cars involve impact with the front part of the car (n = 299 cases). In 23 of these cases the car was parked. Consequently, only 276 cases are included in our consideration of typical accident constellations. Thus, both parties involved were in motion at the time of the accident in these remaining cases.

Figure 2 shows four different impact constellations, to which all the observations that follow apply:

- **A**: The car is traveling straight ahead or turning left or right, and the bicycle is coming from the right.
- **B**: The car is traveling straight ahead or turning left or right, and the bicycle is coming from the left.
- **C**: The car is traveling straight ahead or turning left or right, and the bicycle is approaching head-on.
- **D**: The car is traveling straight ahead or turning left or right, and the bicycle is moving in the same direction.

Constellation A is the most common one (with 116 cases), followed by constellation B (94 cases) and then constellations C (35 cases) and D (31 cases).

The box in the upper-left corner of Figure 2 shows the subset of the cyclist-car accident material to which the information in the main part of Figure 2 applies. The same principle applies to the boxes in Figures 3 to 5.
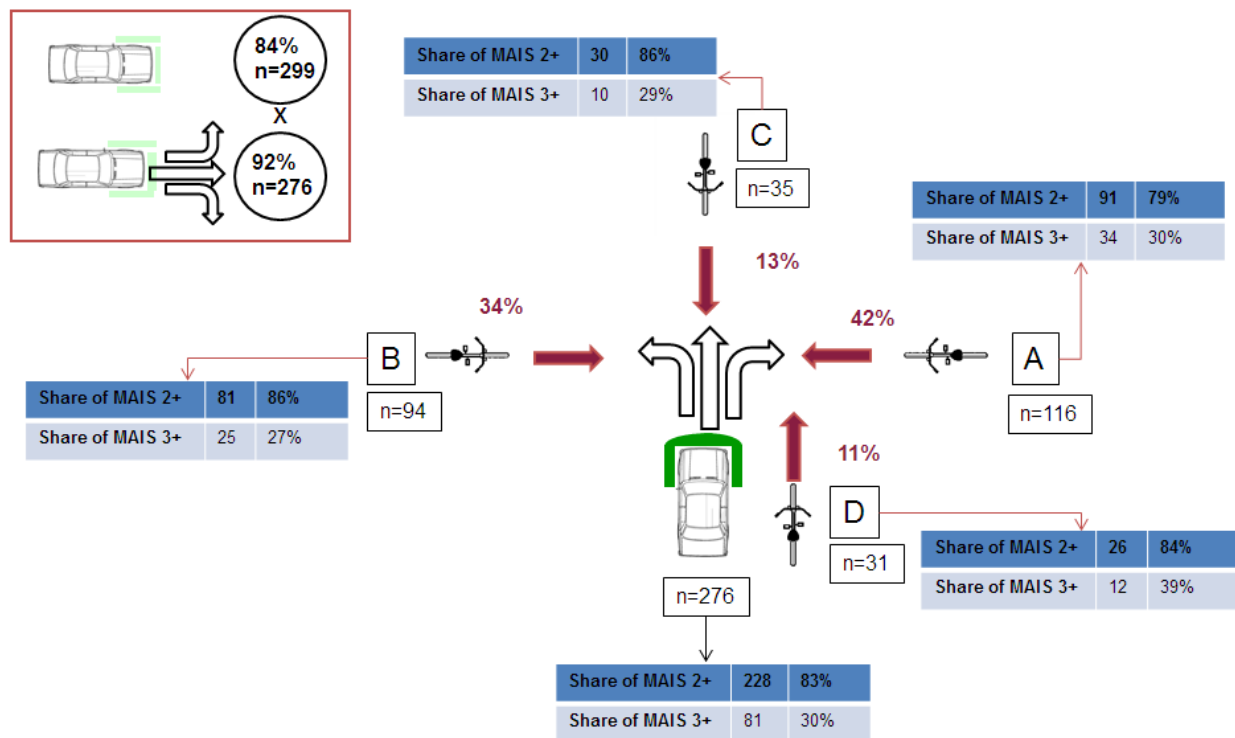
Figure 2. Frequency of different impact constellations at the front part of the car with the corresponding distributions of MAIS 2+ and MAIS 3+ in the cyclists

Speeds of the cars and bicycles and severity of the cyclists' injuries

Figure 3 shows the average speeds of the cars for these four constellations. The average speeds of the cars in constellations A, B and C were very similar (19 km/h to 23 km/h), while for constellation D the average speed was significantly higher (51 km/h).

The different speeds of the cars are also reflected in the maximum level of severity of the injuries of the cyclists involved in the accidents: The percentage of serious to fatal injuries (MAIS 3+) in constellation D was

thus significantly higher (at 39%) than in constellation A (30%), constellation B (27%) or constellation C (29%). As shown in Figure 2, however, constellation D is the least common of the accident constellations investigated here (at 11%).

The insurers' claim files often contain no information, or only very vague information, on the speeds of the cyclists immediately before the collision with the car, which is why these cannot be specified here. However, in an observational study on the speeds of almost 20,000 cyclists [4], the UDV found that their average speed on a clear run was 18.6 km/h. Moreover, the speed measurements indicated that cyclists on mountain bikes (at 20.5 km/h) and road or racing bikes (25.5 km/h) were significantly faster than average, and cyclists on "Dutch" bicycles (17.0 km/h) were significantly slower. The average speed of cyclists on city bikes (18.3 km/h) was about the same as the average speed for all cyclists, and the same can be said for riders of pedelecs 25 (electric-assist bicycles), whose average speed was 18.5 km/h.
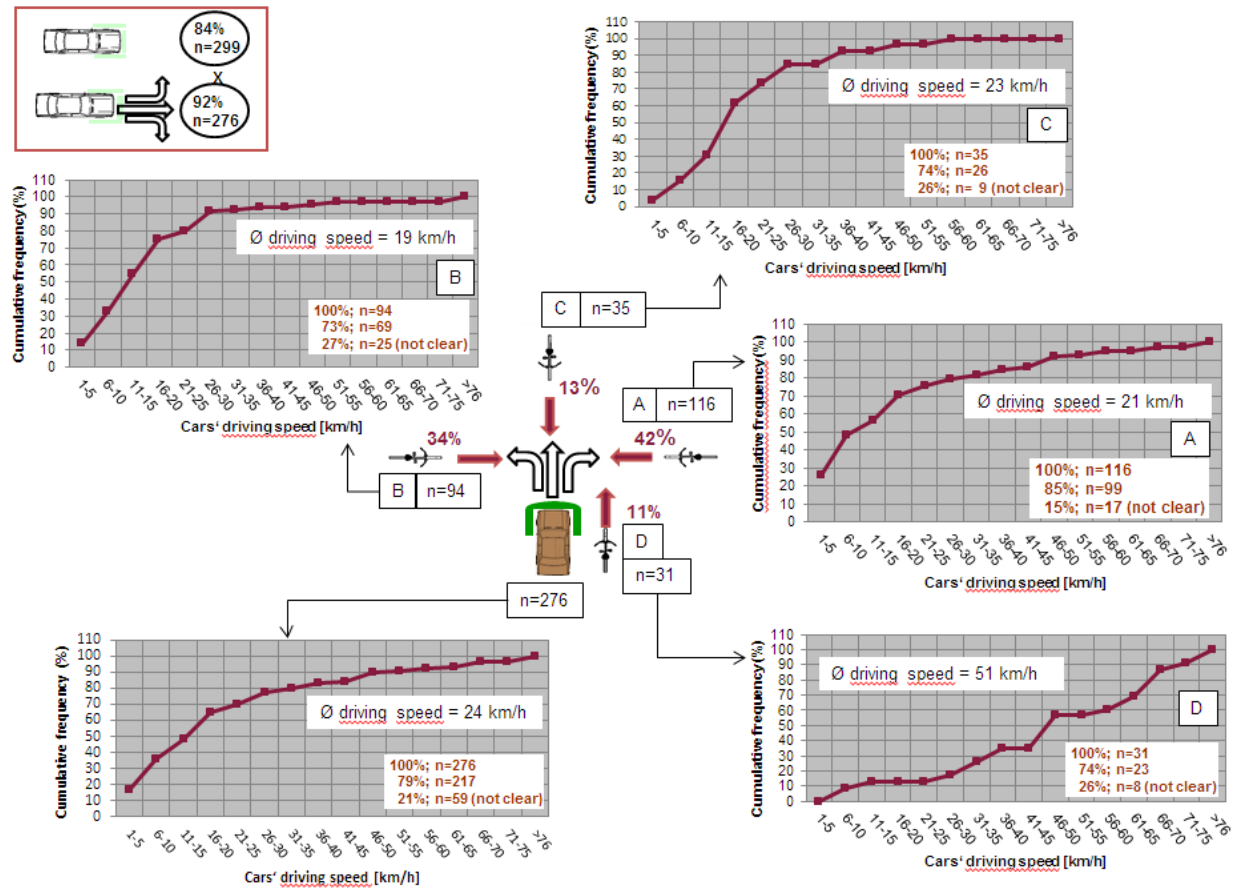
Figure 3.   Average speeds of the cars by impact constellation

In-depth analysis of the two most common accident constellations

It can be seen from Figures 2 and 3 that accident constellations A (116 cases) and B (94 cases) are clearly more common than the other constellations in this accident material. These two accident constellations will be described in depth below.

   Accident constellation A, bicycle coming from the right: Accident constellation A can be subdivided into three separate scenarios (see **Figure 4**):

- A1: The car is turning left, and the bicycle is coming from the right.
- A2: The car is traveling straight ahead, and the bicycle is coming from the right.
- A3: The car is turning right, and the bicycle is coming from the right.

Accident scenarios A2 and A3 occur with almost exactly the same frequency, accounting for 46% and 45% of the cases. Scenario A1, on the other hand, occurs much more rarely (9%). The lower part of Figure 4 sets out concrete situations for each of the three accident scenarios (A1, A2 and A3) that show the circumstances of the cyclist-car collision in more detail.
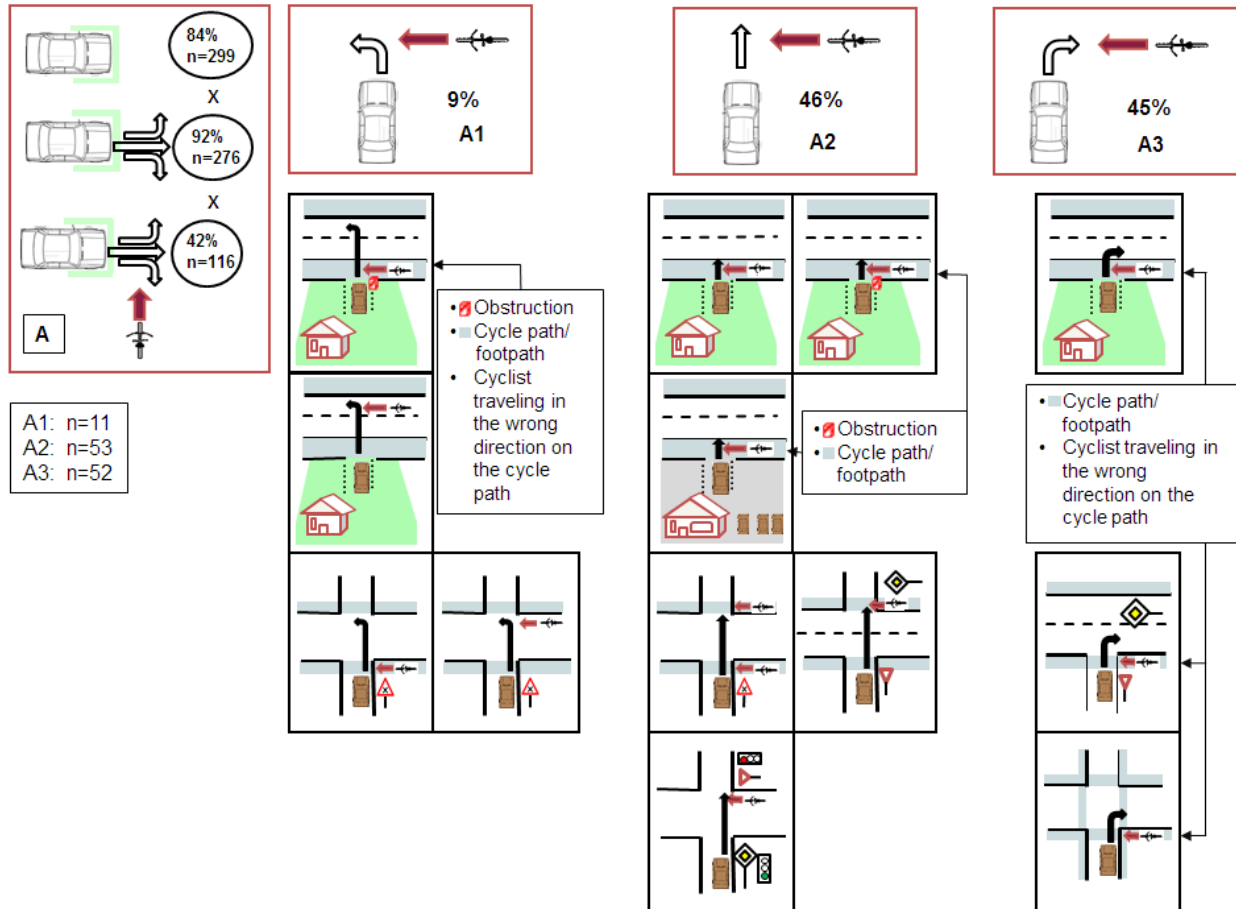
Figure 4.   Distribution of accident scenarios A1, A2 and A3 and illustration of typical cases

The following are typical accident scenarios for A1:

- The car is coming out of an exit and wants to turn left into the road. A cyclist is approaching from the right on the footpath or cycle path and is partially or totally concealed by an obstruction (such as a hedge or wall).
- The car is coming out of an exit and wants to turn left into the road. A cyclist is approaching from the right on the road.
- The car is turning left at an intersection and collides with a cyclist coming from the right.

The following are typical accident scenarios for A2:

- The car is coming out of an exit straight onto the road. A cyclist is approaching from the right on the footpath or cycle path and in some cases may be concealed by an obstruction (such as a hedge or wall).
- The car is coming out of a parking lot (of a supermarket, for example) straight onto the road. A cyclist is approaching from the right on the footpath or cycle path.
- The car is traveling straight ahead across an intersection and collides with a cyclist coming from the right on the footpath, cycle path or road.

The following are typical accident scenarios for A3:

- The car is coming out of an exit and wants to turn right into the road. A cyclist is approaching from the right on the footpath or cycle path.
- The car is turning right into a road where the traffic has priority and collides with a cyclist coming from the right on the footpath or cycle path.
- The car is turning right at an intersection and collides with a cyclist coming from the right on the footpath or cycle path.

Accident constellation B, bicycle coming from the left: Like accident constellation A, accident constellation B can also be subdivided into three separate scenarios (see **Figure 5**):

- B1: The car is turning left, and the bicycle is coming from the left.
- B2: The car is traveling straight ahead, and the bicycle is coming from the left.
- B3: The car is turning right, and the bicycle is coming from the left.
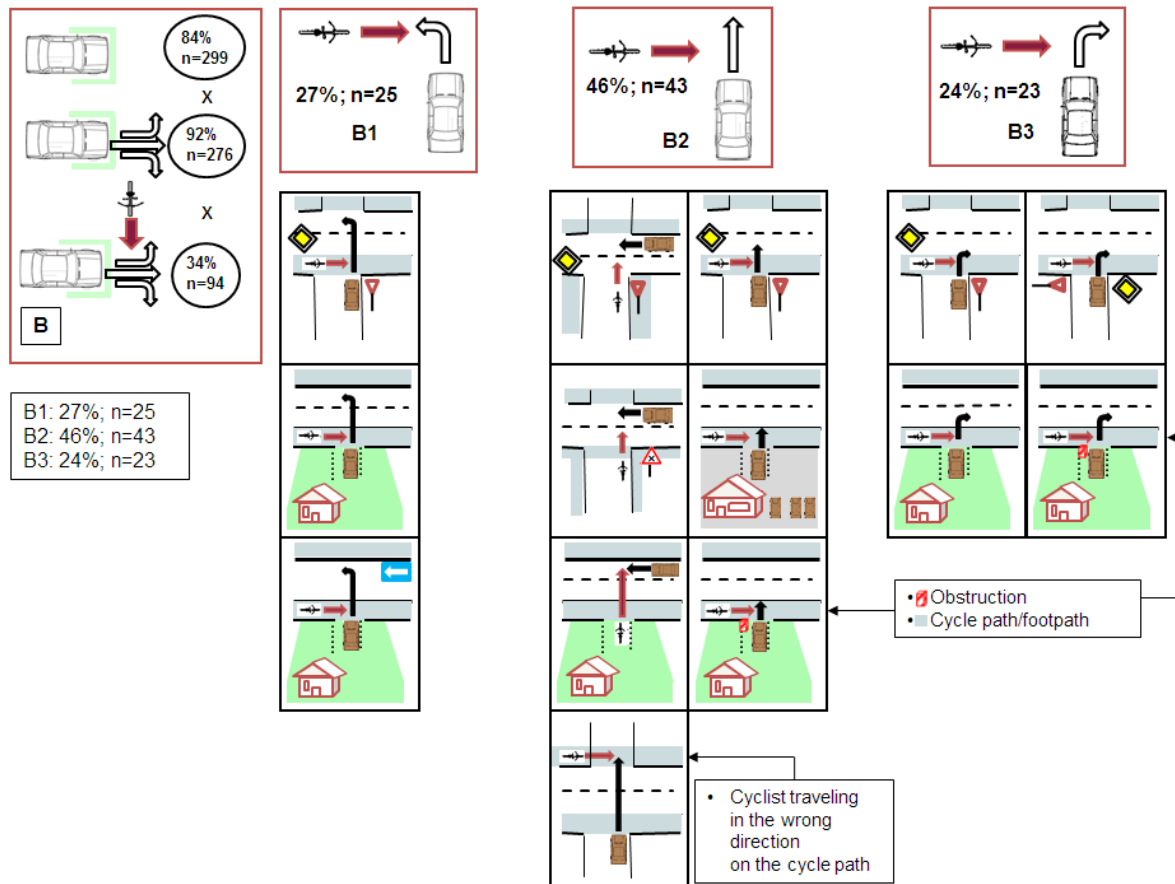
Figure 5. Distribution of accident scenarios B1, B2 and B3 and illustration of typical cases

B2 is the most common accident scenario (accounting for 46% of the cases), while scenarios B1 and B3 occur with a similar frequency (27% and 24%). The lower part of Figure 5 sets out concrete situations that show the circumstances of the cyclist-car collision in more detail.

The following are typical accident scenarios for B1:

- The car, which does not have priority, is turning left at an intersection and collides with a cyclist coming from the left on the footpath or cycle path.
- The car is coming out of an exit and wants to turn left into the road or one-way street. A cyclist is approaching from the left on the footpath or cycle path.

The following are typical accident scenarios for B2:

- The car is traveling straight ahead across an intersection and collides with a cyclist coming from the left on the footpath, cycle path or road.
- The car is coming out of an exit or a parking lot onto the road. A cyclist is approaching from the left on the footpath or cycle path and in some cases may be concealed by an obstruction (such as a hedge or wall).
- The car is traveling straight ahead on a road and collides with a cyclist who comes out of an exit on the left.
- The car is traveling straight ahead across an intersection and collides with a cyclist coming from the left on the other side of the road.

The following are typical accident scenarios for B3:

- The car is turning right at an intersection and collides with a cyclist coming from the left on the footpath or cycle path.
- The car is coming out of an exit and wants to turn right into the road. A cyclist is approaching from the left on the footpath or cycle path and in some cases is concealed by an obstruction (such as a hedge or wall).

Summary assessment of the three most common accident scenarios   In addition to the findings described in this paper, a range of further analyses were also carried out and assigned to the various accident scenarios. Moreover, extrapolation factors were used to extrapolate the cyclist-car accident material described here to all claims reported to the GDV. When all these findings are combined, the picture shown in **Figure 6** is obtained: Scenarios A2 and A3 are the most common, followed by B2. These three scenarios alone account for 42% (15% + 15% + 12%) of all cyclist-car accidents.
Two out of three A2 accidents take place at entrances or exits, the average speed of the car is 30 km/h, and the driver does not brake in 55% of all cases. In scenario A3, 85% of the collisions between cyclists and cars take place at entrances or exits, and the driver does not brake in three of every four cases. This suggests that the driver either does not see the cyclist or does not have enough time to brake. The average speed of the car in scenario A3 is 11 km/h. The percentage of entrances and exits involved in scenario B2 is also very high (47%). The average speed of the cars in scenario B2 is 27 km/h, and the driver does not brake in 42% of the collisions. Further characteristics of scenarios A2, A3 and B2, such as light conditions, the condition of the road and the injury severity and age distribution of the cyclists, are also shown in Figure 6.

CONCLUSIONS

In the past, researchers focused primarily on pedestrians rather than other unprotected road users. However, cyclists are now becoming an increasingly important focus of research. In 84% of the cases in the UDV's cyclist-car accident material, the impact between the bicycle and the car occurred at the front part of the vehicle. The most common accident scenarios are "cyclist coming from the right" and "cyclist coming from the left". There are only a few cases in which the car is behind the bicycle and hits the back of it. In this impact constellation, however, serious to fatal injuries (MAIS 3+) occur more often than in other impact constellations. Accidents in which the cyclist is coming from the right or left

- Location: 62% at junctions and entrances/exits of properties or parking lots
- Movement type of cyclist = cycling
- Cars' average speed = 30 km/h
- Car braked before accident = no in 55% of cases

- Injury severity of cyclists = 70% serious
- Light conditions = 85% daylight
- Road surface conditions = 85% dry
- Age distribution of cyclists = 19% (13-19); 17% (41-47)

Scenario A2 :
*15% (±3.5%) of all cyclist-car accidents
*18% (±4.4%) of all cyclist-car accidents where the main point of impact is on the front part of the car

1. (A2)

- Location: 85% at junctions and entrances/exits of properties or parking lots
- Movement type of cyclist = cycling
- Cars' average speed = 11 km/h
- Car braked before accident = no in 75% of cases

- Injury severity of cyclists = 62% serious; 38% minor
- Light conditions = 88% daylight
- Road surface conditions = 81% dry
- Age distribution of cyclists = 21% (55-61); 17% (41-47); 13% (48-54); 13% (62-68)

Scenario A3 :
*15% (±3.5%) of all cyclist-car accidents
*17% (±4.3%) of all cyclist-car accidents where the main point of impact is on the front part of the car

2. (A3)

- Location: 47% at junctions and entrances/exits of properties or parking lots
- Movement type of cyclist = cycling
- Cars' average speed = 27 km/h
- Car braked before accident = no in 42% of cases

- Injury severity of cyclists = 74% serious
- Light conditions = 88% daylight
- Road surface conditions = 79% dry
- Age distribution of cyclists = 16% (62-68); 14% (6-12); 12% (41-47)

Scenario B2 :
*12% (±1.9%) of all cyclist-car accidents
*14% (±3.9%) of all cyclist-car accidents where the main point of impact is on the front part of the car

3. (B2)

*: Using case-dependent extrapolation factors based on stratification variables of the case material

Figure 6.   The three most common accident scenarios, their significance in relation to all cyclist accidents and characteristic features of these accident scenarios

very often occur at the entrances or exits of properties or parking lots and at junctions. It is essential to take this into account when developing advanced driver assistance systems designed to prevent collisions between cars and cyclists – but also when developing test procedures. Poor light or road conditions, on the other hand, are of only minor significance.

REFERENCES

[1] German Federal Statistical Office. 2014. Verkehrsunfälle 2013 [Traffic accidents 2013].
Fachserie 8, Reihe 7. Wiesbaden, July 2014. Article no. 2080700137004
[2] German Insurance Association (GDV). 2014. Statistical Yearbook of German Insurance – 2014.
Distributed by Verlag Versicherungswirtschaft GmbH, Karlsruhe, Germany. ISSN 0936-1960
[3] Association for the Advancement of Automotive Medicine. 1990. Abbreviated Injury Scale – 1990 Revision.
Des Plaines, IL
[4] Alrutz, D., Bohle, W., Maier, R., Enke, M., Pohle, M., Zimmermann, F., Ortlepp, J. and M. Schreiber. 2015. Einfluss von Radverkehrsaufkommen und Radverkehrsinfrastruktur auf das Unfallgeschehen [Influence of cycling traffic volume and cycling infrastructure on accident occurrence].
German Insurers Accident Research (UDV), Berlin

ANALYSIS OF CHILDREN STROLLERS AND PRAMS SAFETY IN URBAN BUSES

Luis Martínez, Antonio García, Manuel Espantaleón, Enrique Alcalá.
UPM. Universidad Politécnica de Madrid.
INSIA. Instituto Universitario de Investigación del Automóvil.
SPAIN.

Juan Dols.
UPV. Universidad Politécnica de Valencia.
IDF. Instituto de Diseño y Fabricación.
SPAIN.

Paper Number 15-0175.

ABSTRACT

The wide incorporation of low floor buses in our cities encourages that child younger than three years, seated on their stroller could use the buses. Currently, the UNECE Regulation No 107 at its revision 5 has included general provisions for the accessibility and basic safety for this type of users. An applied research has been performed to analyze the level of protection offered for the stroller restraint systems included in R107, by performing dynamic tests with instrumented dummies.

More than 20 dynamic sled tests were performed to assess the child safety in urban buses. Two types of configurations have been tested: a vehicle specific CRS for urban buses and the own stroller with different restraint systems.

The specific vehicle built-in CRS tested is a rearward facing group 0/I that is currently in use in the city of Madrid (Spain) by the public urban buses. This CRS was tested in frontal and rear impact with the acceleration pulse defined in the UNECE regulation No 80.

On the other hand, to make suggestions for using the stroller in urban buses, a very low severity crash pulse (up to 2 g peak acceleration and $\Delta V = 20$ km/h) was defined and used in this study. Four stroller models with three types of restraint devices (safety belt, PRM wheelchair backrest and a folding backrest device) were tested with this pulse. The strollers were selected in order to reduce biasing of the results.

Several dummies (P3, Q3 and Q1) were used to evaluate the injuries and the kinematics. Furthermore, different sources of IRAV have been applied for the Q dummies (R94 and FMVSS 208 scaled by applying Mertz 2003 techniques), an extended range of injury criteria is obtained and an in depth analysis of the protection offered by the different restraints systems used is performed.

INTRODUCTION

The use of public transport is a need and a right for all citizens. However, there are still some groups who experience difficulty travelling on buses – such as users who travel with pushchairs or strollers. These users also face safety problems as it is often necessary for children to be taken out of their strollers and held in the arms of their accompanying person. From the standpoint of operating companies, the use of buses by this group represents a design problem that has not yet been satisfactorily and effectively resolved at the moment of perform this research study.

One of the studies published regarding the use of buses by passenger travelling with pushchair [1], analyze the response of a survey applied to 44 Spanish transport companies (69% of the total). The results show that 32% of bus companies use local legislation to regulate the access to buses by pushchair users, 27% applies internal regulations, 11% respond to regional legislation, and up to 30% of companies do not apply any regulations. Of all the companies surveyed, 45% allow pushchairs to be open inside the bus, while 32% prohibit pushchairs from being open. Most companies (41%) have not defined the number of pushchairs allowed on a bus, while 34% allow access for up to two pushchairs, and 25% allow only a single pushchair. Note that priority is given to wheelchair users over pushchairs by 23% of these companies, while the remainder (77%) does not specify priority. Access for pushchairs is usually (preferably) through the front door, although central door entry is allowed (even without using the ramp), while exiting is normally made through the central or rear doors.

Pushchairs are usually positioned parallel to the longitudinal axis of the vehicle and facing backwards. Some 25% of bus companies require that the pushchair brake is applied to the wheels during transport (as the pushchair is open), while no indication is provided by the remaining 75%. Finally, only 18% of the companies surveyed explicitly deny access to tandem (twin) pushchairs.

Recently, at June 2014, the UNECE regulations (United Nations Economic Commission for Europe) in its regulation 107R05 (current version of the regulation 107 is R06 from March 2015), has modified the accessibility requirements of Class I vehicles (urban buses), extending the previous requirement of at least one wheelchair user to also at least one pram or unfolded pushchair at same time.

The work reported in this paper is focus on the child safety (children under 3 years old) in urban buses. Children under 3 usually used Child Restraint System – CRS (approved under regulation 44 or in future the i-Size category according regulation 129). Nevertheless in urban buses this type of CRS could not be used (technically because there is no safety belt or ISOFIX installed in urban buses seats; and it is not practical for the user that must wear their own CRS for buses). There are clearly two tendencies: on one hand to use a specific built-in child restraint system (with national or regional approval) and on the other hand to establish prescriptions for use the strollers or prams inside the urban buses in order to obtain a certain level of safety (the same direction than regulation 107), however R107 does not require any dynamic evaluation of the restraint system included into vehicles.

To bring some information to the previous mentioned options, dynamic sled tests have been performed in order to assess the safety behaviour in urban buses with different safety devices, and oriented to achieve the following objectives:

- Know the accelerations of a specific built-in child restraint system for urban buses tested with the acceleration profile as defined in the regulation 80 (for coaches). The safety assessment is evaluated objectively in order to obtain the accelerations levels as a maximum in order that this level could be useful to establish a reference for the child safety evaluation in urban buses.
- Evaluation of the child safety behaviour in urban buses using strollers or prams. In this case, it has been developed a low severity pulse in order to assess this behaviour.
- Analyze the safety of different systems (safety belt, PRM backrest or a prototype [2] of folding backrest), using different types of strollers. It is not the objective of the study to evaluate if one stroller is better or worse than others.

METHODS

Two severity pulses are used in this study. For the strollers, several frontal low severity impact sled tests were performed in order to assess the safety performance of different strollers restrained with different systems to the urban bus (a PRM backrest, a folding backrest and a 2P stroller safety belt). Furthermore, for the specific built-in CRS, three sled tests (2 frontals and 1 rear) were performed with the acceleration profile defined in regulation 80R03, more severe than previous ones. The next figure shows the differences of the two severity pulses carried out (these pulses are obtained from real sled test deceleration). The low severity pulses represents conditions more severe than the emergency manoeuvres (limited by the friction coefficient between the tire and the road), but there is not intended to replicate a bus crash, therefore the acceleration should be greater than 1 g. An increase of 50% was imposed (i.e. an acceleration of at least 1.5 g). The duration of the dynamic impact was limited by the capabilities of the sled facility used, with a maximum stroke of 1200 mm. Finally it was established a $\Delta V = 20$ km/h (compatible with the total braking distance available).
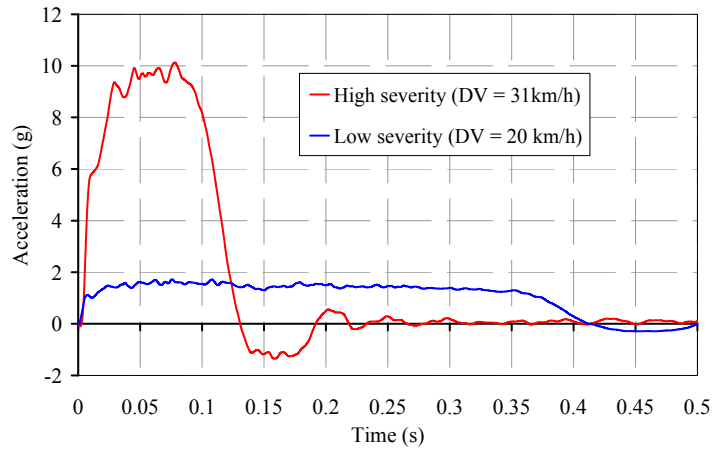
Figure 1. Sled acceleration for the two severities.

Four types of occupants were used to perform the dynamic sled tests:
- Ballasted mannequin of 9MO: with a total mass of 9 kg. Used to assess the kinematics response.
- Q1 dummy. The measurement capabilities used in tests are: head acceleration (X, Y, Z), upper neck forces (X, Y, Z), upper neck moments (X, Y, Z), chest acceleration (X, Y, Z), chest deflection and pelvis acceleration (X, Y, Z).
- P3 dummy with head acceleration (X, Y, Z) and chest acceleration (X, Y, Z).
- Q3 dummy with chest acceleration (X, Y, Z).

Furthermore to the dummy measuring capabilities, two or three high speed cameras (1000 fps) were used to evaluate the impact kinematics of the dummies and the strollers. The next figure shows a sketch of the sled test with the views of the two high speed cameras (the third camera is a zenithal view). As it can be seen, a representative urban bus floor was installed on the sled. This floor includes the PRM backrest, the folding backrest and the 2P stroller safety belt.
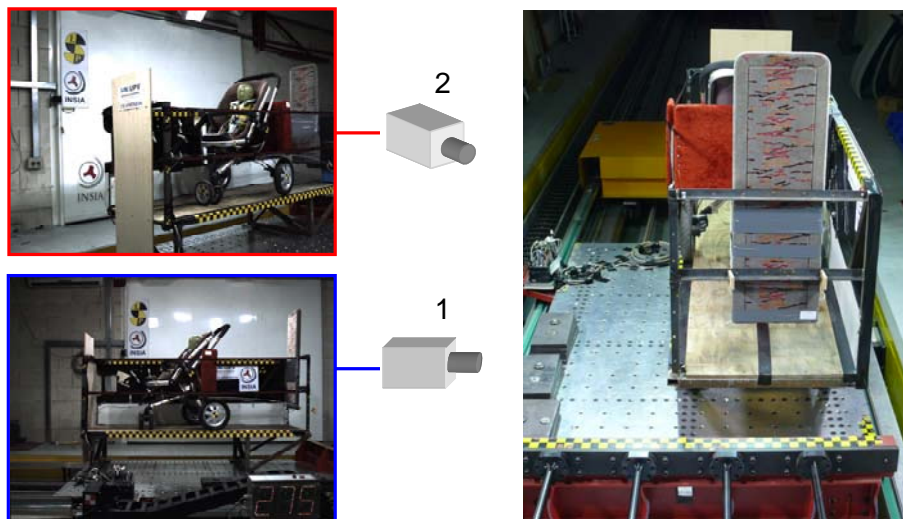
Figure 2. High speed cameras and test ring set up.

The dynamic sled tests were performed in two phases:
- **Phase1**: High severity dynamic tests (according regulation 80R03) with a specific built-in rearward facing child restraint system. The objective of this phase is to obtain the safety performance of a specific child restraint system built in an urban bus.

- **Phase2**: Low severity dynamic tests (ΔV = 20 km/h; 1.5 g) with strollers and baby carriage with different safety devices:
  - o **Phase2A**. Larger number of dynamic tests with: folding backrest, PRM backrest and 2P safety belt as safety devices used to restraint the strollers. Four types of strollers have been tested in this phase. The objective of this phase is to analyze the general behaviour of the strollers and the safety devices.
  - o **Phase2B**. Finally, in this latter phase a Q1 dummy (with larger measurement capabilities) was used in order to study in detail the behaviour of the strollers with the safety devices. Two types of strollers and two types of safety devices were studied.

Samples

Different samples have been tested during the dynamic tests (see Figure 3). For the dynamic tests, the strollers have been used in the configuration of the bigger child (i.e. the worst situation for the restraint and stability of the stroller is produced with the heavier child). The strollers have been selected with different configurations or features but all of them are current market representatives. The main characteristics of them are summarized:

- For the high severity pulse, a **specific built-in** (in an urban bus – **M3 vehicle category, Class I**) child restraint system was used. This CRS is rearward facing oriented and incorporates an integral 5p safety harness. This system is based on the design of the traditional CRS according regulation 44R04 for group I rearward facing oriented. The buckle and the straps fulfil the requirements of the regulation 44R04.
- **Stokke Xplory**. Incorporates a telescopic rod for height adjustment. The main characteristic of this stroller is the height of the centre of gravity that is greater than the other models. The child is restrained to the stroller using a 5p harness.
- **Quinny Buzz**. This stroller has been selected because it has 3 wheels (the frontal is twin wheel). This produced a potential instability of the stroller. The child is restrained to the stroller using a 5p harness.
- **Bebeconfort Streety**. This stroller has a large wheelbase compare with the rest of the dimensions. It was tested in a lateral configuration in order to produce more instability. The child is restrained to the stroller using a 5p harness.
- **Maclaren Quest**. It is the "traditional stroller", with four wheels (same track width front and rear). The child is restrained to the stroller using a 5p harness.

| Built-in (M3-Class I) | Stokke Xplory | Quinny Buzz | Bebeconfort Streety | Maclaren Quest |

Figure 3. Built-in (M3 vehicle) CRS and strollers used (figures are not to same scale).

Injury Assessment Reference Values (IARV) – extended range

The anthropomorphic tests devices (ATD) or dummies are very useful and a good measurement tool as a substitute for the human body under crashes. Thanks to their measurements capabilities is possible to establish a baseline or boundaries to determine whether there is a likelihood of injury.

The injury criteria are primarily developed for adult size dummies (specifically for the Hybrid III 50th male). The reference values for child dummies should be scaled form the data of average size adult occupant. The

injury criteria used in this paper (for the Q1 dummy) are obtained from information contained in the regulation 94R02 and FMVSS 208, scaled with the information provided by Mertz et al [3] (where it is described the scaling process for developing the IARV for different sizes and ages). Current IARV used for Q1 at R129 were not used because the pulse severity used at present study is much lower than in R129 (20 kph versus 50 or 30 kph), also and a extended set of IARV with respect to R129 is used and to avoid any collateral effects for use different sources of the IARV, a common procedure were used to obtain the set of injury criteria.

Dummy part	Parameter	Unit	Limit
Head	HIC_{15}		389.00
	HPC (HIC_{36})		555.71
	Acceleration	g	154.00
	3ms acceleartion	g	68.44
Upper neck	Shear force Fx	N	740.00
	Tension force +Fz	N	783.45
	Compression force -Fz	N	960.00
	Lateral moment Mx	Nm	21.00
	Flexion moment +My	Nm	27.00
	Extension moment -My	Nm	8.31
	Twist moment Mz	Nm	14.00
	Nij		1.00
	· FT	N	1610.00
	· FC	N	1470.00
	· MF	Nm	42.50
	· ME	Nm	18.60
	NIC		Corridor
Chest	Sternum deflection Dx	mm	24.00
	T4 acceleration	g	87.00

NIC Traction (12 MO)

NIC Shear (12 MO)

NOTE: All the values in the table are peak values, except the 3ms head acceleration.

Grey data are obtained based on the regulation 94R02 and scaled to Q1 dummy.

Figure 4. IARV obtained for a Q1 dummy.

RESULTS

This section summarized the results of the dynamic sled tests performed with different severities, strollers, dummies and restraint systems (as mentioned before):
- **Phase1**: High severity dynamic tests (according regulation 80R03) with a specific rearward facing child restraint system.
- **Phase2A**: Low severity dynamic tests ($\Delta V = 20$ km/h; 1.5 g) with strollers and baby carriage with different safety devices (folding backrest, PRM backrest, safety belt).
- **Phase2B**: Low severity dynamic tests ($\Delta V = 20$ km/h; 1.5 g) with the most unstable strollers with folding table and PRM backrest and misuse evaluation. These tests have been performed with a Q1 dummy.

Phase1 (P1)

In this phase, a Q3 instrumented dummy has been used for assess the performance of a rearward facing child restraint system built-in in a urban bus (M3 category, class I). This system was manufactured using components with the individual approval of regulation 44R04 for the group I, therefore this system may offer safety performance equivalent to the CRS used in M1 vehicles. Three tests have been performed in this phase:
- 2 rearward facing impact tests (P1-1 and P1-2).
- 1 forward facing impact test (P1-3).

The next table summarized the chest acceleration of the Q3 dummy in the tests and a picture obtained from the High Speed camera register.

Table 1. Summary results of the phase 1, (urban bus with specific vehicle CRS).

Test ref	Sled Vel (km/h)	Chest AccR 3ms (g)	Chest Vert AccZ (g)	RF (t = 100 ms)	FF (t = 100 ms)
P1-1	30.78	14.82	4.08		
P1-2	31.16	15.64	10.97		
P1-3	31.19	20.83	8.94		
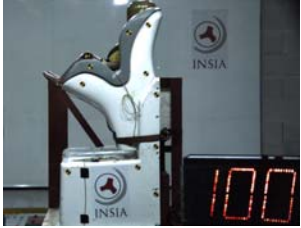
Phase2A (P2A)

The second phase is focused on the assessment of the safety performance of restraint devices with the strollers in the urban bus. Initially (in phase2A) a large number of samples were tested (see Figure 3) with three types of safety devices:

- 2P safety belt (Br3 according regulation 16R08, i.e. two point belt with retractor and automatically locking retractor).
- PRM backrest installed in the urban bus
- Folding backrest (developed in ASUCAR project under P-201131557 patent [2]). It is objective of these test to evaluate this device and provide (if necessary) solution for improved it.

The next figure shows a picture of the sled with a representative section of the urban bus. This section is used for the three types of safety devices.
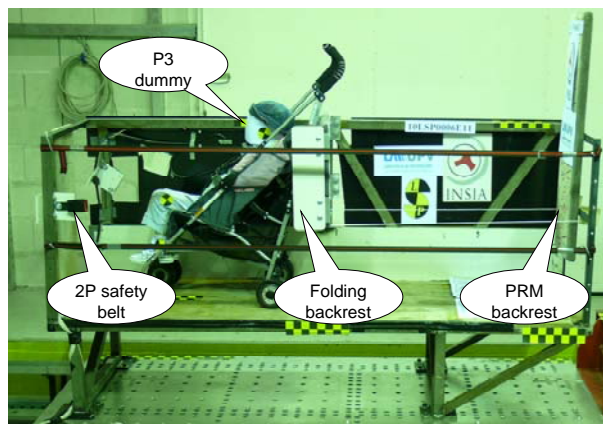
Figure 5. Urban bus module with three safety device types installed.

14 sled tests were performed with:

- P3 dummy and Ballast 9MO dummy. One tri-axial accelerometer was installed in each stroller for measure its acceleration during the dynamic tests.
- 4 types of strollers (see Figure 3).
- 3 types of safety devices (described above).
- Different configurations: rearward facing, forward facing, misuse in the belt path, break and without break the strollers' wheels, etc)

In this phase, kinematics analysis was made in order to verify the restraint of each type of the safety device. The results of these test have allow to design the test matrix for the phase2B, with has been performed with a Q1 dummy (more biofidelic dummy and instrumentation capabilities).

Phase2B (P2B)

The next table shows the test matrix of the phase2B.

Table 2. Test matrix of the phase2B.

Test ID	Stroller	Safety device	Comments
P2B-1	Stokke Xplory	Prototype #1	Stroller placed 89 mm from the first contact of the folding backrest. The stroller breaks are deactivated
P2B-2	Stokke Xplory	PRM backrest	150 mm gap between the stroller and the PRM backrest. The stroller breaks are deactivated
P2B-3	Stokke Xplory	Prototype #2	150 mm gap between the stroller and the folding backrest. The stroller breaks are deactivated
P2B-4	Quinny Buzz	Prototype #3	The stroller in contact with the backrest with the breaks activated (this is the recommended usage).
P2B-5	Quinny Buzz	Prototype #3	150 mm gap between the stroller and the folding backrest. The stroller breaks are deactivated
P2B-6	Quinny Buzz	PRM backrest	The stroller in contact with the PRM backrest with the breaks activated (this is the recommended usage).

As it can be seen, there are three types of prototype folding backrests. The three prototypes are manufactured with metal frame and covered with wooden plates. The first prototype has a total height of 500 mm, whilst the second has 400 mm. The third prototype has as well 400 mm of total height but is covered by a padded surface (similar to a carpet).

All the tests were performed with a Q1 dummy instrumented as mentioned in "**METHODS**" section, except the test P2B-1 with a P3 dummy.

The objective of test **PB2-1** was to verify the structural strength of the pushchair panel prototype#1 using the heaviest dummy (TNO type P3 weighing 15 kg). This configuration was considered as a "misuse" as it aimed to verify the behaviour of the least stable pushchair, with the tallest panel prototype, and without brakes applied to the wheels. The pushchair was placed facing backwards and in its lowest position. The free flight distance between the rear wheels and the restraint system (prototype #1) was 89 mm.

The aim of test **PB2-2** was to verify the structural strength and behaviour of a restraint for wheelchair users (PRM backrest) using the instrumented Q1 dummy (representing a one-year-old child). This configuration is considered as "misuse" as it was intended to verify the behaviour of the least stable pushchair when interacting with the panel used by wheelchair users. In this case, the stroller was configured in its highest position, with a distance from the pushchair grab-bar to the panel (in a horizontal position) of 150 mm – and without brakes applied to the wheels.

The aim of test **PB2-3** was to verify the structural strength of the prototype #2 using the Q1 instrumented dummy. These conditions represented a "misuse" because the stroller was the least stable pushchair and was positioned facing backwards in its highest position with a distance of the centre bar to the panel of 150 mm – and without brakes applied to the wheels.

Test **PB2-4** aimed to verify the structural strength of the prototype #3 using the Q1 dummy. This configuration was considered as "correct use". The stroller was located with the side bars of the pushchair touching the panel – and with brakes applied to the wheels.

Test **PB2-5** was intended to verify the structural strength of the prototype #3 using the Q1 dummy. This configuration is considered a "misuse" as it examined the behaviour of the backward facing stroller when interacting with the prototype #3 when the sidebars of pushchair were 150 mm from the panel – and without brakes applied to the wheels.

Finally, test **PB2-6** aimed to verify the structural strength and behaviour of the panel for wheelchair users (PRM backrest) using the Q1 dummy. This configuration is considered "correct use" as it verified the behaviour of the widest pushchair when interacting with the PRM backrest. In this case, the stroller was located with the handle (horizontal) touching the PRM backrest, and brakes applied to the wheels.

It should be noted that the goal of tests **PB2-2** and **PB2-6** was not only to verify the structural strength of the new pushchair restraint but to compare dynamic behaviour in settings of correct use and misuse in relation to the technical requirements defined in UNECE regulation 107.

The next table shows the results of the Q1 dummy with respect to the IARV obtained in Figure 4.

Table 3. Q1 dummy results relative to the IARV obtained.

Dummy part	Parámetro	Value (% wrt the IARV)				
		P2B-2	**P2B-3**	**P2B-4**	**P2B-5**	**P2B-6**
Head	HIC_{15}	3.5	1.2	0.3	6.1	0.2
	HPC (HIC_{36})	2.5	0.8	0.3	4.3	0.3
	Acceleration	12.6	11.8	4.2	21.6	3.5
	3ms acceleartion	27.6	21.2	9.3	40.8	7.9
Upper neck	Shear force Fx	16.4	10.0	9.7	22.8	3.2
	Tension force +Fz	11.5	10.1	2.4	17.2	3.9
	Compression force -Fz	6.2	4.5	1.0	8.0	1.4
	Lateral moment Mx	8.0	3.2	4.4	4.0	1.4
	Flexion moment +My	7.0	2.3	3.2	11.0	1.1
	Extension moment -My	**112.7**	**94.8**	**58.5**	**126.4**	44.2
	Twist moment Mz	13.7	4.9	9.4	10.6	3.6
	Nij TF (Tensile-Flexion)	5.4	2.9	2.4	8.6	0.8
	Nij TE (Tensile-Extension)	41.1	44.6	20.8	**59.9**	21.5
	Nij CF (Compression-Flexion)	5.3	2.1	0.7	5.4	1.4
	Nij CE (Compression-Extension)	**54.3**	39.3	26.4	**56.3**	10.7
	NIC Tensile	11.4	10.8	5.2	17.0	8.2
	NIC Shear	18.4	10.3	14.4	23.8	7.1
Chest	Sternum deflection Dx	3.4	4.4	0.5	3.1	0.1
	T4 acceleration	13.7	16.5	5.3	21.5	4.0

As it can be seen in the previous table, the extension moment has values that exceed the IARV. All the tests with "misuse" configuration have obtained values greater than 90% (and in two tests over exceed the limit). The tests performed according with the recommendations (PB2-4 & PB2-6) has been obtained values around the 50% of the limit. The rest of the parameters have not got value potentially injurious. Two comparisons in detail are made: P2B-2 vs P2B-3 and P2B-4 vs P2B-5.

P2B-2 vs P2B-3
In this case, two test configurations, classified as misuse, were compared. The least stable stroller due to its high centre of gravity was used, and in one of the tests it was supported by the PRM backrest and in the other test (P2B-3) was supported by the folding backrest (prototype #2). Figure 6 shows a superimposed image of the two configurations with the relative position of the pushchair during free flight of 150 mm towards each of the restraint systems.
Table 3 shows the results of the tests. Although the distance of free flight in both cases were the same (150 mm), the difference in height between the two panels and the contact point of the pushchair with them, produces differing behaviour in each case. Thus, while the contact of the pushchair with the PRM backrest system occurs with the back of the (horizontal) pushchair handgrip, the contact with the folding backrest (prototype #2) occurred lower down with the central telescopic rod on which the chair is mounted. Although the distance of free flight is the same, the horizontal displacement of the pushchair in the case of the PRM backrest is greater, because the handgrip bends when it comes into contact with the panel and the pushchair continues travelling until the telescopic mast strikes the panel (see Figure 7). As a consequence, all the values obtained in the test with the PRM backrest system (P2B-2) are higher than those obtained with the folding backrest (P2B-3).
The most critical parameter in both cases corresponds to neck extension moment of the dummy. The limit was exceeded by 12% in the case of the PMR backrest, while in the case of the folding backrest the values did not reach the limit of tolerance (5% below the limit).
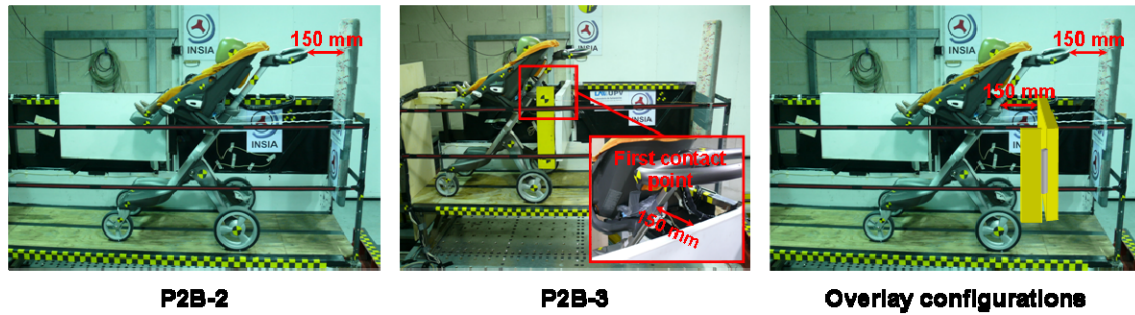
Figure 6. P2B-2 & P2B-3 configurations and a superimposed figure.
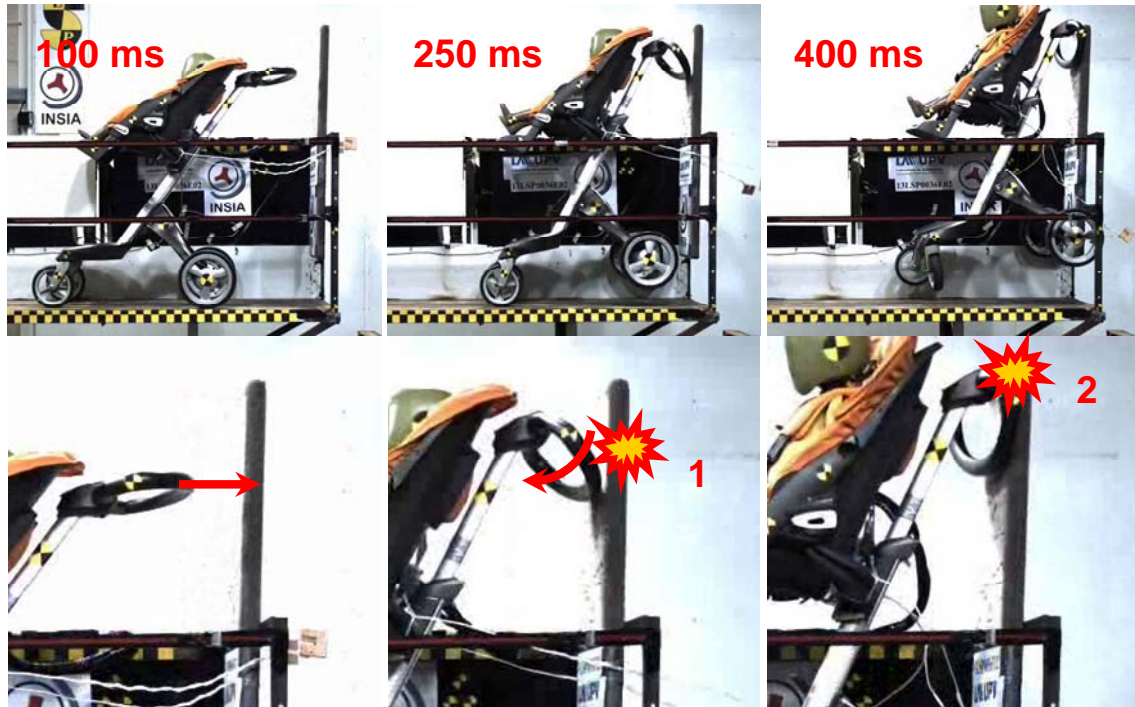
Figure 7. Kinematics analysis of the P2B-2.

P2B-4 vs P2B-5

In this case, two configurations were tested using the same stroller, one of the widest models and a model with three wheels (twin wheels for the frontal). The analysis compared a "correct" configuration (P2B-4 test) in which the stroller was in contact with the folding backrest (prototype #3) and the brakes were applied to the wheels, with a "misuse" configuration (PB2-5 test) with the PRM backrest, with a free flight distance of 150 mm and finally, the brakes were not applied to the wheels.

Table 3 shows the results of the tests, and it can be seen that all the parameters obtained for the PB2-5 test ("misuse") were worse than those obtained for the PB2-4 test ("correct use"). Only a small gap of 150 mm between the pushchair and the panel caused all the registered levels to double or more. The highest critical values exceeding the tolerance level were reached for the vertical extension of the neck, which exceeded the level of tolerated damage by 26%. Values increased by up to four times for head and chest accelerations, although critical values were not exceeded.

CONCLUSIONS

The main conclusions of the analysis of children strollers' safety in urban buses are:
- The safety belt has probed that is able to restraint the strollers and baby carriages in low severity frontal impact. Although there are potential risk configuration (the path of the belt in the strollers), it has not been able to reproduce any unstable configuration in the tests. This system is the only device that guarantees the retention of the child whatever be the impact direction.
- The folding backrest (tested in phase2B) is able to withstand the loads of the stroller occupied by one dummy (total mass 25 kg). As mentioned before, the folding backrest has being developed under patent [2].
- The misuse configuration tested in phase 2B has probed that the measurement on the dummy parts (injury readings) has grown up from 2 up to 5 times with respect to the recommended or standard situation. Therefore, it is highly recommended to follow the directions noted by usage recommendations.
- With respect to the folding backrest or the PRM backrest, neither of them have got positively restrained the stroller. In crash configuration or acceleration fields that are not longitudinal, there may be an uncontrolled movement of the stroller inside the urban bus.
- Despite the low severity tested, potentially injury situations have been reproduced.
- Currently the regulation 107R06 only provides as safety device the PRM backrest for restraint the strollers. The folding backrest (from the ASUCAR project) provides a similar solution that complements the requirements of the regulation. Furthermore, the regulation framework does not provide a solution for cases in which a wheelchair user and stroller coincide on the same journey on the urban bus. Therefore the folding backrest could be an alternative solution for transportation compatibility of different users.
- The specific built-in child restraint system has obtained four times chest acceleration with respect to the "correct use" in low severities, but the same levels with respect to the "misuse" configuration. The specific built-in CRS has been tested with a crash severity more than 6 times greater than the low severity. That means that this system is safer than the other systems (as it has been estimated).

REFERENCES

[1] Dols, J.; Aparicio, F.; Alcalá, E.; Pons, V.; Martínez, L.; Martín, A.L.; Valles, B. (2012). Código de Buenas Prácticas para la utilización de carritos de niños en vehículos de transporte público. Ed. UNIVERSITAT POLITÈCNICA DE VALÈNCIA. ISBN: 978-84-8363-810-1.

[2] Dols, J.; Pons, V.; Alcala, E.; Martínez, L.; Martín, A.; Valles, B. (2011). Sistema de Seguridad Pasivo para carritos de niños en vehículos de transporte público. University Polytechnic of Valencia and University Polytechnic of Madrid. Patent No. P-201131557. Priority country: Spain. 27 SEPT. 2011.

[3] Mertz , H.J., Irwin, A.L. and Prasad P. 2003. "Biomechanical and Scaling Bases for Frontal and Side Impact Injury Assessment Reference Values". Stapp Car Crash Journal, Vol. 47, pp. 155-188 (2003-22-0009).

PERFORMANCE COMPARISON AND REPEATABILITY EVALUATION OF THE FLEX PLI AND THE TRL PEDESTRIAN LEGFORM IMPACTORS

Lan Xu
Sukhbir Bilkhu[1]
Iskander Farooq
Jeff Hickman
Jack Jensen
Ken McCabe
Guy Nusholtz

The USCAR/OSRP Pedestrian Task Group

United States

Paper Number 15-0177

ABSTRACT

The objectives of this study were to compare the response differences of the Flex PLI and TRL legforms under various test conditions and to assess their repeatability. A test fixture with four control factors was designed and fabricated to simulate a generalized front structure of a light truck. Using this fixture, thirty-six impact tests with the Flex PLI and the TRL legforms were performed at an impact speed of 32 km/h.

The responses from the two legform impactors, specifically, moments in the Flex PLI and acceleration in the TRL, MCL elongation in the Flex PLI and bending angle in the TRL, and ACL elongation in the Flex PLI and shear displacement in the TRL were compared. The Taguchi method was applied to compare the responses from these three pairs of measurements. The shape and magnitude of the response time histories were used to evaluate the repeatability of the Flex PLI and TRL legforms.

Some results from this limited study indicate that the two legforms did not consistently respond to the same test conditions in the same way and could potentially drive countermeasures in opposite directions. For example, increasing the protrusion of the lower bumper stiffener relative to the bumper generally resulted in lower moments in the upper tibia with the Flex PLI, but higher accelerations with the TRL legform. However, the MCL from the Flex PLI and bending angle of the TRL legform trended consistently with changes of all four fixture factors, although with differing sensitivity.

A repeatability analysis indicated that most measurement parameters of each legform were repeatable or marginally repeatable across the spectrum of the test conditions. However, the MCL elongation of the Flex PLI and the bending angle of the TRL were non-repeatable in some test conditions.

INTRODUCTION

Currently, two legforms are available for pedestrian impact tests: the TRL Pedestrian Legform Impactor, originally developed by the EEVC (European Enhanced Vehicle Safety Committee) consortium [1] and the Flexible Pedestrian Legform Impactor (Flex PLI) [2]. The TRL Legform was incorporated into the ECE (Economic Commission for Europe) regulations in 2003 [3, 4]. The European New Car Assessment Program (EuroNCAP) has been using the TRL legform since 1997. The Flex PLI was developed by the Japanese Automobile Research Institute (JARI) in the early 2000's and over time, various versions have been evaluated [5]. EuroNCAP included the latest version of the Flex PLI GTR (Global Technical Regulation) in their 2014 vehicle tests [6]. Considering that these two legforms are used for the same type of test, it is important to understand their performance differences.

Various versions of the TRL legform and Flex PLI have been evaluated and compared by a number of organizations under different test conditions. A series of pedestrian impact tests involving five vehicles was performed using both

---

[1] Retired from Chrysler in 2014

legforms [7]. The major findings from these tests were that the two legforms had marked differences in how they interacted with vehicle front structures. Another series of tests on eight vehicles was performed with both legforms [8]. This work concluded that the TRL legform predicted a higher risk of tibia fracture but a lower risk of knee ligament injury than the Flex PLI. In addition, several bumper designs were tested with both legforms [9]. These results indicated that the bumper system that performed well with the TRL legform did not necessarily perform well with the Flex PLI.

The repeatability of the two legforms has also been studied by different organizations. Most repeatability analyses used the Coefficient of Variance, CV, which was based on the International Organization for Standardization document, ISO/TC22/SC12/WG5 N 751, regarding methods to assess the repeatability and reproducibility [10]. A repeatability and reproducibility study using six TRL legforms in 76 tests was conducted by Siems et al. in 2007 [11]. Repeat tests were performed on each legform with a linearly guided impactor. The CV values calculated from the parameter peaks of the repeat tests were all below 5% which indicated "acceptable" repeatability. Another study by Zander et al. [12] concluded that CV values from certification tests with the Flex PLI demonstrated that all tibia moments had acceptable repeatability while some knee ligament elongations had unacceptable repeatability, with CVs >10%. In the same study, two different locations at the front end of two vehicles were each impacted three times with a Flex PLI. Most of the tibia bending moments were repeatable, with CVs <5%; however, some of the knee elongations (ACL, PCL, and MCL) were non-repeatable with CVs >10%. The repeatability of the Flex PLI was then further assessed by the inverse calibration impact tests. The repeatability for the inverse calibration impact was acceptable since all the CV values were less than 4%. Another repeatability study with a later version of the Flex PLI was conducted [13] using two sedans and one (SUV) Sport Utility Vehicle. For each vehicle, two selected locations were each impacted three times. The CV results indicated that all the tibia moments were either repeatable or marginally repeatable. However, elongations of the knee ligaments did not have acceptable repeatability; their repeatability depended on vehicle front end geometry.

The OSRP (Occupant Safety Research Partnership) of USCAR (United States Council for Automotive Research) evaluated these pedestrian legforms. A unique test fixture was designed and used which allowed understanding of the response differences between the two legforms in this evaluation. The objectives were to compare the performance of the TRL legform and Flex PLI, and to assess the repeatability of some of the responses of the two legforms.

METHODOLOGY

Legform Impactors

The TRL legform consists of two rigid segments covered with foam and neoprene skin (Figure A1 in Appendix A) [1, 14]. The segments represent the lower leg (tibia and foot) and upper leg (femur) of an adult, connected by a simulated knee joint that can rotate and translate. The motion of the knee joint is resisted by two deformable elements (ligaments as shown in Figure A1) which are replaced after each test.

The Flex PLI consists of an upper leg (femur) and lower leg (tibia) composed of fiberglass bone cores and several plastic segments attached to its impact side (Figure A2) [2, 14]. The knee element consists of two complex blocks containing over twenty four springs. The entire assembly is wrapped in a thin rubber and neoprene skin.

The TRL legform and Flex PLI instrumentation locations are shown in Figures A3 and A4, respectively [15, 16]. The standard TRL legform instrumentation includes two transducers to measure the relative rotation (bending angle) and relative translation (shear displacement) between the femur and tibia. There is also an accelerometer fitted to the non-impact side of the tibia, close to the knee joint (66mm below its knee as shown in Figure A3).

The Flex PLI has four strain gauges glued to its fiberglass core to estimate the tibia moments at four different locations. These are labeled Leg-1 through Leg-4 in Figure A4, but identified as Tb1 through Tb4 throughout the text. The standard Flex PLI also includes four string potentiometers in its knee to measure the elongations of the Anterior Cruciate Ligament (ACL), Medial Collateral Ligament (MCL), Posterior Cruciate Ligament (PCL) and Lateral Collateral Ligament (LCL). Although the thigh has instrumentation, the moments in the thigh and the LCL elongation were not measured in this evaluation program.

To minimize the potential damage to the Flex PLI (GT version), the owner of the legform (JARI) advised that the maximum tibia bending moment should not exceed 380Nm during any test. A series of tests was performed using the Flex PLI, starting from a low impact speed which was increased gradually, to determine the impact speed for this test program. An impact speed of 32km/h kept the bending moments less than 380 Nm. Both the TRL and the Flex PLI legforms were tested at this speed.

Test Fixture Design

The test fixture was designed to represent a front end of a generic Light Truck and Van (LTV) and is shown in Figure 1. The fixture had three horizontal components which represented the hood edge, bumper, and lower bumper stiffener (LBS). The LBS was adjustable in both horizontal and vertical directions. The fixture was bolted to a heavy bed plate and secured to the test area floor. The foam placed in front of bumper face was expanded polypropylene (EPP) with a density of 32g/l and a thickness of 75mm. It was replaced for each test.
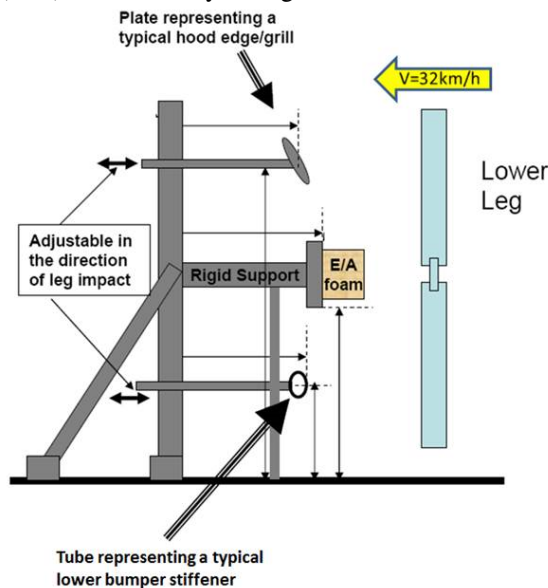
Figure 1. Fixture Design.

Test Matrix Design

 Taguchi method A procedure used to analyze the data from this test series was the Taguchi method [17, 18]. The Taguchi method utilizes orthogonal arrays in the design of experiments to significantly reduce the number of experimental configurations compared to a full factorial array. Control factors such as the bumper foam height and LBS position were varied and evaluated.

 Test matrix An L9 orthogonal array was used in this study. It had four control factors with 3 different levels. This resulted in 9 tests for each legform. The required number of tests, if a full factorial array were used, would be 162. The factors are given in Table 1. Factor A, the bumper foam section height, was the vertical length of the cross section. Factor B, height of the bumper, was the vertical distance from the ground plane to the bumper lower edge. Factor C, LBS fore/aft position, was its alignment with respect to the bumper contact surface in the horizontal direction. Factor D, the height of LBS, was the vertical distance from the ground plane to the LBS. Photographs of the nine test configurations are shown in Figure B1 (Appendix B). To assess the repeatability of the legforms, two tests were conducted for both legforms in each of the nine configurations.

All four control factors were tested using three levels except for the bumper foam height (Factor A). Only two levels of the bumper foam height were used in the test. The Taguchi method allows for substitution for variables that were not represented in testing. Thus, Level 2 of factor A is the same as Level 1 (A2=A1). A 100 mm bumper section was used in test configurations 1 through 6 in this test series. The factor levels are shown in Table 2.

Table 1.
Test Matrix.

L9 Taguchi Experimental Layout Inner Array - Control Factors and Levels				
*Confg.**	*Bumper Foam Height (z)*	*Bumper Lower Edge From Ground*	*Lower Bumper Stiffener offset to bumper face*	*Lower Bumper Stiffener from ground*
	A	**B**	**C**	**D**
1	**1**	**1**	**1**	**1**
2	**1**	**2**	**2**	**2**
3	**1**	**3**	**3**	**3**
4	**2**	**1**	**2**	**3**
5	**2**	**2**	**3**	**1**
6	**2**	**3**	**1**	**2**
7	**3**	**1**	**3**	**2**
8	**3**	**2**	**1**	**3**
9	**3**	**3**	**2**	**1**

*Confg. = configurations

Table 2.
Factor Levels.

Control Factors and Levels for Taguchi L9			
	Level 1	*Level 2*	*Level 3*
A *Bumper Foam Height (mm)*	100	100	200
B-*Bumper lower edge from Ground (mm)*	350	400	450
C-*Lower Bumper Stiffener Offset to bumper face (mm)*	-50	0	+50*
D-*Lower Bumper Stiffener from ground (mm)*	180	230	280

*Positive is in the legform initial travel direction

Data Processing

For the Flex PLI legform, the directions of the tibia moments (Tb1, Tb2, Tb3 and Tb4) were about the legform X axis. The MCL, PCL, and ACL extension measurements were in the local (dummy) coordinate systems (as opposed to the vehicle coordinate system). For the TRL legform, the directions of tibia acceleration and shear displacement were in the Y-direction (legform travel direction), and the knee bending angle was about the leg's X-axis. Data was recorded at a sample rate of 10,000 samples per second and filtered with a SAE CFC180 filter. Sign conventions, filtering and data processing followed standard industry practices (as described in SAE J211.)

Analysis Method

The measurements from the Flex PLI and TRL legforms that were hypothesized and proposed to assess the same injury type were compared. Moments from the Flex PLI and acceleration from the TRL were hypothesized to assess the risk of bone fracture. MCL elongation in the Flex PLI and bending angle in the TRL were hypothesized to assess the risk of injuries to the collateral ligaments. ACL elongation in Flex PLI and shear displacement in the TRL were hypothesized to assess the risk of injuries to the cruciate ligaments. Since some pairs measured different physical metrics, the trends of both their peak responses and their signal to noise ratios for each control factor were compared.

Factor A in the test fixture, size of the bumper foam, controlled the amount of energy that was absorbed. Factor B, the height of the bumper, controlled the relative height between the bumper and the knee and accelerometer location for the TRL legform, and between the bumper and the Tb1 and Tb2 for the Flex PLI. Factor C, LBS fore/aft position,

is the horizontal distance between the contact surfaces of the bumper and LBS. C2 is aligned with the bumper beam, C3 is towards the rear of the fixture (recessed rearward of the bumper surface), and C1 is towards the front of the fixture (protruded forward of the bumper surface). Factor D is the LBS height relative to the ground.

The relationship between moment distribution and loading conditions in a beam is illustrated in Figure C1 of Appendix C. Considering that the shape and construction of the tibia in the Flex PLI is essentially a beam, it is possible to use beam theory for pictorial estimation of the moment distribution in its tibia, as shown by Figure C1. The pictorial estimation indicates that the maximum moments occur near the locations of the reaction forces, which would be the bumper force and LBS force.

The signal to noise (S/N) function used in this analysis is of the smaller-the-better type exhibited in Eq. (1),

$$S/N = -10 \, log(\tfrac{1}{n}\textstyle\sum_{i=1}^{n} y_i^2) \qquad (1)$$

where y_i are responses and n is the number of repeats from a test configuration. In this study, n=2, y_1 and y_2 are the peaks from the two repeat tests.

Repeatability was assessed by shape and magnitude correlation method. The repeatability between the two signals was measured through the use of cross correlations of the time-histories [19]. The two signals are considered repeatable if both the shape correlation is at least 0.98 and the magnitude correlation is at least 0.95. On the other hand, the two signals are considered not repeatable if either the shape is below 0.92 or the magnitude is below 0.9. In between, the repeatability is marginal. The definition of the shape and magnitude correlations and the repeatability criterions are included in Appendix E. All of the correlations were calculated from 0 to 80 milliseconds.

RESULTS AND DISCUSSION

Peak Response Analysis

The data from the PCL transducer could not be recorded because of faulty instrumentation. Therefore, it was not included in this analysis.

Peak tibia accelerations from the TRL legform and peak moments in the Flex PLI from all the tests are presented in Figures 2 and 3 (t1= test 1, t2=test 2) below and Figure D1 in Appendix D. Among the measured moments at four locations in the Flex PLI, the majority of the maximum moments occurred at Tb1 (at the top location), possibly due to the inertial loading from the knee and its contact with the bumper. Moments in Tb2 were close to Tb1 in configurations 7 and 9. Moments in Tb2 were larger than Tb1 in configurations 4 and 8. Beam theory seems to explain this result: the closer the bumper and LBS reaction points are to the transducer location, the higher the moment. For example, in configuration 4, the bumper was below the Tb1 location and both the bumper and the LBS are nearer to Tb2 than to Tb1; in configuration 8, both the bumper and the LBS are nearer Tb2 again. Therefore, only the Tb1 moments from the Flex PLI are compared to the tibia accelerations from the TRL legform in peak response analysis.
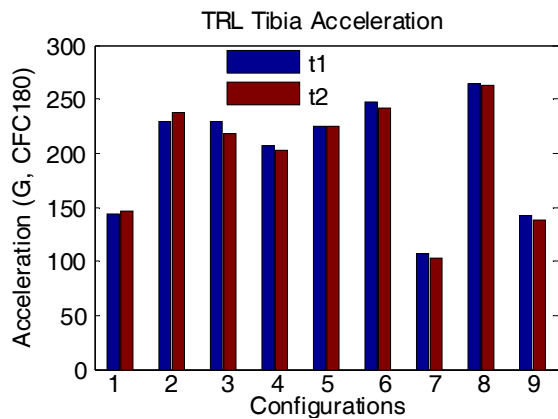
Figure 2. Peak Tibia Accelerations (TRL).   *Figure 3. Peak Tb1 Moments (Flex PLI).*
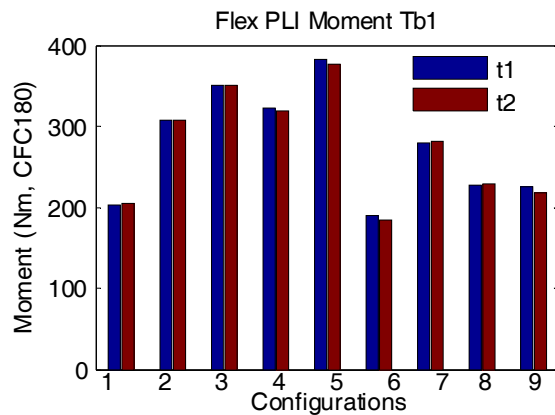
The configurations that produced maximum or minimum peaks for the tibia acceleration and Tb1 moment are presented in Table 3. The configurations that resulted in the maximum acceleration from the TRL legform included C1 (protruded LBS), while the configurations that resulted in the maximum Tb1 moment from the Flex PLI included C3 (recessed LBS). C3 created more rotation around the knee (observed from the video) which increased the moments in the tibia. The highest acceleration in the TRL legform occurred when it was impacted at the top quarter of the tibia, but the highest Tb1 in the Flex PLI occurred when both the top quarter and bottom quarter of the tibia were impacted. Similarly, the TRL legform obtained the minimum accelerations in the configuration that included C3, and the Flex PLI Tb1 tended to obtain the minimum in the configurations that included C1.

Table 3.
Maximum or Minimum Peaks in Terms of Configurations.

Variables	Configurations	Comments
Tibia Acc. Max (TRL)	8: A3B2C1D3	contains C1;
	6: A2B3C1D2	contains C1
Tb1 moment Max (Flex PLI)	5: A2B2C3D3	contains C3;
	3: A1B3C3D2	contains C3;
Tibia Acc. Min (TRL)	7: A3B1C3D2	contains C3;
Tb1 moment Min (Flex PLI)	6: A2B3C1D2	contains C1;

Peaks of the bending angle in the TRL legform and the MCL displacement in the Flex PLI are presented in Figures 4 and 5. Both legforms demonstrated considerable similarity in the ranking of the three maximum peaks. This might be due to the similar parameters measured in the two legforms. Bending angle in the TRL legform measures the relative rotation between the femur and the tibia. As the femur rotates with respect to the tibia, the MCL is approximately proportional to the multiplication of the relative rotating angle (similar to bending angle in the TRL legform) and the distance (almost constant) from the pivot point to the location of the measurement device of the elongation. It was observed that C3 is included in the two maximum peak response configurations (3 and 5).
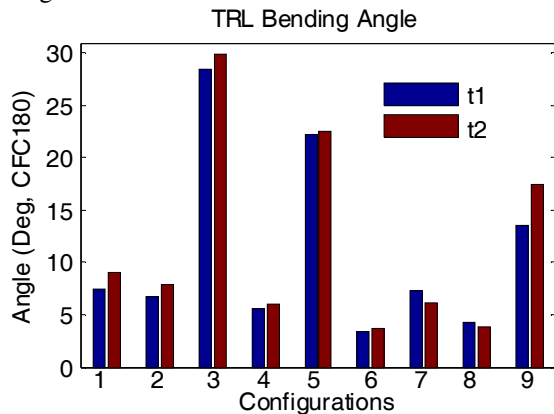
Figure 4. Peak Bending Angles (TRL).
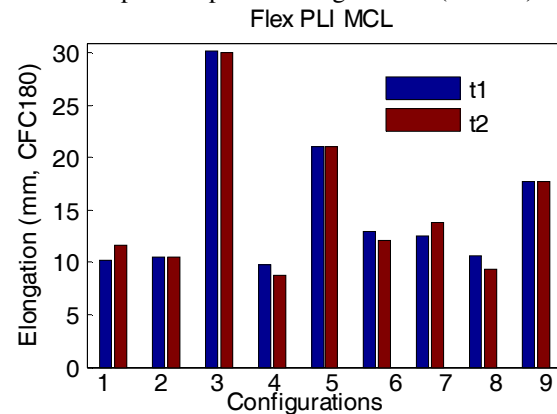
Figure 5. Peak MCL Elongations (Flex PLI).

The peaks of the shear displacement in the TRL legform and the ACL elongation in the Flex PLI are presented in Figures 6 and 7. These two parameters measure the relative translational motion between the femur and tibia. The two legforms responded to most test configurations inconsistently. The trends from one legform could not be predicted from the trends of the other legform. For example, configurations 3 and 9 produced peak shear

displacement responses in the low range for the TRL legform, but they produced peak ACL elongation responses in the high range for the Flex PLI. Configuration 4 produced peak responses in the high range for the TRL legform, but it produced the peak responses in the low range for the Flex PLI.
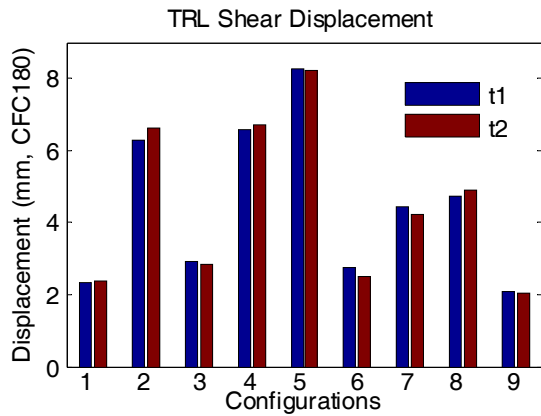
Figure 6. Peak Shear Displacements (TRL).
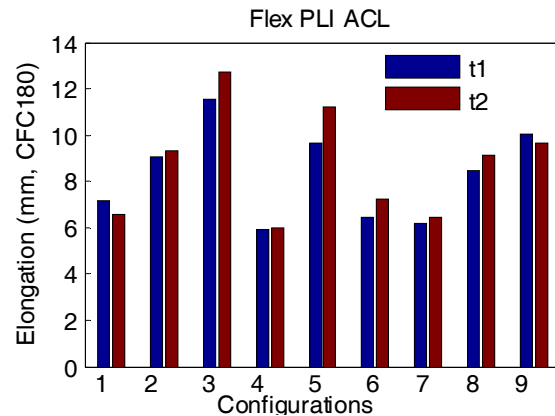
Figure 7. Peak ACL Elongations (Flex PLI).

Control Factor Analysis

The trends and sensitivities of S/Ns (signal to noise ratios) of the two legform responses due to the changes in the levels of the four factors are compared below. S/Ns for tibia acceleration from the TRL legform and Tb1 from the Flex PLI are overlaid in Figure 8. In general, the larger the change in the S/N with respect to an increment in a factor indicates the more sensitive the response is to that factor.

Tibia acceleration and Tb1 moment were affected by Factor A in a similar way, presumably due to the similar transducer locations. Both legform peak responses were influenced by Factor B consistently: there was a bumper position between B1 and B3 that would produce a minimum S/N. However, tibia moment Tb1 peak response in the Flex PLI and the acceleration in the TRL legform were influenced by Factor C in opposite directions. Tibia moment Tb1 peak response in the Flex PLI and the acceleration in the TRL legform were influenced by changing from factor D2 to D3 similarly but with different sensitivities.

The S/Ns for the bending angle from the TRL legform and the MCL elongation from the Flex PLI are presented in Figure 9. All four factors tended to affect the two parameters consistently, but with different sensitivities. The TRL legform was more sensitive to Factors A, C and D than the Flex PLI. The larger bumper section (A3), the lower bumper height (B1), and more forward alignment (protrusion) of LBS (C1) produced less rotation between the femur and tibia. Additionally, it indicates that there was a position between D1 and D3 for the LBS that would produce a maximum S/N.
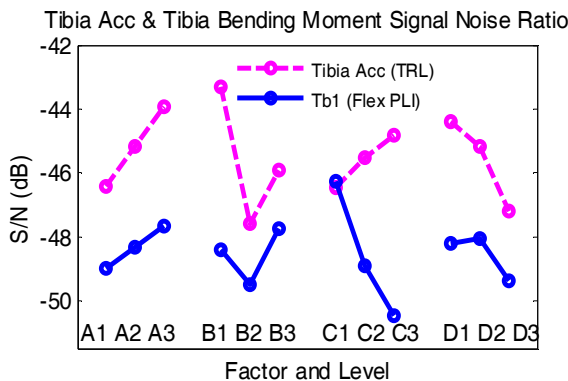
Figure 8. Factor Effects to Tibia Accelerations (TRL) and Tb1 Moments (Flex PLI).
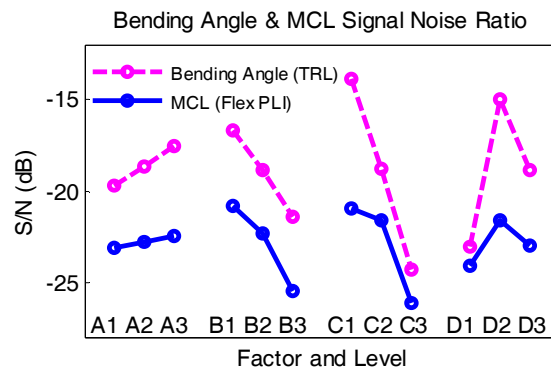
Figure 9. Factor Effects to Bending Angles and MCL Displacements.

The S/Ns for the shear displacement from the TRL legform and ACL elongation from the Flex PLI are presented in Figure 10. The two legforms were inconsistent in their responses to the factors changed in most configurations. With respect to the height of the bumper foam face (Factor A), the Flex PLI ACL was insensitive to the bumper face size. Recall that for control factor A only two values were tested (A1 and A2 were both 100 mm and used for configurations 1 through 6). The differences in S/N ratios between A1 and A2 are attributed to variability in the testing. Because the Taguchi method predicts trends from test outputs and test outputs are affected by test variability and noise factors it is not unusual for an S/N ratio to change for two control factors that are the same. The changes in S/N between A1 and A2 could be considered the limitations of the analysis (at least for control factor A, but not necessarily for the other control factors.) The differences between S/N ratios between A1 and A2 are, however, relatively low, as expected.

Control factor A3 (large bumper face) spans the tibia / femur interface in configuration 9 (see Figure B1). Thus tibia measurement trends would be expected to have discontinuities as the leg is moved up and down with the larger bumper face. This challenges the Taguchi method and trends with respect to control factor A should be interpreted accordingly. However, this geometric configuration is realistic and vehicles could indeed have bumper faces that span this area. As such trends identified in this study (such as the different trends between the two legs) are meaningful.

With respect to the location of the bumper (Factor B), the Flex PLI ACL was insensitive to the bumper height change from B2 (400mm) to B3 (450 mm) above the ground, while the TRL legform shear displacement was significantly sensitive to this change. The trends for both shear displacement and ACL varied differently to the heights of the LBS (Factor D). Only the protrusion of the LBS relative to the bumper (Factor C) affected both legform shear displacement and ACL displacement similarly, however with different sensitivities.

Shear Displacement & ACL Signal Noise Ratio
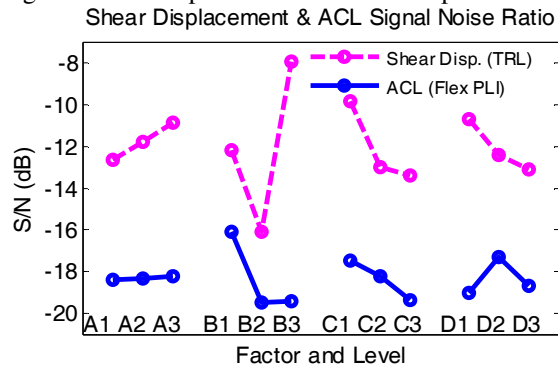
Figure 10. Factor Effects to Shear Displacement and ACL Displacement.

Repeatability Analysis

TRL legform The shape and magnitude correlations for the three parameters from the TRL legform tests are shown in Figures D2 and D3 (Appendix D). The shape and magnitude correlations of the TRL legform measurements are categorized in Table 4. Tibia acceleration of the TRL legform was repeatable in both shape and magnitude for all test configurations. Bending angle was repeatable in both shape and magnitude in only two of the nine test configurations. Shear displacement was repeatable in both shape and magnitude in six of the nine test configurations. Examples of repeatable time-histories for tibia acceleration, bending angle, and shear displacement from test configuration 4 are shown in the subplots of Figure D6, while non-repeatable time-histories for bending angle from test configuration 2 are shown in Figure D7.

Table 4.
Repeatability of TRL Legform Measurements.

Config.	Acc		Bending Angle		Shear Disp.	
	Shp	Mag	Shp	Mag	Shp	Mag
1	Y	Y	Y	N	Y	Y
2	Y	Y	M	N	Y	M
3	Y	Y	Y	M	M	N
4	Y	Y	Y	Y	Y	Y
5	Y	Y	Y	Y	Y	Y
6	Y	Y	Y	N	M	N
7	Y	Y	Y	N	Y	Y
8	Y	Y	Y	M	Y	Y
9	Y	Y	Y	N	Y	Y

Config. = Configuration
Shp=shape; Mag=magnitude;
Y: Repeatable;   M: Marginal;   N: Non-repeatable;

Flex PLI legform The shape and magnitude correlations from the Flex PLI tests for the six parameters are shown in Figures D4 and D5 (Appendix D). The results of the repeatability level for each parameter from the Flex PLI are categorized in Table5. Tb1, Tb2, Tb3, and ACL were repeatable or marginally repeatable in both shape and magnitude for all test configurations. Tb4 had non-repeatable shape for test configuration 3. It also had non-repeatable magnitudes for test configurations 1 and 7, but they were below the non-repeatable criteria (0.9) with small margin (0.90 and 0.89, respectively). MCL had a non-repeatable magnitude for test configuration 8. It was below the non-repeatable criteria (0.9) with a considerable margin (0.61). As an example, repeatable time-histories for moments Tb1 through Tb4 and MCL and ACL elongations from test configuration 4 are shown in the subplots of Figure D6, while non-repeatable time-histories for MCL from test configuration 8 are shown in Figure D8.

Table 5.
Repeatability of Flex PLI measurements by test Configuration.

Config.	Tb1		Tb2		Tb3		Tb4		MCL		ACL	
	Shp	Mag	Shp	Mag	Shp	Mag	Shp	Mag	Shp	Mag	Shp	Mag
1	M	Y	Y	Y	M	Y	Y	N	Y	M	M	Y
2	Y	Y	Y	Y	Y	Y	Y	M	Y	Y	M	M
3	Y	Y	Y	Y	M	Y	N	M	Y	Y	Y	Y
4	Y	Y	Y	Y	Y	Y	Y	Y	Y	Y	M	Y
5	Y	Y	Y	Y	Y	Y	Y	Y	Y	M	Y	M
6	Y	Y	Y	Y	Y	Y	Y	Y	Y	Y	Y	Y
7	Y	Y	Y	M	Y	M	Y	N	Y	M	Y	M
8	M	M	Y	M	Y	Y	Y	Y	M	N	M	M
9	M	Y	M	Y	M	Y	Y	M	Y	Y	Y	Y

Config. = Configurations;
Shp=shape; Mag=magnitude;
Y: Repeatable;   M: Marginal;   N: Non-repeatable;

Repeatability comparison The mean and standard deviation (Std) for the shape and magnitude repeatability were obtained by combining the 9 shape and magnitude correlations[2]. The mean plus and minus one Std of the correlations for all the parameters in the TRL legform and the Flex PLI are presented in Figures 11 and 12. In terms

---

[2] This does not imply that every configuration results in similar measured responses. The correlation coefficient across the two repeat tests for one configuration was then combined with the correlation coefficients from the other 8 configurations.

of the means of shape correlations and magnitude correlations, the tibia acceleration from the TRL legform and Tb1, Tb2, Tb3, and ACL from the Flex PLI were repeatable. The magnitude of bending angle in the TRL legform was non-repeatable. The magnitude of shear displacement in the TRL legform and Tb4 and MCL in the Flex PLI were marginally repeatable. However, the magnitude of the MCL in the Flex PLI had large standard deviation (Figure 12) which indicated that its repeatability was dependent on the test configurations: non-repeatable responses might be produced under some test conditions.
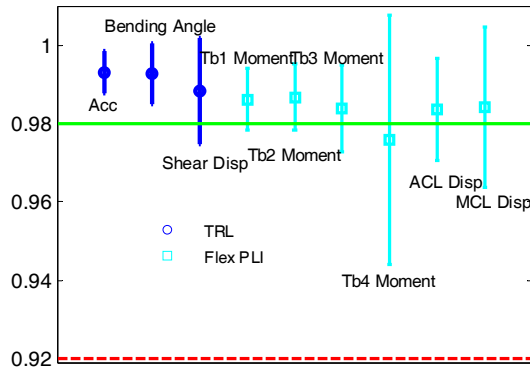
Figure 11. Means and one Std of Shape Correlations.
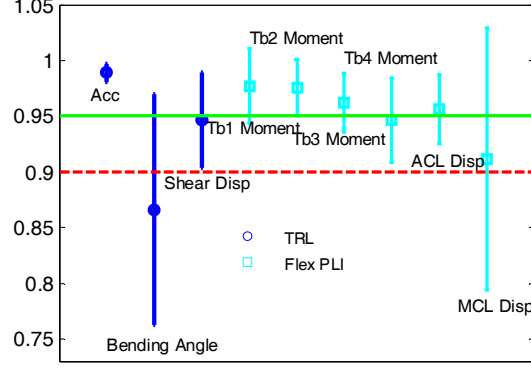
Figure 12. Means and one Std of Magnitude Correlations.

Limitations

The result on the level of the repeatability for these two legforms is limited in this study as there were only two repeat tests in this analysis. More repeat tests should be conducted to confirm the observations of this study.

The control factor analysis provided insights into the trends for the measured parameters with respect to the factor level changes. These trends could be further verified through additional confirmation tests. As an example, the limitation of only 2 repeat tests may have failed to fully quantify the trends associated with bumper foam height. The analysis suggested trends between A1/A2 (which were the same physical dimension) and A3 (which was larger) were insignificant, however more testing repeats may have better quantified the effects of the larger bumper foam height.

All tests were conducted at 32 km/h and neither legform was damaged. Additional tests at 40 km/h or higher should be conducted to confirm the durability of the legforms and if the repeatability changes.

Summary

Tibia acceleration in the TRL legform and tibia Tb1 bending moment in the Flex PLI reached their maximum peaks from different test configurations. The trends from the two legforms were inconsistent (in opposite directions) with respect to the change of LBS alignment with the bumper. This is possibly due to the difference in the mechanisms for producing the force/acceleration and the mechanism for producing the moment. As an example, for producing force/acceleration, the impact to the legform only occurs at one point. However, to produce a significant moment, either two (or more) impact points or one impact point and one (or more) fixed point reactions is required.

Shear displacement in the TRL legform and ACL elongation in the Flex PLI achieved the maximum peaks from different test configurations as well. In addition, to the increments of the four adjustable factors in the fixture, their sensitivities were different and some trends were inconsistent. The inconsistency might be due to the differences in transducer locations and knee designs.

Bending angle in the TRL legform and MCL elongation in the Flex PLI reached the maximum peaks from various configurations consistently, but with different levels of sensitivity.

Observations from the data indicate that the lowest responses (optimal responses) from the instrumentations between two legforms do not occur at the same vehicle front geometries. This could guide the design of the vehicle front structure differently.

Repeatability analysis indicated that across the spectrum of the test conditions in this study, some measured parameters had acceptable repeatability, but others were only marginal. Bending angle in the TRL legform had unacceptable repeatability. The MCL elongation in the Flex PLI is borderline non-repeatable under some test conditions, considering that its mean of overall magnitudes was close to the non-repeatable criteria (magnitude =0.9, Figure 12) and it exhibited a large standard deviation.

CONCLUSIONS

In general, inconsistencies in the responses between the TRL and Flex PLI legforms for the same changes to a generic LTV front geometry are identified in this study. These inconsistencies likely would drive differing vehicle designs depending on what legform was used.

The change to the horizontal alignment between the bumper and the lower bumper stiffener (Control Factor C) affected the "risk of leg bone fracture" assessment values (tibia acceleration in the TRL legform and tibia moments in the Flex PLI) in opposite directions. Contradictory design directions are likely depending on which legform is used.

The "risk of leg ligament tear by bending" assessment values (tibia bending angle in the TRL legform and MCL elongation in the Flex PLI) produced consistent trends but with different sensitivities in most impact configurations.

The "risk of leg ligament tear by shear" assessment values (shear displacement in the TRL legform and ACL elongation in the Flex PLI) produced inconsistent trends in most impact configurations.

Overall, the MCL displacement responses in the Flex PLI were marginally repeatable.

With the TRL legform, the tibia acceleration response was repeatable, but bending angle was not repeatable in some test conditions.

ACKNOWLEDGEMENT

JARI/JAMA loaned their Flex PLI Pedestrian Legform Impactor which made this evaluation program possible.

REFERENCES

[1] TRL, Transport Research Laboratory, *TRL Pedestrian Legform User Manual, version 2.0*, 2000

[2] Humanetics Innovative Solutions*, Flex PLI GTR User Manual, GRR9-3-04,* 2011

[3] UNECE, European Directive 2003/102/EC, 2003

[4] UNECE, European Directive 78/2009/EC, 2009

[5] GTR 9, Flex PLI SubGroup - Informal Group on Pedestrian Safety - Flex-PLI Technical Evaluation Subgroup at http://www.unece.org/trans/main/wp29/wp29wgs/wp29grsp/pedestrian_flexpli.html, 2005-2010

[6] EuroNACP Group, EUROPEAN NEW CAR ASSESSMENT PROGRAMME (Euro NCAP); PEDESTRIAN TESTING PROTOCOL, Version 7.1.1, December 2013

[7] Mallory, A., Stammen, J., and Legault, F., "*Component Leg Testing of Vehicle Front Structures*", ESV 2005, 05-0194. 2005

[8] Matsui, Y., Takagi, S., Tanaka, Y., Hosokawa, N., Itoh, F., Nakasata, H., Watanabe, N., and Yonezawa, H., "*Characteristics of the TRL Pedestrian Legform and the Flexible Pedestrian Legform Impactors in Car-front Impact Tests*", ESV, 09-0206, 2009

[9] Kinsky, T., Friesen, F., and Buenger, B., "*The Flexible Pedestrian Legform Impactor and Its Impact on Vehicle Design*", ESV, 11-0328, 2011

[10] Mertz, B., "*Calculation Method & Acceptance Levels for Repeatability and Reproducibility*", ISO/TC22/SC12/WG5 N 751, Dec. 6, 2004

[11] Siems, S., Zander, O., Leβmann, P., Gegring D., Bortenschlager, K., Barnsteiner, K., Ferdinand, L., Hartlieb, M., Kramberger, D., and Zeugner, M., "*Evaluation of the Effects of Test Parameters on The Results of the Lower Legform Impactor*", ESV 07-0009, 2007

[12] Zander, O., Lorenz, B., Gehring, D., and Lebmann, P., "*Prediction of Lower Extremity Injury Risks During an Impact on Modern Car Fronts with a Flexible Pedestrian Legform Impactor and the Pedestrian Legform Impactor According to WWVC WG17*", ESV 07-0206, 2007

[13] Zander, O.B., Gehring, D., Lebmann, P., and Bovenkerk J., "*Evaluation of a Flexible Pedestrian Legform Impactor (Flex-PLI) for the Implementation within Legislation on Pedestrian Protection*", ESV 09-0277, 2009

[14] GRSP, "*Difference Of TRL Legform Impactor/Injury Criteria And Flex Pedestrian Legform Impactor/Injury Criteria*", Informal Document GRSP-49-24 (49th GRSP, 16-20 May 2011

[15] 7 EEVC Working Group 17 Report, *IMPROVED TEST METHODS TO EVALUATE PEDESTRIAN PROTECTION AFFORDED BY PASSENGER CARS* (December 1998 with September 2002 updates).

[16] Dr. Konosu / JARI, UNECE,http://www.unece.org/fileadmin/DAM/trans/doc/2006/wp29grsp/teg-002e.pdf, 2006

[17] Wu, Y., Wu, A., "*Taguchi Methods for Robust Design*", 2000

[18] Taguchi, G., Chowdhury, S., Wu, Y., *"Taguchi's Quality Engineering Handbook"*, 2004

[19] Xu, L., Agaram, V., Rouhana, S., Hultman, R., Kostyniuk, G., McCleary, J., Mertz, H., Nusholtz, G. and Scherer, R., *"Repeatability Evaluation of the Pre-Prototype NHTSA Advanced Dummy Compared to the Hybrid III"*, SAE2000-01-0165, 2000

APPENDIX A: TWO LEGFORMS

The TRL legform and Flex PLI are illustrated in Figures A1 and A2. The locations of their instrumentations are presented in Figures A3 and A4.
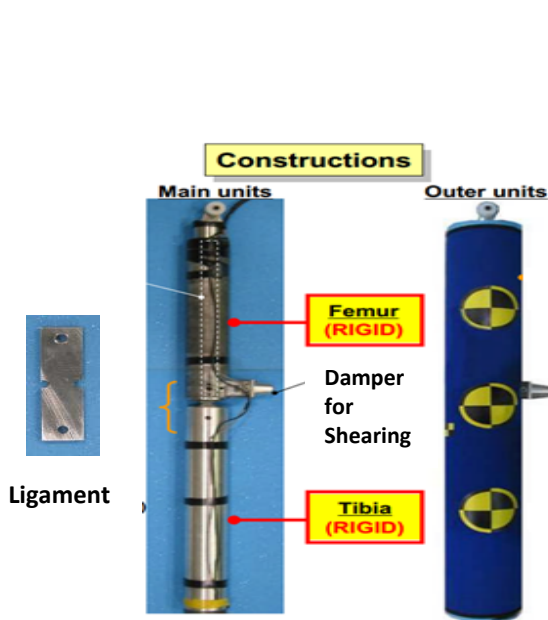
Figure A1. TRL Legform Construction.
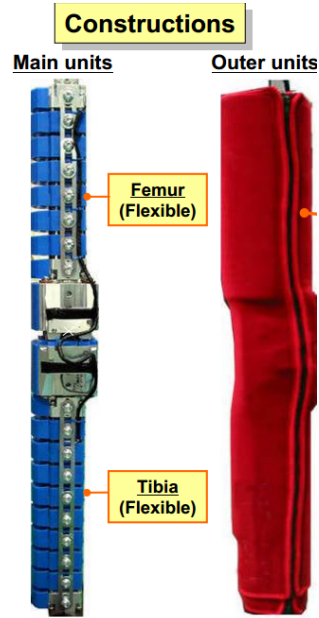
Figure A2. Flex PLI GT Legform Construction.
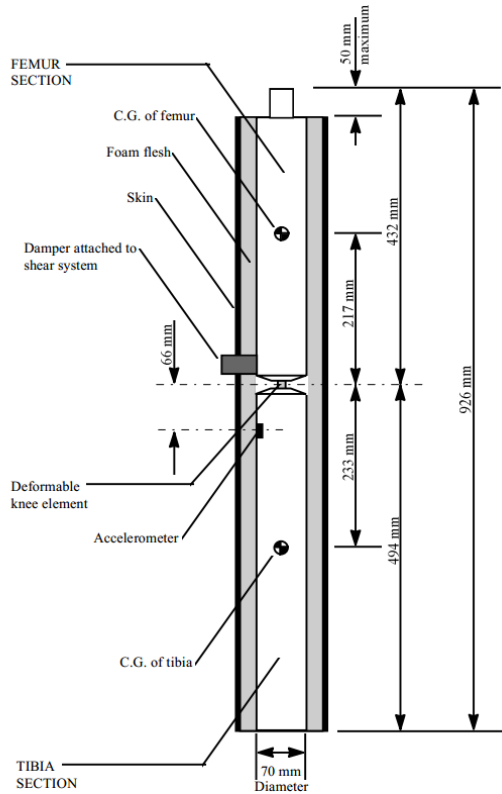
Figure A3. TRL Legform Instrumentation.
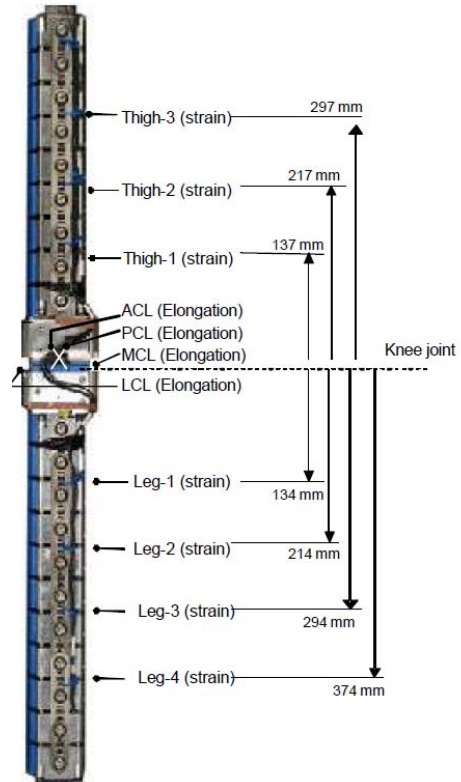
Figure A4. Flex PLI Instrumentation.

Xu, 13

APPENDIX B: TEST CONFIGURATIONS

Nine test configurations with the TRL legform and its alignment with the fixture are presented in Figure B1. The configurations with the Flex PLI are similar. The distances from the bottom of the legform to the ground are different for the two legforms: 25mm for the TRL legform and 75mm for the Flex PLI according to the test protocols for the standard tests. With the additional information provided in Tables 1 and 2, as well as in Figures A3 and A4, the positions of the transducers in the legforms with respect to the test fixture can be obtained.

| Configuration 1 A1B1C1D1 | Configuration 2 A1B2C2D2 | Configuration 3 A1B3C3D3 | Configuration 4 A2B1C2D3 | Configuration 5 A2B2C3D1 |
| Configuration 6 A2B3C1D2 | Configuration 7 A3B1C3D2 | Configuration 8 A3B2C1D3 | Configuration 9 A3B3C2D1 | |
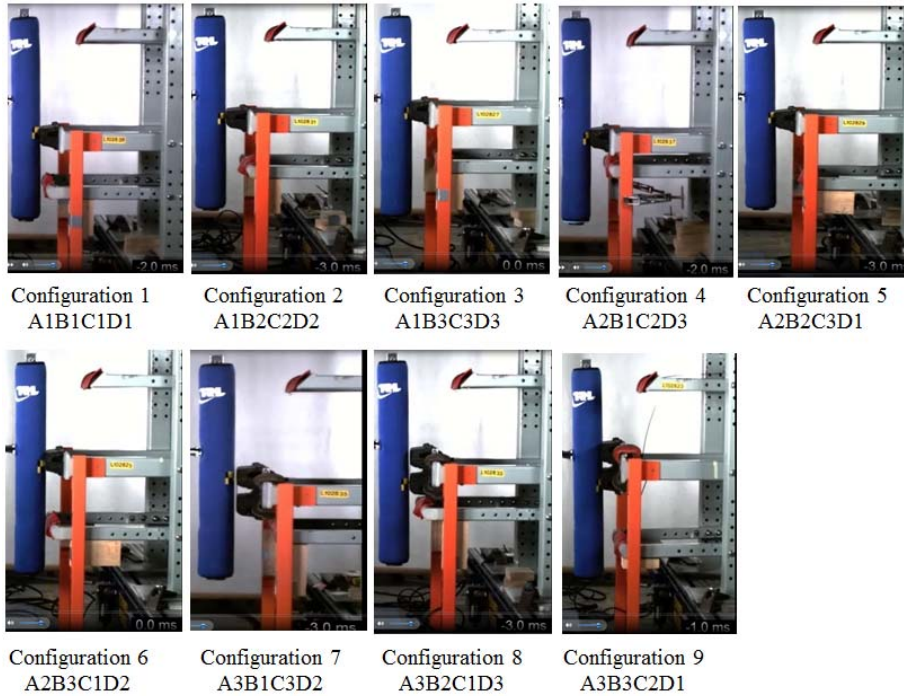
Figure B1. Nine Test Configurations.

APPENDIX C: ILLUSTRATION OF LOAD AND MOMENT TO THE LEGFORM

The moment distribution estimated from elementary linear beam theory for a beam subjected to concentrated and distributed loads is shown in the Figure C1. F_{kn} represents the force from the knee and w_1 and w_2 represent the inertial loading distributions.

$$M_1 = w_1 l_1^2/2 + F_{kn} l_1$$

$$M_2 = w_2 l_2^2/2$$
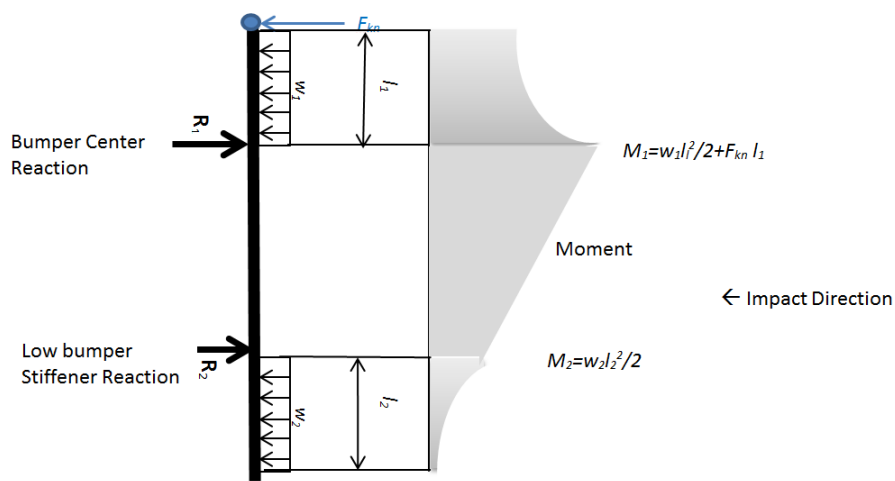
Figure C1. Illustration of Moments in a Beam.

APPENDIX D: TEST RESULTS

Peak Moment Response and Signal to Noise Ratio

Peak responses (absolute peak values) for four tibia moments from the Flex PLI are presented in Figure D1.
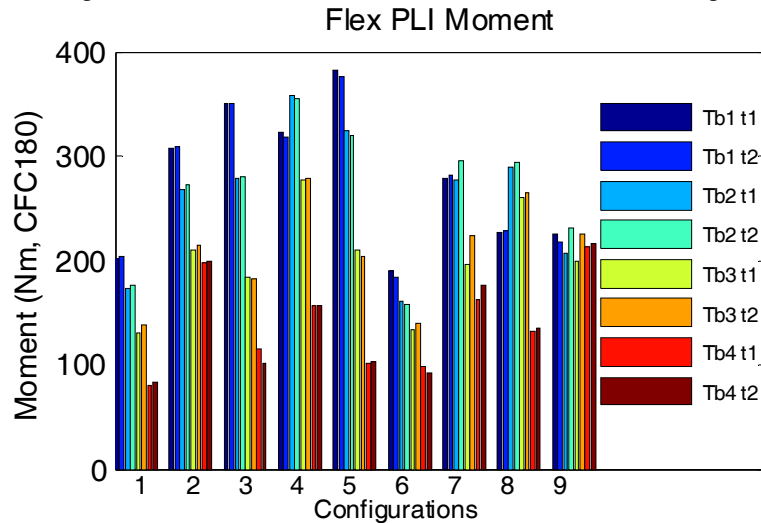
Figure D1. Peak Moments from the Flex PLI.

Signal to noise ratios, S/Ns, are contained in Table D1. The S/Ns for each factor level are in Table D2. The procedure to compute the S/Ns from B1, B2, B3, C1, C2, C3, D1, D2, and D3 are similar: take the S/Ns from the three configurations that include a factor at the same level, and then average them. As an example, when calculating the effect from factor B1 for parameter Tb1 (column 5), the S/N values in Table D1 from configurations 1, 4, and 7 (rows 3, 6, and 9) are used.

There is a slight difference in calculating the effects from factor A, considering A2=A1 in this series of tests. When calculating the effects from A1, the average of six S/N values from six configurations including A1 is the S/N value from A1. The calculation of S/N from A3 is the same as those from the Bs, Cs, and Ds. Once the S/Ns from A1 and A3 were obtained, the S/N from A2 is just the average of the S/Ns from A1 and A3.

Table D1.
Signal Noise Ratios from the TRL and the Flex PLI Legforms.

	Acc	Angle	Shear	Tb1	Tb2	Tb3	Tb4	MCL	ACL
Configuration									
1 A1B1C1D1	-43.2	-18.3	-7.4	-46.2	-44.8	-42.6	-38.2	-20.8	-16.8
2 A1B2C2D2	-47.4	-17.4	-16.2	-49.8	-48.6	-46.5	-45.9	-20.5	-19.3
3 A1B3C3D3	-47.0	-29.3	-9.2	-50.9	-48.9	-45.3	-40.7	-29.6	-21.7
4 A2B1C2D3	-46.2	-15.2	-16.4	-50.1	-51.0	-48.9	-43.9	-19.4	-15.5
5 A2B2C3D1	-47.0	-27.0	-18.3	-51.6	-50.1	-46.3	-40.2	-26.5	-20.4
6 A2B3C1D2	-47.8	-11.0	-8.4	-45.4	-44.1	-42.7	-39.6	-22.0	-16.7
7 A3B1C3D2	-40.4	-16.6	-12.7	-49.0	-49.1	-46.4	-44.6	-22.4	-16.0
8 A3B2C1D3	-48.4	-12.2	-13.7	-47.1	-49.3	-48.4	-42.5	-20.1	-18.9
9 A3B3C2D1	-43.0	-23.9	-6.3	-46.9	-46.8	-46.6	-46.6	-25.0	-19.9

Table D2.
Signal Noise Ratios Affected by Different Control Factors and Levels.

Factor	Acc	Tb1	Tb2	Tb3	Tb4	Angle	MCL	Shear	ACL
A1	-46.4	-49.0	-47.9	-45.4	-41.4	-19.7	-23.1	-12.7	-18.4
A2	-45.2	-48.3	-48.2	-46.2	-43.0	-18.6	-22.8	-11.8	-18.3
A3	-43.9	-47.7	-48.4	-47.1	-44.6	-17.6	-22.5	-10.9	-18.2
B1	-43.3	-48.4	-48.3	-46.0	-42.2	-16.7	-20.8	-12.2	-16.1
B2	-47.6	-49.5	-49.4	-47.1	-42.9	-18.8	-22.3	-16.1	-19.5
B3	-45.9	-47.7	-46.6	-44.8	-42.3	-21.4	-25.5	-8.0	-19.4
C1	-46.5	-46.3	-46.1	-44.5	-40.1	-13.8	-20.9	-9.8	-17.5
C2	-45.5	-48.9	-48.8	-47.3	-45.5	-18.8	-21.6	-13.0	-18.2
C3	-44.8	-50.5	-49.4	-46.0	-41.8	-24.3	-26.1	-13.4	-19.4
D1	-44.4	-48.2	-47.3	-45.2	-41.7	-23.1	-24.1	-10.7	-19.0
D2	-45.2	-48.1	-47.3	-45.2	-43.4	-15.0	-21.6	-12.4	-17.3
D3	-47.2	-49.4	-49.8	-47.5	-42.4	-18.9	-23.0	-13.1	-18.7

Shape and Magnitude Correlations

The results for shape and magnitude correlations are presented in Figures D2 to D5. The green lines are the repeatable criterions and the red lines are the non-repeatable criterions in those figures (conf.=configurations).
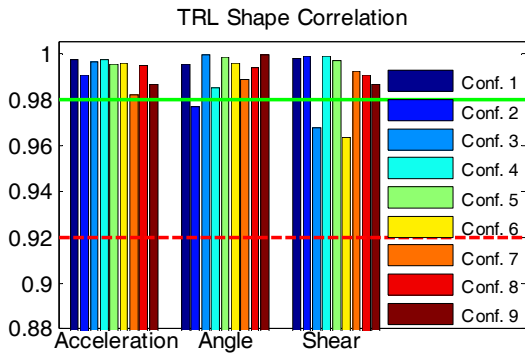
Figure D2. Shape Correlations (TRL).
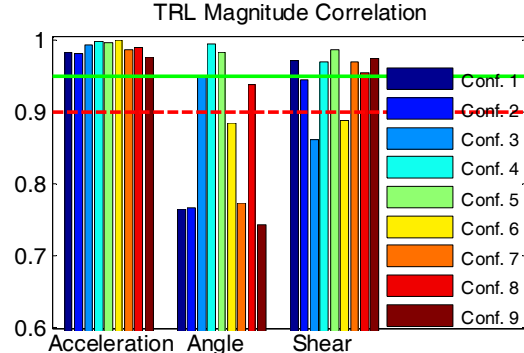
Figure D3. Magnitude Correlations (TRL).
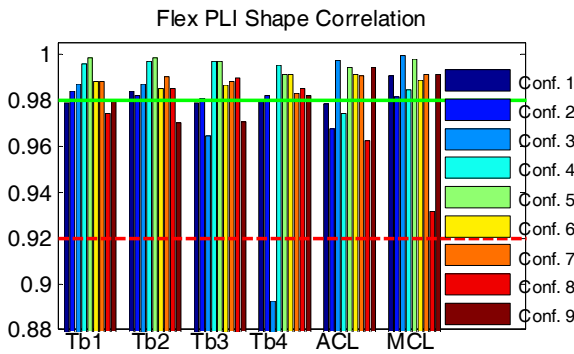
Figure D4. Shape Correlations (Flex PLI).
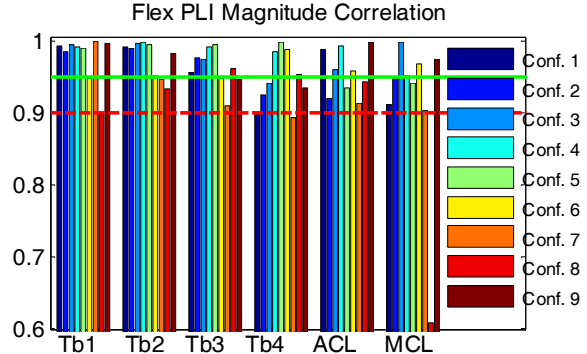
Figure D5. Magnitude Correlations (Flex PLI).

Selected Time Histories

The time histories from test configuration 4 for nine measurements of both legforms are presented in Figure D6 to illustrate the repeatable time-histories. The time histories for the bending angles from test configuration 2 and MCL from test configuration 8 are presented in Figures D7 and D8 to illustrate the non-repeatable time-histories.
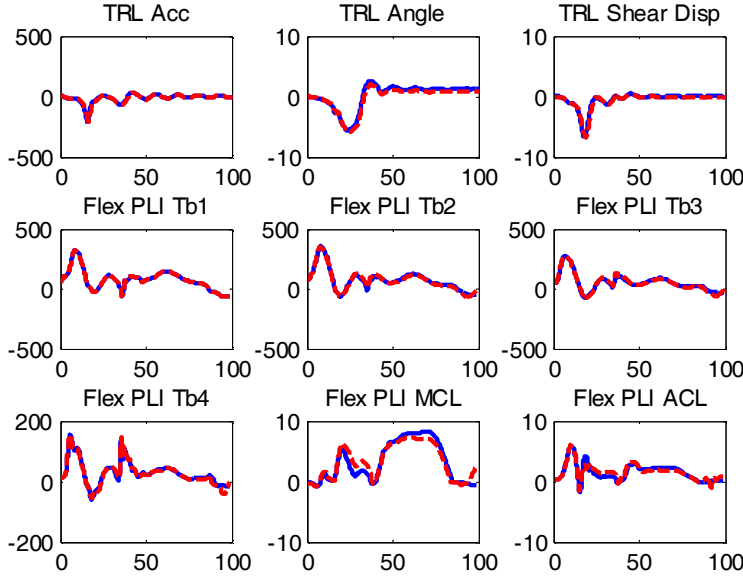
Figure D6. Nine Measurement Response Time-histories from Test Configuration 4.
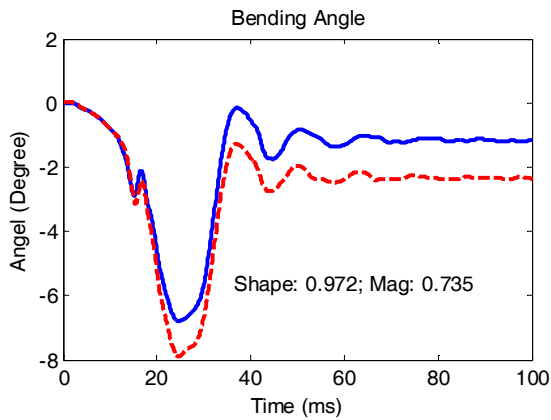
Figure D7. Bending Angles from Test Configuration 2.
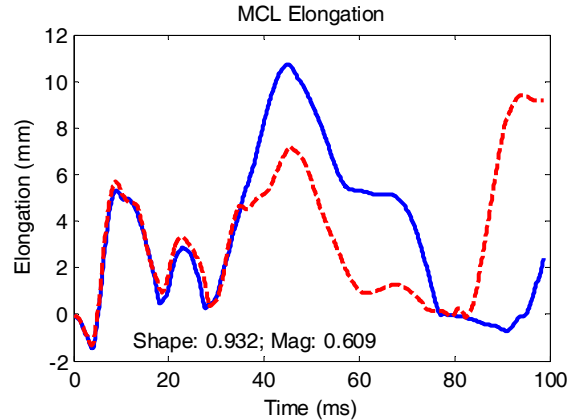
Figure D8. MCLs from Test Configuration 8.

APPENDIX E: SHAPE AND MAGNITUDE CORRELATION METHOD

Definitions

Given two signals denoted as, X: x_i; and Y: y_i. The definitions for the shape correlation and magnitude correlation between X and Y are given in the following.

1.   Norm $||X|| = \sqrt{\sum x_i^2}$; $||Y|| = \sqrt{\sum y_i^2}$;
     The average of the two is
     $Mxy = (||X|| + ||Y||)/2;$ (E1)

2.   *Shape* correlation:

In general, the shape correlation is defined as

$$\max(\sum_j x_i * y_{i+j}/(||X|| * ||Y||)) \qquad\qquad\qquad (E2)$$

3. Magnitude correlation: $Mx= ||X|| /Mxy;$ $My= ||Y|| /Mxy;$ $Mx+My=2$ (E3)

It should be noted that one of the magnitudes is greater than or equal to one and the other less than or equal to one. Magnitude that is less than or equal to one is used throughout this study.

Repeatability Standards

Two signals with both the shape correlation greater than 0.98 and the magnitude correlation greater than 0.95 are deemed to have acceptable repeatability. Two signals with the shape correlation less than 0.92 or the magnitude correlation less than 0.9 are deemed to have unacceptable repeatability. Two signals with the shape correlation between 0.92 and 0.98 and the magnitude correlation of 0.9 or above, or with the magnitude correlation between 0.9 and 0.95 and the shape correlation of 0.92 or above are deemed to have marginal repeatability.

Figures E1 illustrated the signals that have both repeatable shape and magnitude correlations (shape > 0.98 and magnitude >95) for any set of two curves. Figures E2 illustrated the signals that have both non-repeatable shape and magnitude correlations (shape < 0.92 and magnitude <0.9) for any set of two curves.
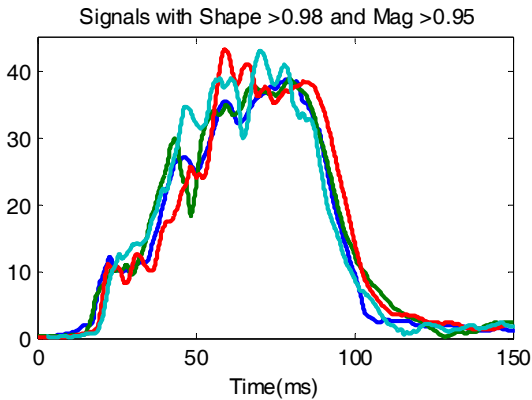
Figure E1. Repeatable Signals.   *Figure E2. Non-repeatable Signals.*
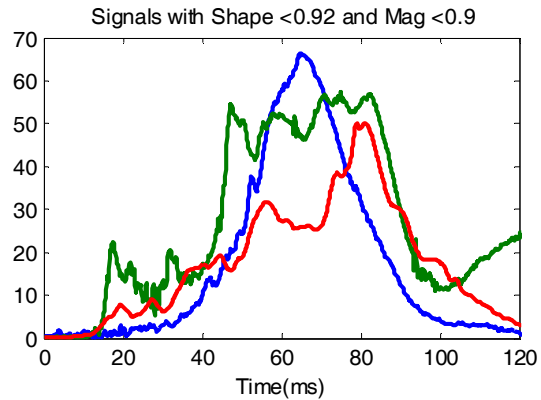
IMPROVEMENT OF THE PROTECTION OF LOWER EXTREMITIES OF VULNERABLE ROAD USERS IN THE EVENT OF A COLLISION WITH MOTOR VEHICLES

Oliver Zander
Marcus Wisch
Federal Highway Research Institute (BASt)
Germany

Dirk-Uwe Gehring
BGS Boehme & Gehring GmbH
Germany

ABSTRACT

Since the beginning of the testing activities related to passive pedestrian safety, the width of the test area being assessed regarding its protection level for the lower extremities of vulnerable road users has been determined by geometrical measurements at the outer contour of the vehicle. During the past years, the trend of a decreased width of the lower extremity test and assessment area realized by special features of the outer vehicle frontend design could be observed. This study discusses different possibilities for counteracting this development and thus finding a robust definition for this area including all structures with high injury risk for the lower extremities of vulnerable road users in the event of a collision with a motor vehicle.

While Euro NCAP[1] is addressing the described problem by defining a test area under consideration of the stiff structures underneath the bumper fascia, a detailed study was carried out on behalf of the European Commission, aiming at a robust, world wide harmonized definition of the bumper test area for legislation, taking into account the specific requirements of different certification procedures of the contracting parties of the UN/ECE[2] agreements from 1958[3] and 1998[4].

This paper details the work undertaken by BASt, also serving as a contribution to the TF-BTA[5] of the UN/ECE GRSP[6], towards a harmonized test area in order to better protect the lower extremities of vulnerable road users. The German In-Depth Accident Database GIDAS is studied with respect to the potential benefit of a revised test area. Several practical options are discussed and applied to actual vehicles, investigating the differences and possible effects. Tests are carried out and the results studied in detail. Finally, a proposal for a feasible definition is given and a suggestion is made for solving possible open issues at angled surfaces due to rotation of the impactor.

The study shows that, in principle, there is a need for the entire vehicle width being assessed with regard to the protection potential for lower extremities of vulnerable road users. It gives evidence on the necessity for a robust definition of the lower extremity test area including stiff and thus injurious structures at the vehicle frontend, especially underneath the bumper fascia.

The legal definition of the lower extremity test area will shortly be almost harmonized with the robust Euro NCAP requirements, as already endorsed by GRSP, taking into account injurious structures and thus contributing to the enhanced protection of vulnerable road users.

---

[1] Euro NCAP: European New Car Assessment Programme
[2] UN/ECE: United Nations Economic Commission for Europe
[3] Agreement concerning the adoption of uniform technical prescriptions for wheeled vehicles, equipment and parts which can be fitted and/or be used on wheeled vehicles and the conditions for reciprocal recognition of approvals granted on the basis of these prescriptions
[4] Agreement concerning the establishing of global technical regulations for wheeled vehicles, equipment and parts which can be fitted and/or be used on wheeled vehicles
[5] TF-BTA: Task Force Bumper Test Area
[6] GRSP: Working Party on Passive Safety

After finalization of the development of a torso mass for the flexible pedestrian legform impactor (FlexPLI) it is recommended to consider again the additional benefit of assessing the entire vehicle width.

INTRODUCTION

Since the year 2000, the Japan Automobile Research Institute (JARI) has been developing a new flexible pedestrian legform impactor (FlexPLI) with the purpose of properly assessing the protection potential of vehicle frontends in terms of passive pedestrian safety. From the year 2005 on a Technical Evaluation Group[7] had evaluated the impactor towards introduction within legislation related to pedestrian safety. Subsequently, since 2011 an Informal Group[8] of the Working Party on Passive Safety has been working on a framework and the preconditions for including the flexible pedestrian legform impactor within the global technical regulation on pedestrian safety (GTR No. 9) as well as the UN regulation on pedestrian safety (UN-R 127). The impactor with humanlike kinematic behaviour and biofidelic human responses in the knee and the tibia area has been found ready for legislation by working party 29[9] of UN/ECE. Subsequently, the FlexPLI has been introduced within the 01 series of amendments of UN-R127 (UN/ECE, 2015). Due to an amendment of framework Directive 2007/46/EC of the European Parliament and of the Council (European Union, 2007), pedestrian protection requirements for the purpose of european type approval can be either tested according to Regulation (EC) No. 78/2009 in conjunction with Commission Regulation (EC) No. 631/2009 (European Union, 2009) or according to UN-R 127 in conjunction with UN-R 13H, latter one ruling the type approval provisions of passenger cars with regard to braking. Therefore, since 22 January 2015 and during a transitional period that lasts until 1 September 2017 all new vehicles to be type approved according to UN-R127 can be subjected to tests with the FlexPLI instead of the lower legform impactor according to EEVC[10] (UN/ECE, 2015). After the expiration of this transition period the FlexPLI is to be used mandatorily for type approval tests according to UN-R 127.

In parallel to the work performed by the Informal Group, the Task Force Bumper Test Area, chaired by the European Commission, was established under the umbrella of the Informal Group. Aim of this Task Force was to re-define the bumper area that is subjected to tests with the lower legform impactor according to UN-GTR 9 or UN-R 127 respectively, in order to avoid small bumper test areas that prevent large zones of the bumper from being tested, and to counteract some manufacturer's practice of downsizing the width by design means of the outer vehicle contour.

This paper details the investigations performed by the Task Force and in particular the contributions of BASt that finally led to the proposal for the supplement 1 of the 01 series of amendments to UN-R 127 (UN/ECE, 2014) that was endorsed by GRSP at its December 2014 session.

In case of angled test areas a rotation of the lower legform impactor may occur which is, to some extent, not always coincident with the behavior of the human leg, possibly leading to unrealistic test results. In order to limit this possible rotation a pedestrian torso mass may be applied to the lower legform impactor. However, the ongoing validation of the torso mass still needs to be finalized, including tests to a broad variety of vehicle frontend designs.

PROBLEMS RELATED TO UN-GTR9 (PHASE 1) AND UN-R 127 (00)

The UN Regulation on pedestrian safety as transposition of the Global Technical Regulation No. 9 into national legislation entered into force in November 2012 (UN/ECE, 2013). The Regulation defines performance requirements for passenger cars with regard to the protection potential of their frontends when subjected to impactor tests with the adult and child headform impactors against the bonnet and the upper or lower legform impactor against the bumper fascia.

---

[7] Flex-TEG: Flexible Pedestrian Legform Impactor Technical Evaluation Group
[8] IG GTR9-PH2: Informal Group on phase 2 of GTR No. 9
[9] WP.29: Working Party 29 / World Forum for Harmonization of Vehicle Regulations
[10] EEVC: European Enhanced Vehicle-safety Committee

The test area defined for the legform to bumper test is described by the part of the bumper fascia that is limited by two points 66 mm laterally inboard of the corners of bumper, see Figure 1a. The corners of bumper are defined as the vehicle's points of contact with a vertical plane making an angle of 60 degrees with the vehicle vertical longitudinal centerplane.

In the past years, the application of specific vehicle design features resulted in a limitation of the bumper test area defined by legislation, as can be seen in Figure 1b. It is obvious that the definition of the corner of bumper which in the end defines the bumper test area rather depends on the outer contour of the vehicle than on the underlying hard structure that is responsible for the ocurrence of lower leg injuries that should be mitigated by fulfilling the requirements described in the Regulation.

Figures 1a (left) and b (middle and right). Bumper test area according to GTR9 / UN-R 127 and its limitation by design means.

To counteract the phenomenon of misrepresenting the bumper test area by means of the current procedure, based on the outer vehicle design, the task force bumper test area elaborated different options for an appropriate revision that will be described in the following.

EURO NCAP MARKUP PROCEDURE

The problem of defining the bumper test area using vertical contact planes was already recognized by the technical working group of the European New Car Assessment Programme (Euro NCAP) in 2008. Until version 4.2 of the pedestrian testing protocol the width of the bumper test area was, also in line with the european legislation, in principle limited by the corners of bumper. Only in case of potentially injurious structures outboard of the described area Euro NCAP reserved the right of performing tests to those structures (Euro NCAP, 2008). However, an assessment of the results was not explicitly foreseen. An ad hoc group of Euro NCAP discussed the problems related to this procedure and concluded that, in principle, injurious structures outboard the corners of bumper shall be tested and the results shall be used for the final vehicle assessment. Additionally, the minimum distance requirements of 66 mm from the corners of bumper to define the bumper test area were removed from the protocol from its version 4.3 onwards (Euro NCAP, 2009). The bumper test area was then defined as the area limited by the corners of bumper or the outermost ends of the bumper beam/lower rails/cross beam structures, whichever area was wider. Figure 2a illustrates the markup of the bumper test area that was further divided into thirds, each of them subdivided into halves, until the end of 2013. As from 2014 onwards, along with the introduction of the FlexPLI, a homogeneous grid markup procedure for the legform area was introduced. However, the width of the test area basically remained unchanged. Additionally, since the introduction of the grid markup, in case of the distance between the outermost grid points and the end of the test area being greater than 50 mm, an additional grid point is to be marked at a lateral distance of 50 mm to the last grid point onto the upper bumper reference line. One example for the current Euro NCAP lower legform markup is depicted in Figure 2b.
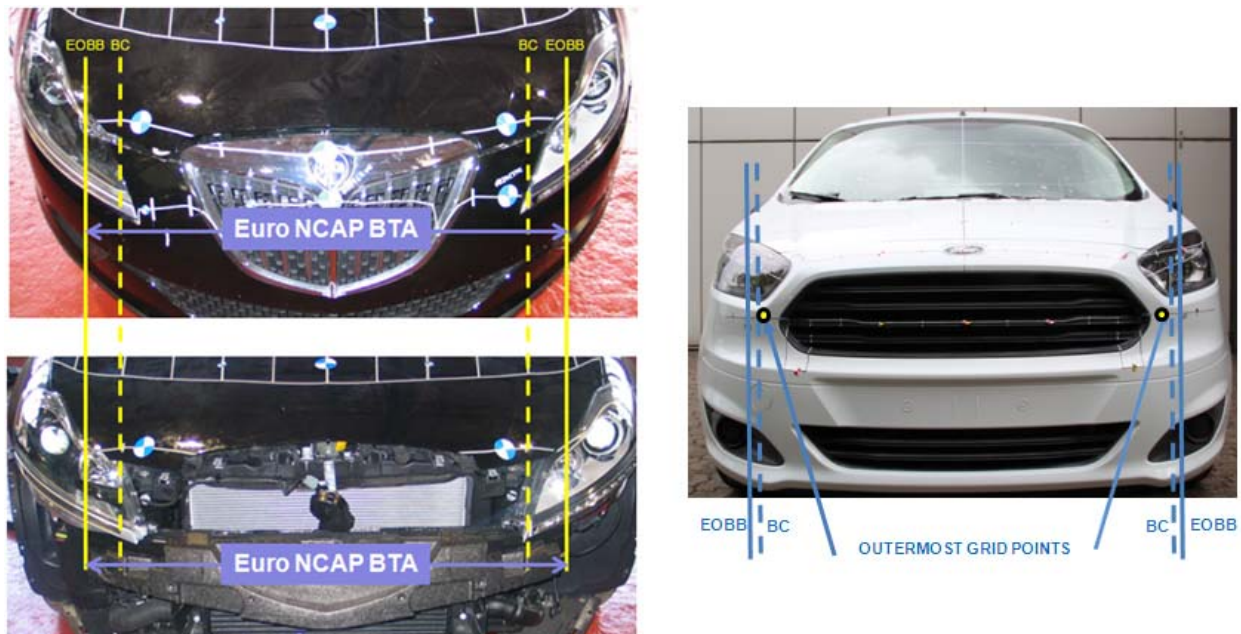
Figures 2a (left) and b (right). Euro NCAP worst point and grid markup.

USE OF WHOLE VEHICLE WIDTH

Already during the discussions within the Euro NCAP ad hoc working group, BASt brought up a proposal to modify the bumper test area in a way that, in principle, the possibility is given to test, where appropriate, the entire width of the vehicle frontend. At that point in time, passenger cars were still tested according to the principle of worst point selection. Therefore, despite the provisions changed according to protocol version 4.3, the selection procedure of injurious points outside the bumper corners remained unclear. It was not further defined how far outboard a point was allowed to be selected; furthermore, no advice was given which point finally to be selected in case of the outermost point being equally but not more injurious as the remaining points. Also, the assessment procedure in case of selecting impact points outside the corners of bumper was not yet further specified, e.g. whether these points to be additionally assessed or to replace adjacent points, whether manufacturers were given the option to additionally nominate the adjacent sixths or whether the maximum number of points would increase. BASt concluded that an extension of the test area using the entire vehicle width (without mirrors) while sustaining the remaining markup procedure would be the most pragmatic way forward. The proposal would give Euro NCAP the possibility of testing, where appropriate, outside a test area described by the outer vehicle contour without further essential changes to the test and assessment procedure. However, it was also suggested that in cases where the tangential vertical plane making an angle of less than 60 degrees to the vehicle longitudinal centerplane a test could possibly lead to unrealistic test results due to a high rotation around the yaw axis and the physical limitations of the impactor.

In the course of the work performed by the TF-BTA, the description of the bumper test area based on the entire width of the vehicle was examined again in detail by Zander et al (2014).

Accident data

Passenger car to pedestrian accidents with maximum two parties involved were the starting point for a study of German in-depth road accident data from the years 2000 until 2012 using GIDAS. The study focused on accidents with pedestrian impact locations between the most forward vehicle part and 20 percent of the total vehicle length rearward under consideration of injury causing vehicle parts being located on the vehicle frontend only, i.e. bumpers, grilles, headlamps, front spoilers, license plates and indicators. In total, 567 cases were found fulfilling the given prerequisites, with an equal distribution of first pedestrian contact along the passenger car front in crashes with at least one injury suffered from contact with a part of the vehicle frontend, as depicted in Figure 3:
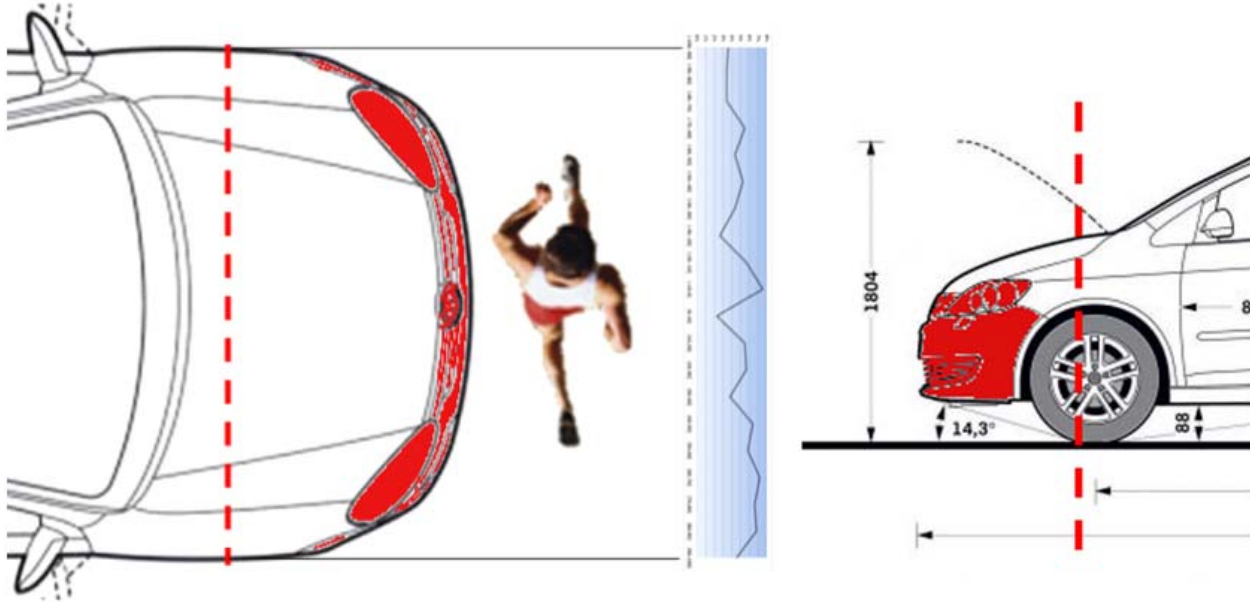
Figure 3. Passenger car to pedestrian impact distribution (2000-2012) extracted from GIDAS database.

Altogether, the study gives no indication for neglecting outboard areas of passenger cars being less impacted by pedestrians during accidents.

Test data

Besides the impact distribution in real world accidents, the significance of the impacted areas in terms of injury causation was examined in more detail. Within the Euro NCAP test programme, injurious points, reflected by impactor readings beyond the limits for the introduced injury criteria, have been continously found outside the test area described by the corners of bumper. It was thus concluded that the area to be considered should include all injurious structures underneath the bumper cover which are in most cases not indicated by the outer design. Therefore, a consideration of those structures, e.g. by dismantling of the fascia was found indispensable for a detection of hard structures.

Furthermore, a comparative test that was conducted outside the corners of bumper was examined with respect to the validity of the kinematics, see Figure 4. High speed film analysis revealed that until the timing of maximum readings the kinematic behaviour was comparable to the one during the baseline test on a location inside the corners of bumper.
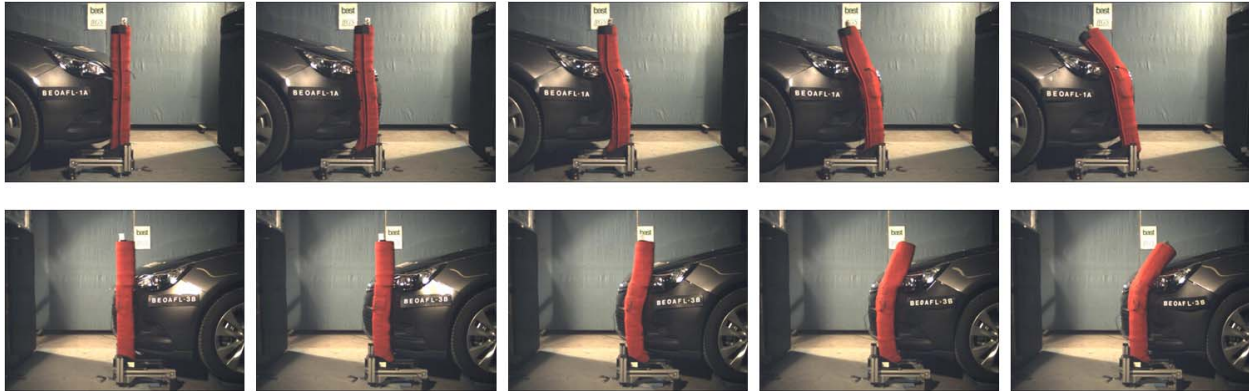
Figure 4. FlexPLI kinematics during biofidelic impact phase inside (above) and outside (below) corners of bumper.

MODIFICATION OF DEFINITION OF CORNERS OF BUMPER

Apart from assessing the entire vehicle width by testing injurious structures of the vehicle frontend, TF-BTA discussed possibilities for modifying the corners of bumper definition.

The first option investigated was related to changing the angle between the vertical tangential planes and the vehicle vertical longitudinal centerplane from 60 to 45 degrees and thus enlarging the test area to a certain extent. This option that was investigated in detail within a study on behalf of the European Commission by Carroll et al. (2014) was already brought forward by the Transport Research Laboratory TRL during their studies for the Working Group on Pedestrian Safety (WG 17) of the European Enhanced Vehicle-Safety Committee in 2002. At that point in time, the proposal was justified with actual vehicles partly having very small bumper test widths, just between the inner ends of the headlights. It was noted that the performance of the legform at impact points with these tangential surface angles could be limited due to spinning of the impactor; however, the legform was expected to still be able to indicate particularly dangerous structures. Not testing these areas would open the door for putting bumper supports, longitudinal members or other hard structures in a non-evaluated area. (TRL, 2002)

The second option was evolved from the current corner of bumper definition described in US bumper standard 49 CFR part 581 (NHTSA, 2011). Instead of a vertical plane, a vertical corner gauge with the dimensions of the face of the impact device as described in part 581, making an angle of 60 degrees to the vehicle vertical longitudinal centerplane, is contacting the vehicle frontend with its vertical centerline while its horizontal centerline is moved between heights of 75 mm and 1003 mm above ground level, representing the lower and upper end of the FlexPLI during an impact, but not falling below the lower bumper reference line and not exceeding the upper bumper reference line. The outermost contact point between the corner gauge and the fascia is then defining the corner of bumper. In the end, the test area is limited by the corners of bumper minus a lateral distance of 42 mm on both sides of the car, taking into account half of the width of the FlexPLI femur and tibia section. This distance requirement was meant to avoid as far as possible any rotation or sliding of the impactor possibly leading to unrealistic test results during an impact against angled surfaces.

In a final stage, the second option was further modified, changing the original corner gauge dimensions to a 236 mm * 236 mm square.

BASt investigated the consequences in case of modifying the markup procedure by just using the corners of bumper defined by the modified corner gauges. When checking the robustness of the procedure against any changes in the outer contour, BASt found that by simple design features the test area could still be narrowed in future design concepts, as illustrated in Figure 5:

Figure 5. Corner point due to gauge contact with daytime running light intake.

Although the example given shows a comparatively small difference between the definition using the end of the bumper beam and the corner of bumper (12 mm plus 42 mm as distance requirement on each side), this design exemplarily demonstrates that in case of an inboard movement of the intake for the daytime running lights (DRL) the width of the test area could be easily minimized significantly. BASt concluded again the indispensability of defining the bumper test area using the underlying injurious structures. In a first step, addressing nowadays vehicle frontends, it seems reasonable to define the test area using the width of the bumper beam. A robust definition of the bumper beam is given by the Research Council for Automobile Repairs (RCAR). In the RCAR bumper test procedures it is described as the structural cross member under the bumper fascia protecting the front or rear of the vehicle, not including foam, cover support or pedestrian protection devices. The bumper beam width is to be measured from the outermost left to the outermost right section of the bumper beam, but only taking into account outer ends meeting the qualifying bumper beam heights. Latter ones are to be measured from a vertical plane contacting the beam up to a distance of 10 mm in direction of the profile (RCAR, 2010):
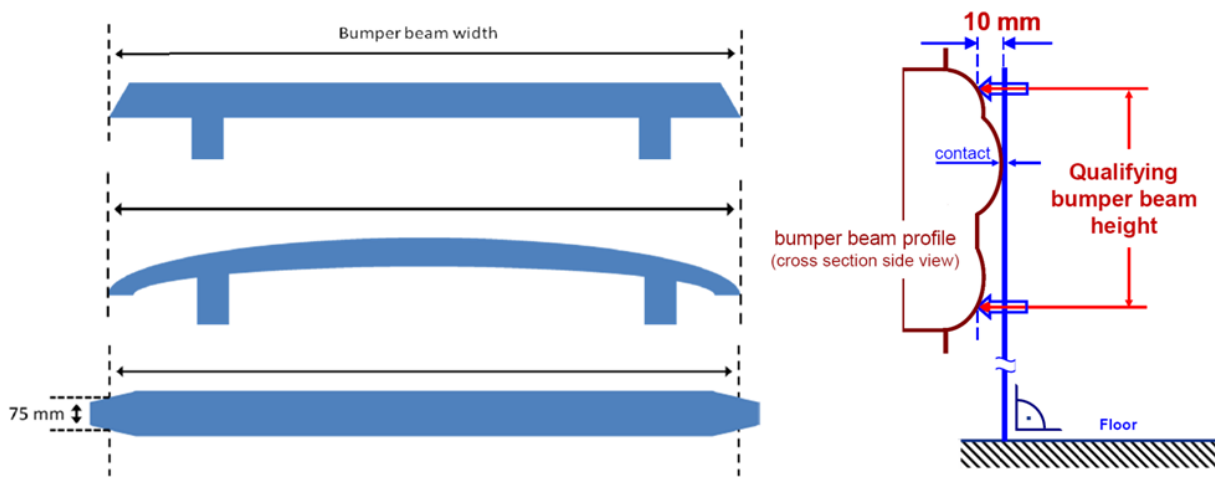
Figure 6. Definition of the bumper beam width (RCAR, 2010).

COMBINATION OF MARKUP REQUIREMENTS

BASt examined the test areas resulting from the different markup procedures and compared them with the markup according to GTR9 (Phase 1) or UN-R 127 (00) respectively. Figure 7 exemplarily illustrates the differences in width of test areas:

Figure 7. Comparison of different markup procedures and resulting test area widths.

The example given in Figure 7 results in the different markups having a range of 530 mm just between the corners of bumper defined by 45 degree planes and the GTR9 (Phase 1) / UN-R 127 (00) markup. The difference between the bumper beam width and the markup with corner gauges is still 159 mm.

The Task Force Bumper Test Area concluded its work in forwarding two different proposals to GRSP for an amendment of GTR9 (Phase 2) and a supplement of UN-R 127.01. The first proposal reflects, while keeping the angle between vertical tangential plane and vehicle vertical longitudinal centerplane unchanged, the idea of defining the bumper test area by a revision of the bumper of corner definition only, using vertical 236 mm * 236 mm corner gauges and laterally moving 42 mm inboard on both sides, see Figure 8. The second proposal adds to the corner gauge definition a second definition of the bumper test area described by the width of the bumper beam. The maximum of both definitions is then to be used to describe the bumper test area:
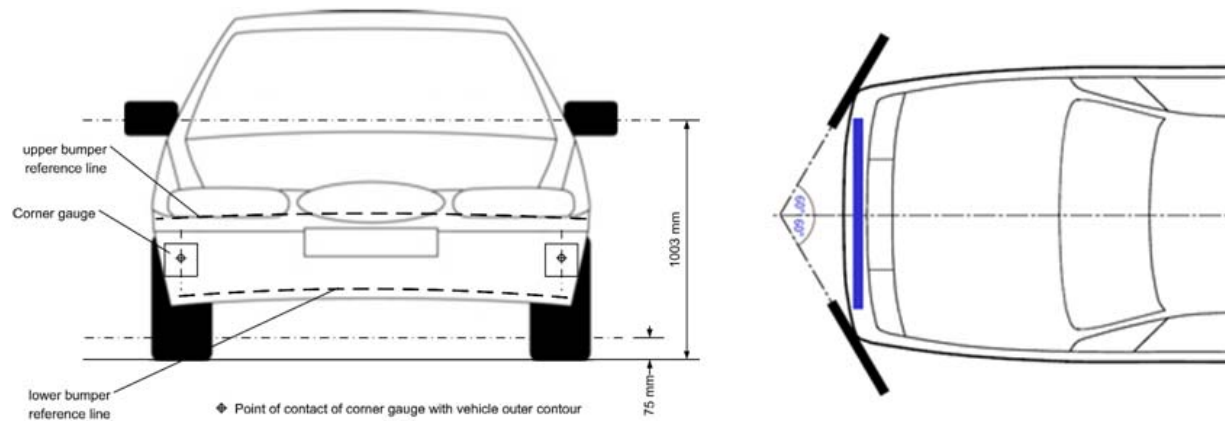
Figure 8. Definition of bumper test area endorsed by GRSP in December 2014 (UN/ECE, 2014).

It has to be noted that supplement 1 to the 01 series of amendments to UN-R127 relates to the FlexPLI only. Therefore, if tested in accordance with UN-R 127 in its original version, the tests conducted with the EEVC lower legform impactor will be limited to the bumper test area defined by the vertical 60 degree planes, whose contact points afterwards laterally moving 66 mm inboard on each side of the vehicle.

OUTLOOK

Real world accident data has shown that pedestrians are generally impacted by locations along the entire vehicle width. Test results with the FlexPLI have proven that in many cases injurious impact locations occur outside the test area described by the corners of bumper. However, technical services need to take care of the fact that on angled surfaces a rotation of the impactor can lead to sometimes unrealistic test results. The rotation of the impactor that is not reflected to that extent by lower extremity rotation as seen in road traffic accidents, is expected to be compensated by the application of an upper body mass, representing the mass of the pedestrians' torso during an accident. An upper body mass for the FlexPLI has been developed within the European FP6 project APROSYS (Advanced PROtection SYStems) by Bovenkerk et al. (2009) and is being evaluated by Zander et al. (2011 and 2013). Subsequently, amongst other things, during the European FP 7 project AsPeCSS (Assessment methodologies for forward looking Integrated Pedestrian and further extension to Cyclist Safety Systems), BASt carried out comparative tests conducted with baseline FlexPLI and FlexPLI with applied UBM on angled vehicle frontend surfaces (Ferrer et al., 2014), see Figure 9:
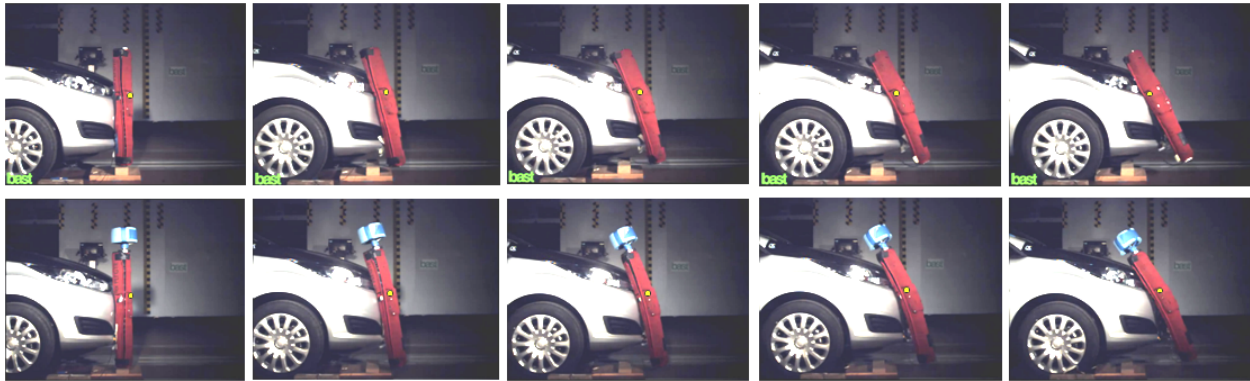
Figure 9. Influence of applied upper body mass during impact on oblique surface.

The depicted screenshots demonstrate that the application of an upper pedestrian mass can significantly reduce the rotation around its yaw axis as well as the sliding of the FlexPLI during impacts on angled areas, leading to an improved simulation of the lower extremity kinematics of a pedestrian. This observation can be underlined by the test results especially in the knee area:

Table1.
Comparative test with Flex PLI baseline and with applied UBM on oblique surface.

Impactor	Impact speed [m/s]	Tibia-1 BM [Nm]	Tibia-2 BM [Nm]	Tibia-3 BM [Nm]	Tibia-4 BM [Nm]	ACL-EL [mm]	PCL-EL [mm]	MCL-EL [mm]
FlexPLI	9,58	111,5	79,8	132,8	86,0	2,5	6,5	10,8
FlexPLI-UBM	9,69	206	154,4	136,9	65,0	7,1	7,1	22,1

y = 505 mm

DISCUSSION

In depth accident data gives evidence of an equal distribution of first pedestrian contact at the front of passenger cars in crashes with at least one injury suffered from contact with a part of the vehicle frontend (Zander et al., 2014). For vehicles with market launch after 2006, a further study of the German In Depth Accident Data (GIDAS) showed an even distribution of the injury severities outside the current bumper test area while having a higher portion of uninjured or slightly injured pedestrians inside the current bumper test area. (Fries et al., 2014). Thus it can be concluded that vulnerable road user safety improvements are focused on the currently assessed areas. Also several stakeholders state the potentially injurious nature of hard structures outside the current bumper test area as defined in UN Regulation No. 127 and consequently confirm the need to assess the structural parts behind the bumper cover (Carroll et al., 2014).

During testing, injurious points have been continuously found outside test areas defined by measurements depending on the outer contour, especially at the ends of the bumper beam (Euro NCAP, 2012). Thus, the assessment of injury risks for vulnerable road users should basically consider the entire vehicle width. However, if a limitation of the test area is necessary, at least no potentially injurious structures should be prematurely excluded from the test area.

The contractor of the European Union states that it would be entirely reasonable to expect that vehicle front-end designs would react to any definition only related to the outer contour and in the future the bumper test area widths return to something similar as todays. Thus, it could be imagined that the same issue may occur again in several months or years (Carroll et al., 2014). The presented study already gives an example of an actual vehicle where outer design features could be easily used for downsizing the bumper test area, see Figure 5.

As procedures based on the outer vehicle contour do not necessarily include the relevant injurious vehicle structures (e.g. bumper beam), at least the entire bumper beam should be included within the test area.

It has been proven that the flexible pedestrian legform impactor works outside the current bumper test area as defined in UN Regulation No. 127, e.g. within the width of the bumper beam (Zander et al., 2014-2). A robust definition for the bumper beam is provided by RCAR (2010).

The above mentioned issues show that the use of the bumper beam for defining the BTA is inevitable.

The work undertaken within the TF-BTA resulted in different options on how to define the vehicle bumper area to be subjected to tests with the lower legform impactor. All options are basically following two different philosophies, either describing the test area by means of the outer vehicle contour or by elements of the underlying stiff structures. Starting from leaving the area as it is described within current legislation, the consequences of a modification of the angles between the tangential vertical planes and the vertical longitudinal vehicle centerplane from 60 degrees to 45 degrees as well as the modificaton of the markup tool for the corner of bumper definition from planes to gauges were investigated as means of leaving the test area definition depending on individual single details of the outer vehicle contour. A new definition of the test area using the ends of the bumper beam, following and harmonizing with the procedure that had been already introduced within Euro NCAP in 2009, reflects the philosophy of assessing the underlying injurious structures rather than the bumper fascia. A third philosophy aims at addressing the real world accident data which results in a homogeneous lateral impact distribution of pedestrians over the entire vehicle width, which therefore is suggested to be assessed. It thus should be, in principle, left to the testing authority to test over the entire width, considering the applicability of tests on angled structures.

CONCLUSIONS

The present study gives evidence of the bumper test area of passenger cars currently assessed within the type approval procedures in terms of pedestrian safety not anymore adequately addressing the purpose of protecting the lower extremities of pedestrians involved in accidents with passenger cars, mainly due to the downsizing of the test area width by means of outer vehicle design in many cases. It was demonstrated that any proposed method for a revision of the test area using tools related to the outer contour will most unlikely be of a permanent effect in terms of avoiding small test areas. Requirements for passive pedestrian safety unconditionally need to include the stiff structures, mainly located under the bumper fascia, which are responsible for injuries to the lower extremities. Therefore, for the time being, the test area definition using the bumper beam is indispensable. However, in the long run, giving consideration to current accident data which shows an equal distribution of pedestrian impacts along the entire vehicle width, the technical services should be given the opportunity to assess the complete vehicle width. Following this procedure, in case of angled test areas a rotation of the lower legform impactor may occur which is, to some extent, not always coincident with the behavior of the human leg, possibly leading to unrealistic test results. In order to limit this possible rotation a pedestrian torso mass may be applied to the FlexPLI. However, further research is needed and the ongoing validation of the torso mass still needs to be finalized, including tests to a broad variety of vehicle frontend designs. It is recommended to introduce the test and assessment procedure for the entire vehicle width after final validation and evaluation of the upper body mass, limiting impactor rotation during impacts on angled surfaces.

REFERENCES

Bovenkerk J., Zander O. 2009. "Evaluation of the extended scope for FlexPLI obtained by adding an upper body mass." Deliverable D333H of the European FP6 research project on Advanced Protection Systems (APROSYS).
Carroll J A., Barrow A., Hardy B J., Robinson B. 2014. "Pedestrian legform test area assessment. Final Report. " Client Project Report CPR 1825 of the Transport Research Laboratory on behalf of the European Commission. Framework Contract Number 121/PP/2011/FC. 2014.

European New Car Assessment Programme. 2008. "Pedestrian Testing Protocol Version 4.2." Euro NCAP, June 2008.

European New Car Assessment Programme. 2009. "Pedestrian Testing Protocol Version 4.3." Euro NCAP, February 2009.

European New Car Assessment Programme (Ellway J.). 2012. "EC Task Force Legform Test Procedure" Doc TF-BTA-1-04 of 1st Meeting of the TF-BTA. 4 September 2012.

European Union. 2007. "Directive 2007/46/EC of the European Parliament and of the Council of 5 September 2007 establishing a framework for the approval of motor vehicles and their trailers, and of systems, components and separate technical units intended for such vehicles (Framework Directive)." Official Journal of the European Union, 09. October 2007.

European Union. 2009. "Regulation (EC) No 78/2009 of the European Parliament and of the Council of 14 January 2009 on the type-approval of motor vehicles with regard to the protection of pedestrians and other vulnerable road users, amending Directive 2007/46/EC and repealing Directives 2003/102/EC and 2005/66/EC." Official Journal of the European Union, 04. February 2009.

European Union. 2009. "Commission Regulation (EC) No 631/2009 of 22 July 2009 laying down detailed rules for the implementation of Annex I to Regulation (EC) No 78/2009 of the European Parliament and of the Council on the type-approval of motor vehicles with regard to the protection of pedestrians and other vulnerable road users, amending Directive 2007/46/EC and repealing Directives 2003/102/EC and 2005/66/EC." Official Journal of the European Union, 25 July 2009.

Ferrer A., del Pozo E., Rodarius C., Ott J., Zander O., Schaub S., Caspar M., Fredriksson R., Nuß F. 2014. „Experimental and virtual testing." Deliverable D3.2 of the European FP7 research project on Assessment methodologies for forward looking Integrated Pedestrian and further extension to Cyclist Safety Systems (AsPeCSS).

Fries A., Schenk T., Roth F. 2014. "Injury risk of lower leg outside of 30° tangent-area." Doc TF-BTA-7-09 of 7th Meeting of the TF-BTA. 29 August 2014.

National Highway Traffic Safety Administration (NHTSA). 2011. "49 CFR 581 – Bumper Standard." Code of Federal Regulations (annual edition), Title 49 – Transportation, Part 581 – Bumper Standard, 2011.

Research Council for Automobile Repairs (RCAR). 2010. "RCAR Bumper Test, Issue 2.0." Issue 2.0, September 2010, available on www.rcar.org.

Transport Research Laboratory (TRL). 2002. "Suggestions for EEVC WG 17 test procedures and for EC Draft Directive." EEVC WG 17 Doc 186. 20 May 2002.

United Nations Economic Commission for Europe. 2013. "Agreement Concerning the Adoption of Uniform Technical Prescriptions for Wheeled Vehicles, Equipment and Parts which can be Fitted and/or be Used on Wheeled Vehicles and the Conditions for Reciprocal Recognition of Approvals Granted on the Basis of these Prescriptions (Revision 2, including the amendments which entered into force on 16 October 1995). Addendum 126: Regulation No. 127 – Entry into force: 17 November 2012. Uniform provisions concerning the approval of motor vehicles with regard to their pedestrian safety performance." Website of the UN/ECE, Doc. ECE/TRANS/505/Rev.2/Add.126. 7 January 2013

United Nations Economic Commission for Europe. 2014. "Proposal for amendments to global technical regulation No. 9 (Pedestrian safety)" Website of the UN/ECE, 56th session of GRSP, 9-12 December 2014, Doc. GRSP-56-39.

United Nations Economic Commission for Europe. 2014. "Proposal for Supplement 1 to the 01 series of amendments to Regulation No. 127 (Pedestrian safety)" Website of the UN/ECE, 56th session of GRSP, 9-12 December 2014, Doc. GRSP-56-41.

United Nations Economic Commission for Europe. 2015. "Agreement Concerning the Adoption of Uniform Technical Prescriptions for Wheeled Vehicles, Equipment and Parts which can be Fitted and/or be Used on Wheeled Vehicles and the Conditions for Reciprocal Recognition of Approvals Granted on the Basis of these Prescriptions (Revision 2, including the amendments which entered into force on 16 October 1995). Addendum 126: Regulation No. 127 01 series of amendments to the Regulation – Date of entry into force: 22 January 2015. Uniform provisions concerning the approval of motor vehicles with regard to their pedestrian safety performance." Website of the UN/ECE, Doc. ECE/TRANS/505/Rev.2/Add.126/Rev.1. 4 February 2015

Zander O., Gehring D., Leßmann P. 2011. "Improved assessment methods of lower extremity injuries in vehicle-to-pedestrian accidents using impactor tests and full scale dummy tests." Paper no. 11-0079 of 22nd ESV conference proceedings.

Zander O., Pastor C., Leßmann P., Gehring D. 2013. "Towards a world-wide harmonized pedestrian legform to vehicle bumper test procedure." Paper no. 13-0175 of 23rd ESV conference proceedings.

Zander O., Wisch M., Gehring D.-U. 2014. "Proposal for a modification of the lower/upper legform to bumper test area in GTR9-PH2 and UN-R 127 01 series of amendments." Doc TF-BTA-6-07 of 6th Meeting of the TF-BTA. Paris, France, 15 May 2014.

Zander O., Gehring D.-U. 2014. "Testing outside bumper corners." Doc TF-BTA-7-11 of 7th Meeting of the TF-BTA. 9 September 2014.

FINITE ELEMENT STUDY OF EFFECTIVENESS OF MODIFIED FRONT-END STRUCTURE WITH ALUMINIUM FOAM IN REDUCING PEDESTRIAN INJURY

Wachirut,Kongsakul
Faculty of Engineering, King Mongkut's University of Technology North Bangkok
Thailand

Julaluk, Carmai
The Sirindhorn International Thai-German Graduate School of Engineering
King Mongkut's University of Technology North Bangkok
Thailand

Sujeepapha, Charoenthong
Faculty of Engineering, King Mongkut's University of Technology North Bangkok
Thailand

Paper Number 15-0416

ABSTRACT

Pedestrians are vulnerable road users. Unlike Occupant in cars, they do not have protection equipment and are often involved in serious accidents leading to fatalities. The reduction of pedestrian injuries has recently become one of the most important road traffic accident priorities. For the bonnet type of vehicle, leg and head injuries are the most prevalent type of injury associated with car-to-pedestrian collision. The possible reduction of leg and head injuries can be done through the design of vehicle bumper structure. Strong and stiff front structure of vehicle usually leads to severe injury to pedestrians in the accident. The use of new class of material like aluminium foam as part of bumper structure can provide better energy absorption capability and hence reduction of impact force to pedestrians. However, in order to design or modify the front structure to be safer for pedestrians, it is necessary to understand kinematics and injury mechanisms of car-pedestrian collisions, which are usually analyzed through costly full scale crash tests of a dummy or a cadaver. Finite element simulations with a human body model are an alternative mean, which offers information of post-crash kinematics and injury mechanisms. This paper has therefore employed the finite element model of pedestrian-city car collisions to study the effectiveness of the modified front-end bumper with aluminium foam in reducing the level of pedestrian injuries. The front bumper structure has preliminary been modified to include the aluminium foam as part of energy absorber. Two relative densities of aluminium foam were selected. The lower density one gave a better injury reduction performance. It was used to simulate a crash with THUMS to study detail injuries of pedestrian. The modified bumper model showed improved performance of injury reduction. The results exhibited the potential use of low density Al-foam in minimizing pedestrian injury and the benefit of using the human body finite element model which provides detailed injury information to help in the design and development of vehicle for pedestrian safety with cheaper cost compared to the actual full-scale crash tests.

INTRODUCTION

Road traffic injuries are a significant global public health problem around the world. Accidents which involve pedestrians mostly result in severe injury or death. Most of car manufacturers have given less priority to pedestrian safety. This is due to the fact that many countries in particularly developing countries have no such regulations. However, many regional New Car Assessment Programs (NCAP) have included pedestrian safety assessment into their car-rating system. This has encouraged many car manufacturers to develop cars with better pedestrian protection. NCAP has assessed pedestrian safety through the impact tests of the front structure with legform and headform since the front structure of vehicle is the part that mostly hits pedestrians. Strong and stiff front structure of vehicle usually leads to severe injury to pedestrians in the accident. Impactor crash test is poor in giving information about the injury mechanisms and kinematics of the pedestrian during crash. Car manufacturers have lately begun to use design principles that have proved successful in protecting car occupants to develop vehicle design concepts that reduce the likelihood of injuries to pedestrians in the event of a car-pedestrian crash. There is a possibility to protect a pedestrian

lower limbs during impact by introducing an appropriate cushion and support of the lower extremities for example the bumper energy absorber. Aluminium foam is a material which has excellent energy absorption capacity. It has been recently introduced to automotive industry to make a crashbox for crashworthiness design [1]. This paper aims at introducing aluminium foam to the front-end structure of a passenger car to study its potential in reducing pedestrian injury level. For purpose of vehicle development, full-scale crash tests are required. However, the actual crash tests are costly compared to alternative computer simulations. Finite element (FE) analysis has been employed widely in vehicle components design and optimization. It is therefore, introduced in this work to simulate pedestrian-car collisions. By firstly, simplified the vehicle model to include only necessary components to reduce computation time. The simplified vehicle model was validated against the actual crash test. The front-end structure of this simplified model was modified by introducing aluminium foam with two relative densities aiming to minimise the pedestrian injury level. The modified bumper structure with two relative densities were numerically assessed with legform impactor. The best safety performance one was selected for car-to-pedestrian simulation. The dynamic responses and injury level were compared with those obtained from the original front-end structure.

SIMPLIFIED FE MODEL OF A PASSENGER CAR

A passenger car finite element model was taken from the National Crash Analysis Center (NCAC) [2]. In the present study, only frontal collision with a pedestrian was considered. Therefore, some unnecessary components were deleted to simplify the car model. The main body in white structure were kept upto the B-pillar. The doors were removed. All components below the hood were kept in place. Since some components and structures were removed, extra mass needed to be added and distributed correctly to obtain the same mass and Centre of Gravity (C.G.) location as in the actual car. Figure 1 shows the simplified FE vehicle model and comparisons of mass and C.G. location with the complete vehicle model. All extra nodes that carried extra mass were constrained to the C.G. of the car. All nodes at area A and B in figure 1 were not allowed to translate in *y* and *z* directions also not to rotate around *x* and *z* axes. The mass and the C.G. of the simplified model were almost identical to the complete model. In order to validate the simplified car model, a full frontal wall crash was simulated and compared the results with the actual crash test data of NHTSA [3]. The car model was set to impact a rigid wall at 56 km/h. The overall global deformation of the actual car was very similar to the actual crash test as shown in figure 2. The acceleration response taken from the engine top and bottom were compared as shown in figure 3. Reasonably good agreement can be seen.
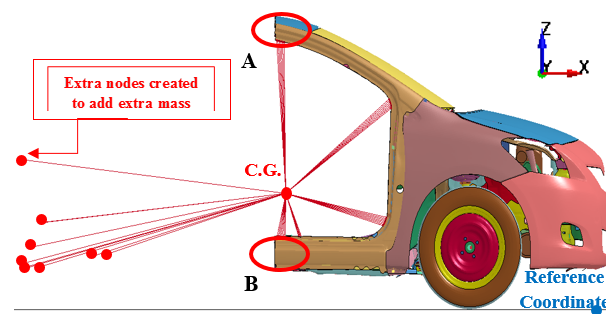
Figure 1. Simplified finite element model of Toyota Yaris sedan

FRONT-BUMPER MODIFICATION TO IMPROVE PEDESTRIAN

For the bonnet-type vehicle, leg and head are body regions that have high risk of severe injuries. The proposed design modification aims at illustrating the potential application of aluminium foam (Al-foam) together with add-on stiffeners to primarily reduce lower extremity injury. Three components made of Al-foam were attached to the front-end of the car as shown in figure 3. They were upper and lower stiffeners as well as a cushion part attached in front of the bumper beam. Two relative densities of Al-foam were used. Material behaviour of Al-foam was required for finite element implementation. The Crushable Foam material model in LSDYNA [4] was employed for this purpose. It requires mass

density, Young's modulus, Poisson's ratio and stress-strain curve. Compression tests of Al-foam were conducted for relative densities of 0.051 and 0.185.

a)

b)

c)
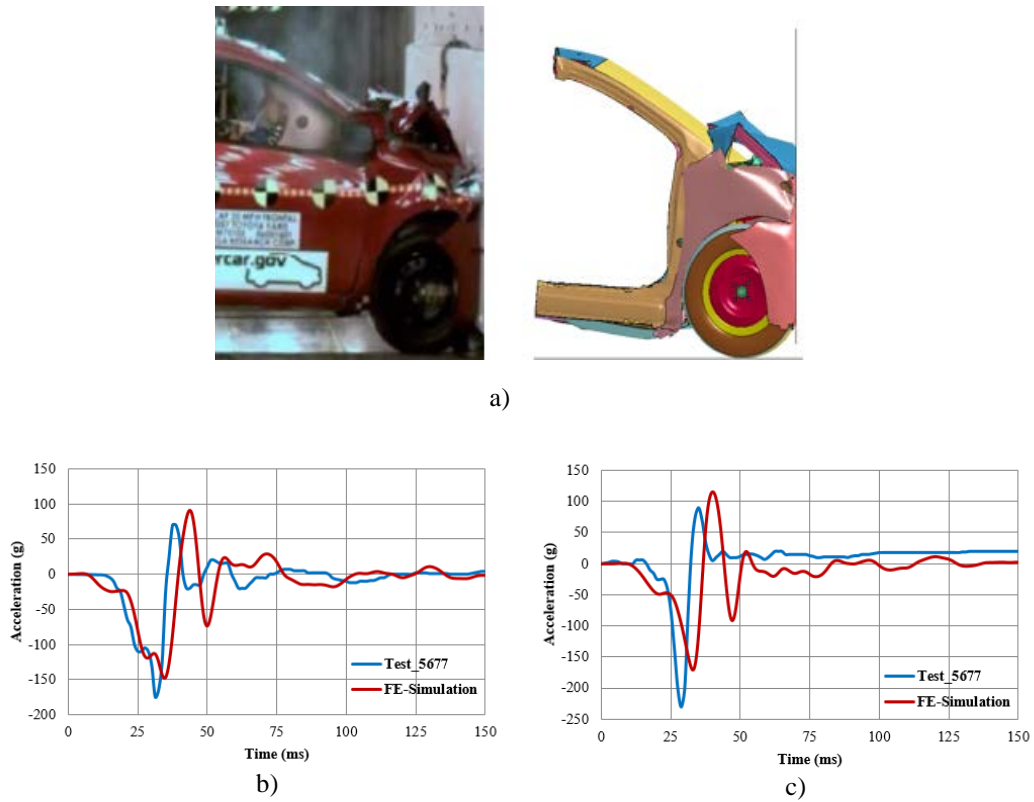
Figure 2. Comparisons of a) global deformation b) engine top acceleration c) engine bottom acceleration.
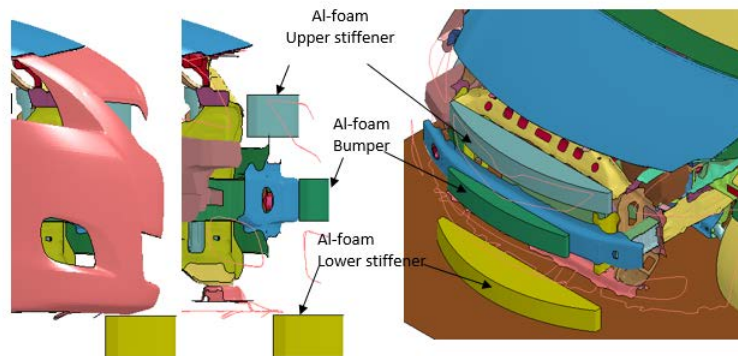
Figure 3. Front bumper modification with aluminium foam parts.

PEDESTRIAN CRASH FINITE ELEMENT MODEL SET UP

Two configurations of crash tests were simulated in this paper. One was legform-car impact test, the other was car-to-pedestrian crash test. A 50 percentile Total Human Body Model for Safety (THUMS) was employed for pedestrian model in this paper. THUMS model is capable of predicting detail injury of brain ligament, bones and internal organs. The set-up of both configurations are shown in figure 5. The legform-to-car model was set up according to the Euro NCAP protocol [5]. The legform was set to move towards the centre of the car bumper at a speed of 40km/hr. For the car-to-pedestrian model, the human body model was initially positioned in front of the car centerline. The car was set

to impact the pedestrian from the right side at a speed of 40 km/hr. The contact friction coefficient between THUMS and the car was 0.3 and the ground friction coefficient was 0.9. Both the car and THUMS were placed in the acceleration field of gravity.
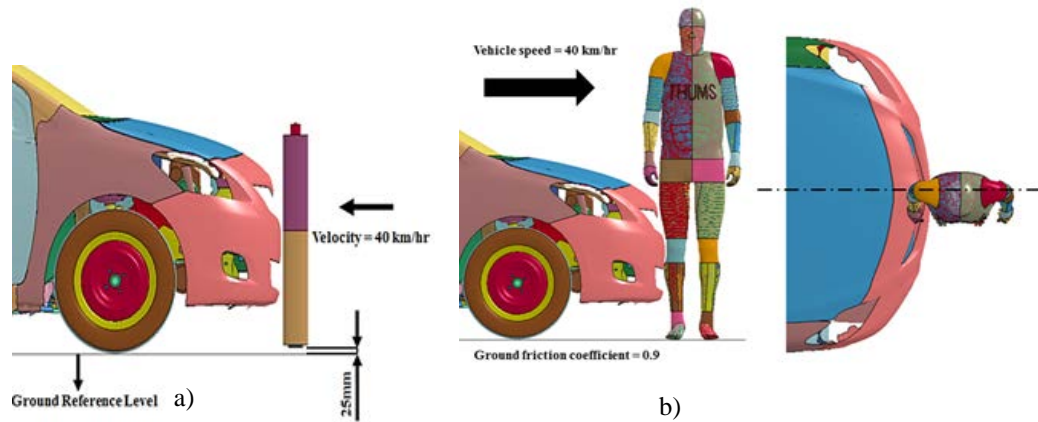
Figure 4. FE model of a) Car-to-Legform impact set-up b) Car-to-Pedestrian collision set-up.

SIMULATION RESULTS

Two set of simulation results are presented. The first set was from the car-to-legform impact test which was employed to assess performance of the original bumper structure and the modified bumper structure with two relative densities of Al-foam. The best performance among the two relative densities was selected to crash with THUMS for detail injury analysis which provided the second set of simulation results.

Legform-car impact simulations

Three cases were conducted. According to the Euro-NCAP protocol [5], three injury parameters including the upper tibia acceleration, the knee shearing displacement, the knee bending angle were used to assess the pedestrian protection performance of the front-end bumper. The maximum value of each injury parameter for each cases are given in table 1. It is obvious that the modified structure with 0.051 relative density Al-foam has all values of injury parameters below the limit specified by Euro NCAP.

Table 1.
The maximum value of each injury parameters for each simulation cases.

Injury parameters	Euro NCAP limit [5]	Original structure	Modified structure with 0.051 relative density al-foam	Modified structure with 0.185 relative density al-foam
Tibia acceleration (g)	150	228	117.7	208.08
Knee shear displacement (mm)	6	-4.8	-1.54	-2.47
Knee bending angle (degree)	15	30	12.06	20.36

Car-to-pedestrian simulations

Two cases were simulated. The first one used the original structure of the car to hit with THUMS in order to obtain the baseline results. The second one used the modified structure with 0.051 relative density al-foam to hit with THUMS. The detail injury were compared and analysed.

Post-crash kinematics behaviour and dynamic responses Figure 5 shows a comparison of kinematics behaviour of pedestrian crashed by the car with original front-end structure and with modified front-end structure. For both cases, the knee was firstly struck by the bumper followed by the thigh and the tibia almost at the same time. The front bumper deformed and the lower extremities bent along the car frontal contour. The upper body rotated around the vehicle front area leading to the pelvis collision with the bonnet leading edge. The elbow were collided with the lower windshield portion. The chest and shoulder collided with the windshield portion at the back end of the hood. Since the neck behaved like a joint which allowed rotation degree of freedom, the head was angularly accelerated and made contact with the windshield. Finally the whole body bounced off the car. The differences can be seen clearly at 40ms, the simulation with the modified bumper model shows less knee bending angle than the original design. In addition, at 60 ms the left leg started to project away from the right leg. This was because the lower part of tibia was in contact with the lower stiffener which tried to resist the tibia movement. The left leg moved away from the car faster than the right leg because some of the right leg energy was absorbed by the lower stiffener aluminum foam. The time and location of head impact were also different. At 130 ms, the one with original bumper structure hit the windshield at 442 mm from the lower end of windshield where are the one with the modified bumper structure hit to the windshield at 410 mm.
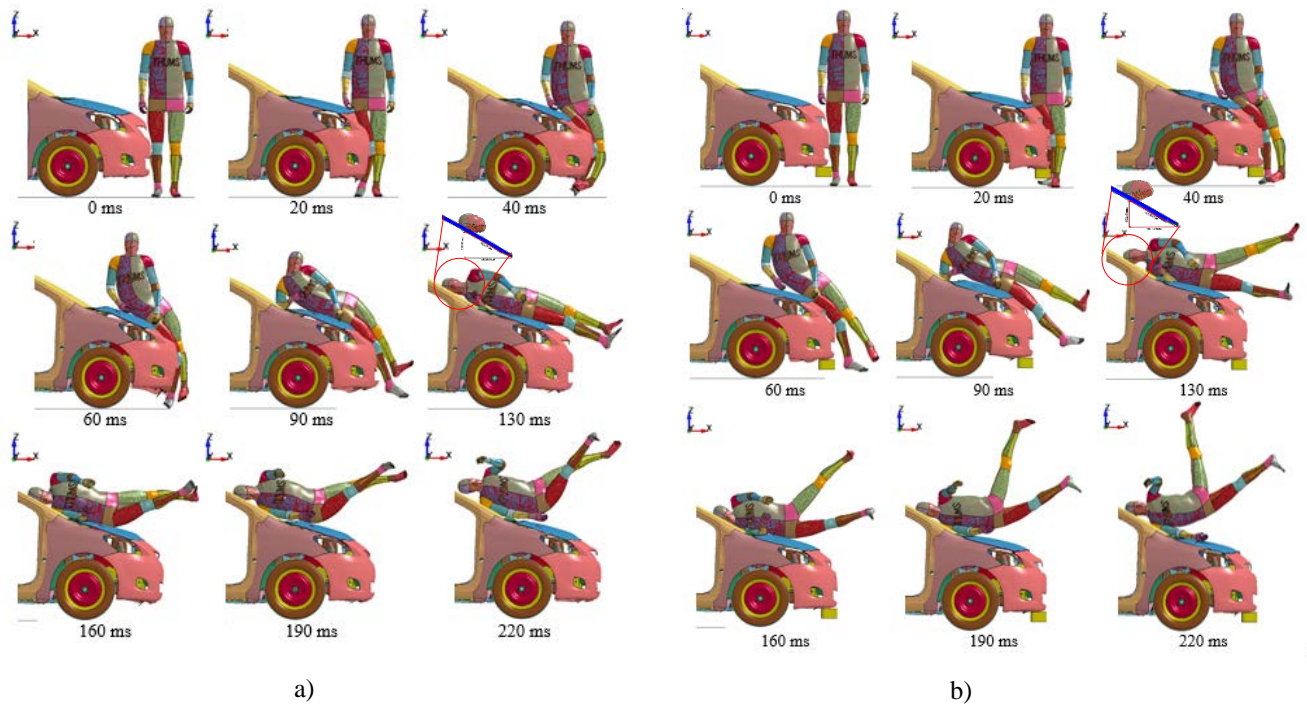
Figure 5. Pedestrian kinematics obtained a) original bumper model b) modified bumper model.

Figure 6 shows comparisons of dynamic responses. The patterns of contact force during collision were similar. The graphs consisted of 5 peak forces corresponding to the impact of plastic cover-leg, bumper beam-leg, elbow-lower part of windshield, chest-hood and head-windshield respectively. The highest peak force was when bumper beam in contact with the knee. The contact force obtained from simulation with the modified bumper was in overall less than those of the original bumper model except the highest peak. This was due to the introduction of the lower stiffener which tried to resist the movement of the lower part of the tibia causing the high contact force at the knee area. The introduction of bumper foam components slowed down the pedestrian body as observing from head and chest relative velocity graphs. The head impact acceleration was decreased from 175.7g to 150g. The HIC_{15} obtained from the simulation with original bumper model was 1059 which implied high risk of severe head injury with AIS3 50% injury

risk [6]. The HIC_{15} was reduced to 913.8 for simulation with the modified bumper model, hence lower risk of head injury.
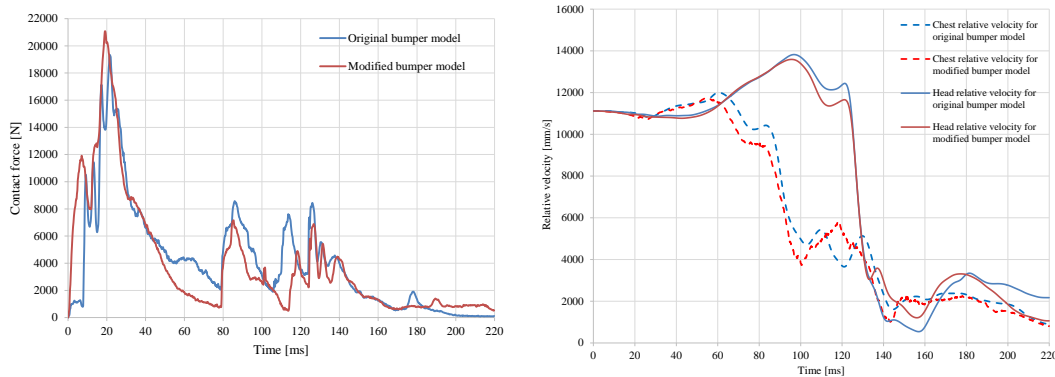
Figure 6. Dynamic response a) the contact reaction force during collision b)relative velocity.

Pedestrian injuries Figure 7 shows comparisons of bending moment and resultant force time histories at various height along the lower extremity. The threshold for 50% injury risk of AM50th was 447 Nm for femur [7-8] ,134 Nm for knee [7-8] and 340 Nm for tibia [9]. The patterns of bending moment were different. For the original bumper model, the maximum bending moment of the right lower extremity was the largest at the tibia height 400 mm above ground. It was 256.52 Nm but still within the tolerance limit of tibia for 50% injury risk of AIS2. While at the knee area with height of 500 mm above ground the maximum bending moment was 231.45 Nm. This value exceeded the tolerance limit of knee for 50% injury risk. The maximum bending moment of the femur was lower than that of tibia and knee. The values were still within the tolerance limit for 50% injury of AIS3. However, for the modified bumper model, the highest maximum bending moment of 400 Nm was shifted to the femur. This value was still within the limit of femur fracture. The knee and tibia bending moment taken from the modified bumper simulations had lower value than the original bumper model. They were all within the limit of bone fracture and knee joint damage.
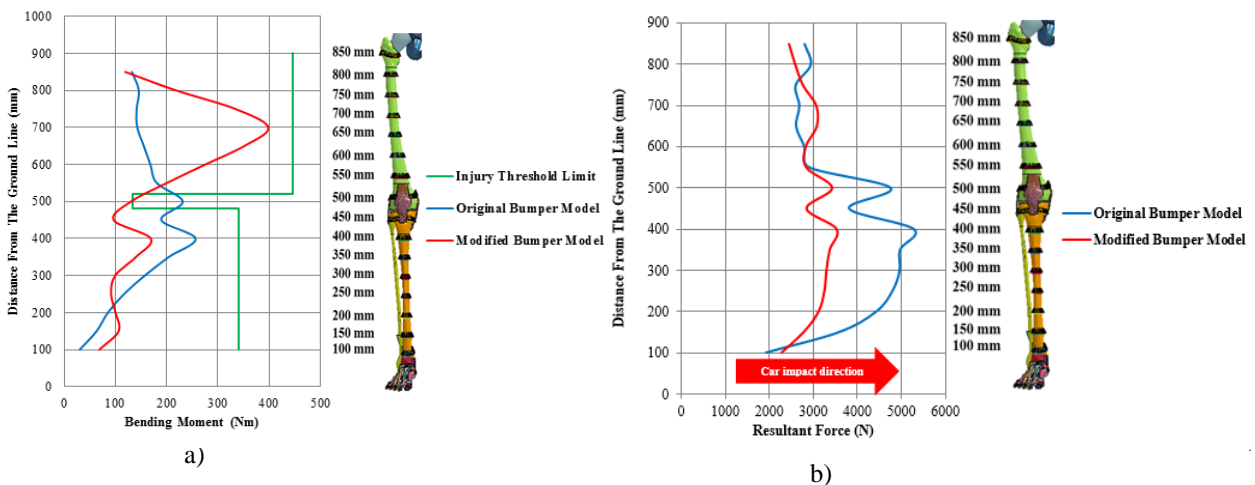
Figure 7 a) bending moment and b) resultant force along the right lower extremity.

Resultant force expressed the same trend as shown in figure 7 b). The resultant force obtained from the simulation with the modified bumper was less than those of the original bumper for every distance.

Apart from dynamic responses, the biofidelity of the human body model can also give detailed injuries of all parts of the pedestrian body. Figure 8 shows comparisons of stress and strain distributions on the extremities. For the original bumper design, high stress of 141 MPa occurred at the front fibula and tibia. However, the magnitude of the stress was still within the bone fracture stress threshold of 150 MPa [10-12]. It was found that stress distribution changed for the simulation with the modified bumper. High stress occurred on femur rather than on the tibia. The highest magnitude was 122.67 MPa which was still below the femur fracture limit of 150 MPa. However, the overall magnitude of stress within the lower extremities was reduced for the simulation with the modified bumper. The maximum strain on knee ligaments for the case of the original bumper was at 0.25 which was beyond the rupture strain limit of 0.16 [13]. The simulation with the modified bumper structure showed improvement of the strain value. The maximum strain value reduced to 0.18. Very high stress also found at the humerus (upper part of an arm) due to the impact of elbow to the lower part of the windshield. For the original bumper simulation case, the stress was 232.5 MPa which exceeded the bone fracture limit of 150 MPa. For the modified bumper case, the stress value was much lower. The modified bumper model helped reducing the injury risk of humerus fracture.
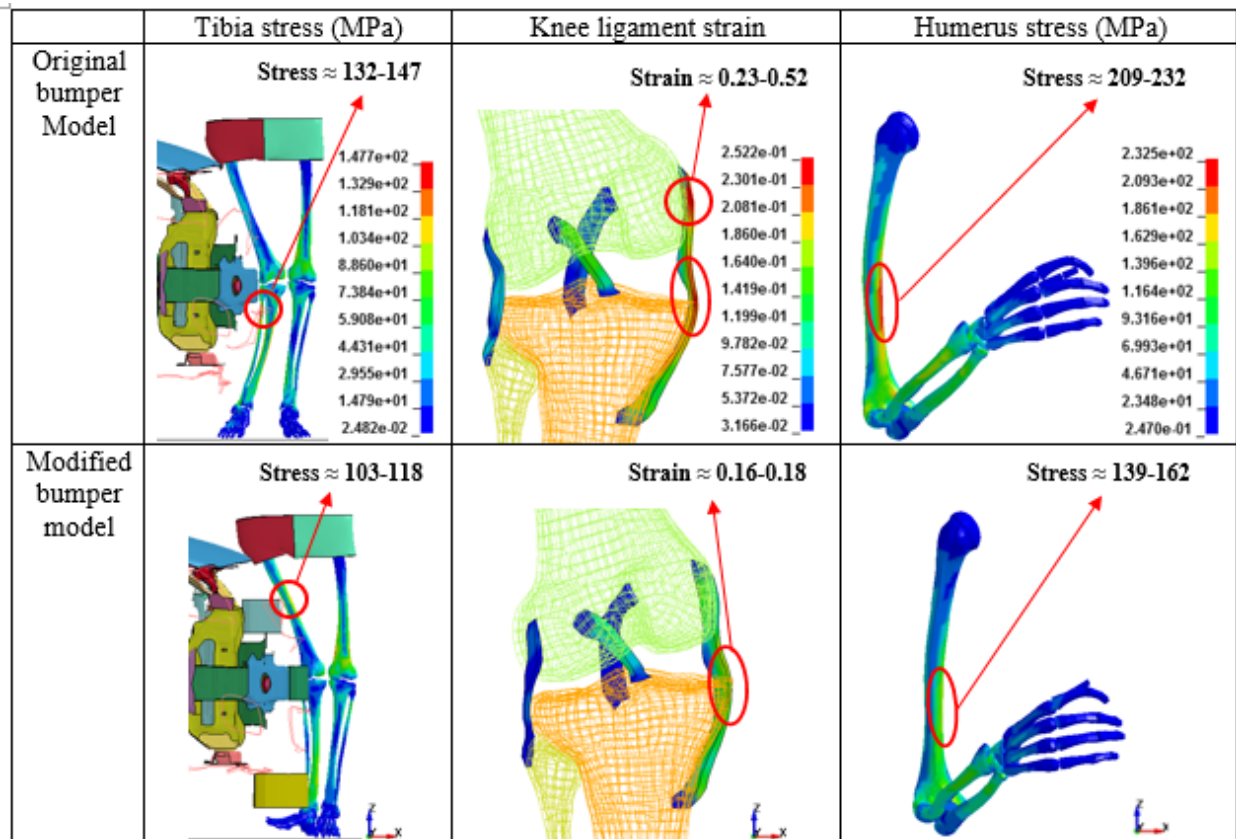
Figure 8. comparisons of stress and strain distributions on the extremities.

Figure 9 shows comparisons of detailed injury for the upper body. The thorax experienced high stress due to the impact of thorax to the back of the hood. For the original bumper model, two ribs, number 3 and 5 had quite high effective stress of around 149.2 MPa which was at the borderline for rib fractures. This impact also induced high pressure within the lung as shown in figure 9. The limit of human lung usually uses pressure to define threshold [12]. The limit is at ±10 kPa. From the simulation results, the red area represents the area that pressure exceeds 10kPa and the dark blue area represents area that pressure is less that -10kPa. The right lung showed damage as the pressure was greater than 10 kPa for almost all area of the right lung. With the modified bumper model, a drastically improvement was seen for

the ribcage stress and the lung pressure. The maximum stress on rib number 5 reduced to 94 MPa which was much below the fracture limit. In addition, the pressure within the lung was also considerably reduced. However, when comparing strain on brain, it was found that the strain within the brain expressed advert effect. For the case with modified bumper, the strain increased to 0.52 which exceeded the limit value of 0.3 for soft tissue damage. This implied that the modified bumper structure induced brain contusion. Although, the head acceleration and HIC value were reduced, the brain strain did not follow the same trend. The argument is that the HIC is calculated from the translation acceleration. There have been some studies illustrating that the relational velocity and acceleration have effects on the brain injury [13-14]. Since post-crash kinematics of head were different, it could affect the strain pattern and magnitude
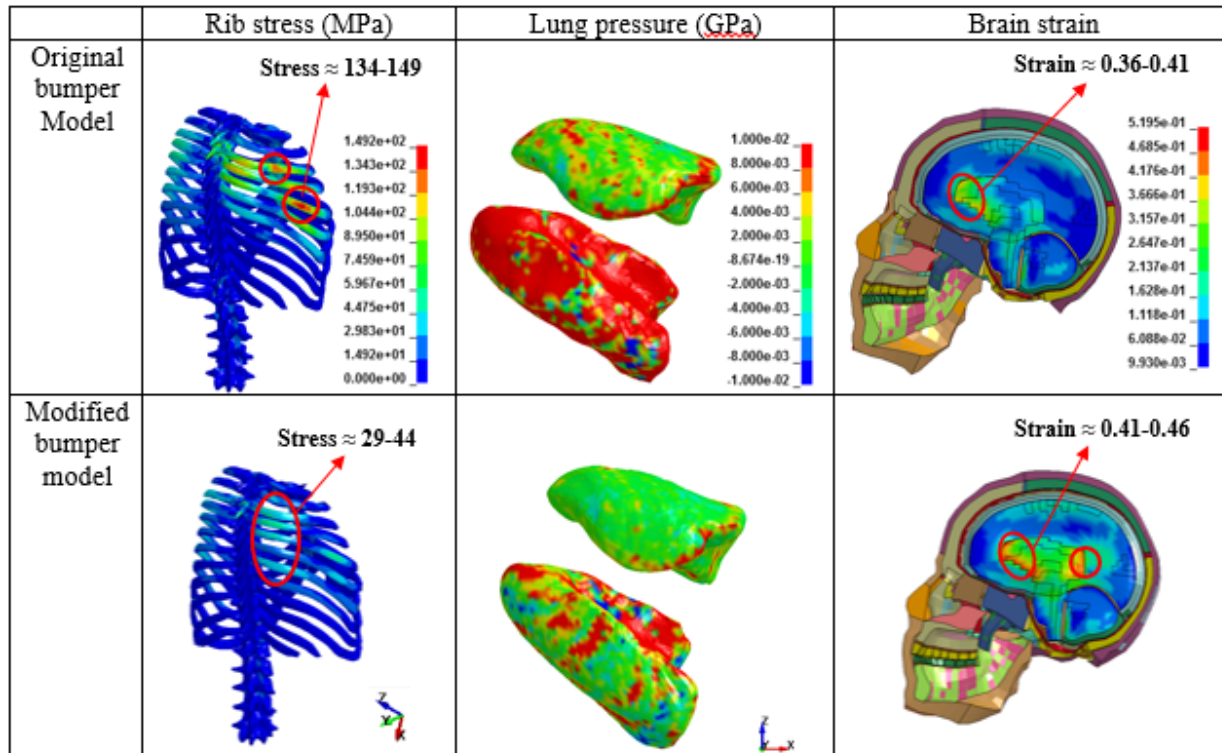
Figure 9. Comparisons of stress and strain distributions for upper body part.

CONCLUSIONS

This paper aimed at studying the potential use of aluminium foam as part of front-end structure to reduce pedestrian injury. The detail injury analysis was performed though the use of finite element human body model. A modification to the bumper structure was done but with limitation of the shape of the bumper cover of the existing car. Three components made of aluminium form were added to the front bumper structure as part of energy absorber. Two relative densities of aluminium foam, 0.051 and 0.185, were considered. The modified design with lower relative density of 0.051was selected based on the legform injury parameters performance. It was used to simulate a crash with THUMS in order to study detailed injuries of pedestrian. The post-crash kinematics showed some differences at the lower extremities and head. The dynamic responses and level of injury were improved with the modified front bumper using low density aluminium foam. However, when simulating car-to-THUMS collision, some detailed injury information showed that the modified bumper caused slight problem in brain area. The results illustrated that the low density aluminium foam could be employed in the design for pedestrian friendly vehicle. The design and development process needed to take into account the injury of other body regions also especially the brain

which could not be simulated using a headform or a dummy. The current study also supported the benefit of using THUMS in the design development of pedestrian friendly bumper.

REFERENCES

[1] Cymat Technologies. "Aluminum Foam Technology Applied to Automotive Design"

[2] NCAC. 2011. "Development and Validation of a Finite Element Model for a 2010 Toyota Yaris Sedan" NCAC 2011-T-001, prepared for FHWA.

[3] MGA Research Corporation. 2006. "Final Report of New Car Assessment Program Testing of a 2007 Toyota Yaris." NHTSA Test No. 5677.

[4] LS-DYNA. 2012. "Keyword User's Manual Volume II Material Models" Version 971 R6.1.0, Livermore Software Technology Corporation (LSTC).

[5] Euro NCAP. 2013. "Pedestrian Testing Protocol V.6.2.1." (Belgium, Feb).

[6] Prasad P and Mertz H. 1985. "The Position of the United States Delegation to the ISO Working Group 6 on the Use fo HIC in the Automotive Environment." SAE Government/Industry Meeting and Exposition, SAE paper no. 851246.

[7] Kerrigan, J.R., et al. 2003. "Experiments for Establishing Pedestrian-Impact Lower Limb Injury Criteria." SAE World Congress & Exhibition.

[8] Ivarsson, J., et al. 2004. "Dynamic response corridors and injury thresholds of the Pedestrian lower extremities." International IRCOBI Conference on the Biomechanics of Impact.

[9] United Nations Economic and Social Council. 2012 "Proposal for amendmentsto global technical regulation No. 9 ECE/TRANS/WP.29/GRSP/2010/2." (Usa).

[10] Han,Y., Yang, J. and Mizuno, K. 2011. "Virtual Reconstruction of Long Bone Fracture in Car to Pedestrian Collisions Using Multi body System and Finite Element Method." Chinese journal of mechanical engineering, 1-12.

[11] Han, Y., et al. 2012. "A study on chest injury mechanism and the effectiveness of a headform impact test for pedestrian chest protection from vehicle collisions." Safety Science, 1304-1312.

[12] Shigeta, K., Kitagawa, Y. and Yasuki, T. 2009. "Development of Next Generation Human FE Model Capable of Organ Injury Prediction." Enhanced Safety of Vehicles, 1-20.

[13] Watanabe, R., et al. 2011. "Research of collision speed dependency of pedestrian head and chest injuries using human FE model (THUMS Version 4)." Enhanced Safety of Vehicles, 1-13.

[14] Kimpara, H. and Iwamoto, M. 2012. "Mild traumatic brain injury predictors based on angular accelerations during impacts." Annals of Biomedical Engineering, 114-126.

IMPROVEMENTS TO THE FLEXIBLE PEDESTRIAN LEGFORM IMPACTOR: THE DEVELOPMENT OF NEW BONE CORES

Thomas KINSKY, Adam Opel AG / General Motors Europe Engineering, Germany[*]
Martin FRITZ, 4a Engineering GmbH, Austria
Peter LESSMANN, BGS Boehme and Gehring GmbH, Germany
Franz ROTH, AUDI AG, Germany[*]

[*] representing the Task Force Pedestrians of the European Automobile Manufacturers' Association (ACEA)

ABSTRACT

During the first decade of the 21st century, pedestrian safety in general was one of the main subjects of vehicle safety development. For the legform testing, the impactor developed by the European Enhanced Vehicle-Safety Committee was the standard impactor but experts from Japan introduced a new impactor, the so-called Flexible Pedestrian Legform Impactor (FlexPLI). The FlexPLI is capable to quantify the load of a human long bone, which is a significant advantage when developing vehicles with reduced bone fracture risk.

With the impactor being developed by a single company spare part availability was limited. In addition, potential improvement in terms of robustness in maximum load were identified. Therefore, a joint project was initiated, in which automobile manufacturers and their partners developed universal spare parts for the FlexPLI bone cores. These parts can withstand higher bending loads, are available from stock and do not need to be adapted to a specific legform. Furthermore, a reduction in variation of properties due to a different production process was achieved. This reduces performance variation within the legs and is comparable to the initial bone core mean performance. The document introduces the details of the project.

INTRODUCTION

During the first decade of the 21st century, pedestrian safety in general was one of the main subjects of vehicle safety development. For the legform testing, the legform impactor developed by the working groups of the European Enhanced Vehicle Safety Committee (EEVC) was state of the art at that time. However, to enhance the representation of a true human leg, experts from Japan introduced a new legform impactor when others still tried to understand how to work with EEVC Legform Impactor (EEVC LFI).

The new Japanese impactor, nowadays called Flexible Pedestrian Legform Impactor (FlexPLI), provides one significant advantage compared to the EEVC LFI: In addition to the assessment of knee injuries, it is able to also assess injury risks to the long bones of a human leg.

To promote the introduction of the new legform and to allow experts of other regions also contributing to the development, the Japan Automobile Research Institute (JARI) and the Japan Automobile Manufacturers Association (JAMA) lend different build levels of the impactor to labs outside Japan.

The European Automobile Manufacturers' Association (ACEA) was equipped with several FlexPLI's by Japan for several years. This allowed ACEA members to conduct tests at different labs such as Concept Technologie GmbH in Austria (Concept), the Bundesanstalt fuer Strassenwesen / Federal Highway Safety Research Institute (BASt) and BGS Boehme and Gehring GmbH[1] as well as Bertrandt Ingenieurbuero GmbH (Bertrandt) in Germany. During those tests, learnings and expertise were generated. These were brought into the activities of the UNECE Informal Group on Pedestrian Safety (INF GR PS) (working from 2002 to 2006), the UNECE Technical Evaluation Group (TEG) (working from 2005 to 2010) as well as the UNECE Informal Group on gtr No. 9 – Phase 2 (IG GTR9-PH2) (working from 2011 to 2013).

---

[1] BGS Boehme und Gehring GmbH is the company operating the test laboratory of the German Bundesanstalt fuer Strassenwesen / Federal Highway Safety Research Institute (BASt).

Finally, the efforts of the working groups mentioned before led to the introduction of the FlexPLI into UN Regulation 127 as of January 2015 as well as to a corresponding draft amendment for the gtr No. 9, which is in the process of adoption. The design of the FlexPLI has achieved a build level that will allow its future use for regulatory purposes. However, room for further improvements to this build level is seen and one of the respective solutions is presented in this document.

CONCERNS WITH THE DESIGN OF THE FLEXIBLE PEDESTRIAN LEGFORM IMPACTOR

During one of the first test series conducted on behalf of ACEA by the company Concept in 2004, Knotz reported about concerns with the – at that time too low – stiffness of the FlexPLI. Knotz tested an early version, the version 2003, of the new impactor. He noted that the legform had a tendency to bend extremely and to follow the contour of the tested vehicles (Knotz 2004, page 25). Experts of ACEA members raised the concern whether this could result in damages to the bone cores of the FlexPLI and whether this indeed represents the behavior of a human leg.

From their testing with the next generation of the FlexPLI, the version 2004, Mallory, Stammen and Legault reported about damages to the bone cores of the impactor in three out of five tests (Mallory, Stammen, Legault 2005, page 8).

Feedback generated in such tests lead to one major design change that was introduced in 2005 with the FlexPLI version G: Starting with this version, all FlexPLIs have a squared design of tibia and femur sections, compared to the round tibias and femurs of the earlier versions. In the corners of the respective sections, steel cables are placed to limit the maximum bending of tibia and femur and therefore prevent the impactor from being excessively bent.

Figure 1 shows a principal drawing of the latest build level of the new impactor. "The FlexPLI consists of a femur and a tibia, which are composed of bone cores made of fiber glass, and several nylon segments attached to them. The overall design of femur and tibia represents the human bones and their ability to be bent. Strain gauges, glued to the fiber glass core, are used to measure the bending moments at the different segments and thereby assess the risk of bone fractures. The knee element consists of two complex blocks, where string potentiometers represent the human knee ligaments. Their elongations assess the risk of ligament injuries… Human skin and flesh are formed by several layers of rubber and neoprene sheets. To closer follow the geometry of a human leg, the number of layers is different for femur, knee and tibia…" (Kinsky, Friesen, Buenger 2011, page 2ff.)
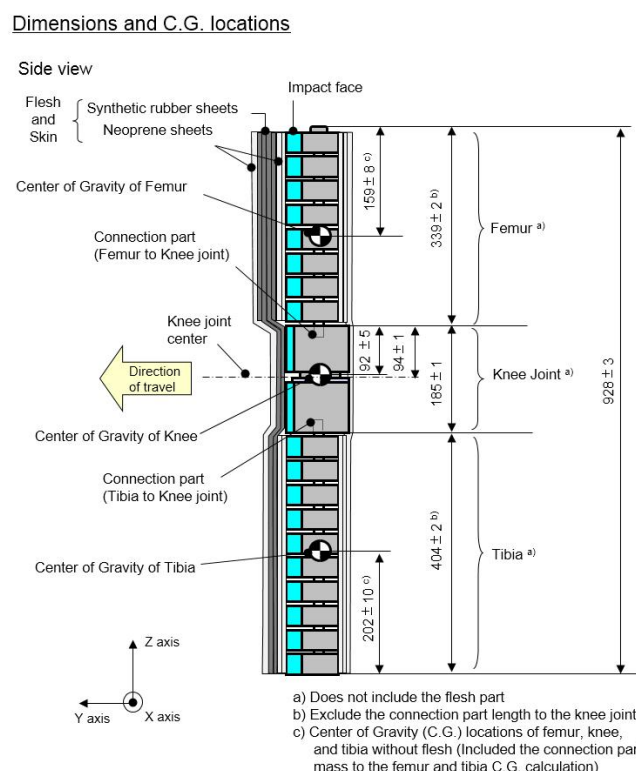
Figure 1: Latest design of the FlexPLI as introduced in the 01 series of amendments to UN R127 (UNECE 2015, page 26)

In 2008, Been and colleagues summarized the development status of the FlexPLI in its intended final version GTR[2] (Been et al. 2008). Been and colleagues introduced the 3-point quasi-static bending test applied to the bone cores individually as well as to the total assemblies to prove the material robustness. This test was carried into calibration and certification procedure of the assemblies for official impact tests. However, in all these tests the bone cores were, by that time, never loaded with bending moments of more than 400 Nm – moments, which could be expected frequently when considering that the maximum bending moments in discussion at that time were in this range. Been et al. also explained that the plastic material surrounding the glass fibers was changed at that time from polyester to vinylester to improve the durability (Been et al. 2008, page 34) and that the old and the new bone core material had been overload-tested with bending moments of 500 Nm to prove the optimization (Been et al. 2008, pages 35ff.). However, experts from ACEA members felt that this still will not be sufficient for development tests were the initial performance of new cars may still to be quantified.

In 2011, Kinsky reported on a first long-time durability assessment with one of the prototypes of the FlexPLI version GTR (Kinsky 2011). Kinsky noted significant wear and visible white cracks on the surface of the bone cores by matrix failure in the bone core material (Kinsky 2011, pages 13 ff.). The report raised also concerns about the availability of spare parts for the impactor.

Additionally, experts of Humanetics, producing the FlexPLI version GTR, stated in 2011 that the fiberglass bone cores are tailor-made for each single legform (Humanetcis 2011). This was explained with the production process of the fiberglass material that cannot guarantee stable material properties. The material is produced in a pultrusion process as a straight profile (see figure 2). Since, according to Humanetics, the glass fibers are not necessarily orientated in line and the thickness of the profile is reduced by machining by about one third, the final batch of material has varying quality (high variation of strength and stiffness). Therefore, the bone cores are produced as blanks and then are slightly reworked to fine-tune the performance in the tibia and femur assemblies. According to the drawings, the bone cores finally vary in thicknesses between 10.3 and 10.9 mm (Humanetics 2015), which in principle makes each bone being unique. Also, the experts of Humanetics stated that the ultimate strength of the straight profile is foreseen for a maximum of 250 MPa (which approximately corresponds to a bending moment of 185 Nm) but that Humanetics tested them up to 400 Nm bending moment (which would require a minimum strength of 540 MPa)
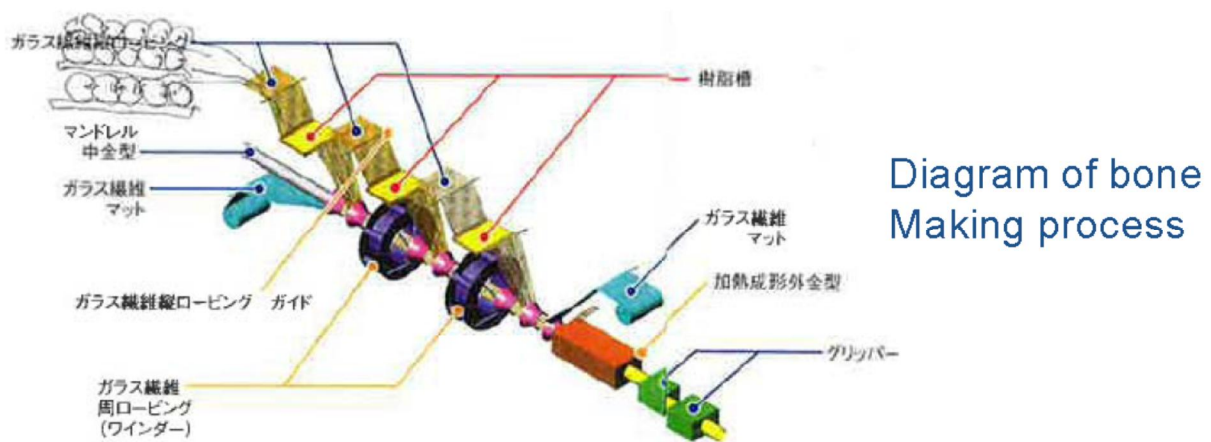
Figure 2: Diagram of the production process for the bone core material, which is then processed in several further steps to the tailor-made bone core for each FlexPLI (Humanetics 2011, page 21)

Based on the statements of Humanetics, concerns were raised by automobile industry experts: Will the FlexPLI withstand higher loads then the legislation limits, also if these loads occur more than once? Will spare parts be available on short notice? How can the required impactor's finite elements (FE) model address variation of the actual parts? Etc.

---

[2] Early versions of the FlexPLI had been named according to their year of introduction. Since 2005, the new versions were named G, then GT and finally GTR, indicating that the development steps should lead to the use in the global technical regulation (gtr) on pedestrian safety.

DEVELOPMENT OF NEW BONE CORES FOR THE FLEXPLI

Experts of ACEA finally decided to support enabling alternative suppliers of the bone cores. The product specifications included:
- The new bone cores should have the ability to withstand bending moments of at least 20 percent above the limits foreseen for legislation (with legislation limits still being in final discussion at that time);
- The material behavior should be reproducible with just small variations in the product performance;
- The dimensions of the new bone cores should fit the dimensions of the other parts of the FlexPLI to avoid a need of further modifications to the impactor;
- The new bone cores should preferably be available as spare parts on stock, without a need to fine-tune them for their use in a specific legform impactor;
- The new bone cores should allow for the use of the different data acquisition systems already in use by different ACEA members;
- A material model should be made available for the simulation;
- Further improvements to the bone cores as well as to the whole FlexPLI could be discussed, if possible.

A preceding project on this topic had been conducted by Partnership for Dummy Technology and Biomechanics (pdb) in Ingolstadt/Germany and Adam Opel AG in Ruesselsheim/Germany with the company 4a Engineering GmbH (4a) in Traboch/Austria. Therefore, ACEA decided for a joint project also with 4a. 4a is a technically oriented research and development company with the focus on plastics engineering and composite material science. They choose to cooperate with the well-experienced test labs BGS in Bergisch Gladbach/Germany and partially also with Bertrandt in Gaimersheim (near Ingolstadt)/Germany. Both labs were experienced in testing the FlexPLI. BGS conducted tests with all earlier versions of the FlexPLI since 2004 and contributed to joint projects with ACEA aiming to improve the impactor. Bertrandt was one of the very first owners of the latest FlexPLI version in Europe and conducted many tests with this version that also helped to improve the design.

After an initial assessment, following objectives were defined for 4a to achieve: The bone cores should be made of a new composite material with narrow variation of the material properties. The fiber matrix combination in this material should be optimized for maximum fatigue strength. Also, the cross section and the bending behavior should be optimized compared to the original bone cores. Finally, 4a also suggested using an improved fixation concept for the bones, taking into account the anisotropy of the material.

In a first step, 4a sourced a new fiberglass material for the bones. The new material is specifically produced for the purposes of the legform impactor with a thickness very close to the final dimensions of the bone cores. Then, the surfaces are grinded down just a few tenth of a millimeter to have flat surfaces that allow the attachment of the strain gauges. The new material has a bending strength of at least 750 MPa (corresponding to 550 Nm bending moment), compared to 250 MPa of the original part as mentioned before. Also, 4a guarantees that the new bone cores are produced with very narrow production tolerances while having the specified material properties.

The strain gauges are bonded to the front and rear surfaces of the bone cores. Initially, the concept of using wires for each single strain gauge was maintained. However, during the frequent assembling and disassembling of the bone cores during the project it was noted, that the wiring always causes a risk of failure due to pinching, braking etc. 4a therefore finally developed folia-printed flexible circuit boards (PCB's) that are attached to the bone core surfaces and that allow minimized wiring. Just one wire per PCB is needed that is placed on the non-struck side close to the knee element.

Using the PCB's also solved issues with the electrical resistance, specifically the bridge resistors. It was observed that in some cases Wheatstone bridges for the strain gauges were also fitted to the data logger board, in addition to resistors in the plugs. The respective wiring depended on the data acquisition system and was impactor specific. Therefore, in these cases the sensors could not be calibrated without the data acquisition system. This would have created issues when producing the bone cores as universal spare parts. The PCB now allows placing all bridge resistors on the PCB, independent of the data logger or the plugs used. Of course, affected FlexPLIs need to be modified accordingly in the beginning but this finally guarantees easy supply of spare parts.

Finally, the bones are covered by heat-shrink tubes. This guarantees the proper dimensions of the bone cores while, at the same time, protecting the strain gauges and the PCB's as well as the bone cores' surfaces from external damaging.

To attach the bone cores to the FlexPLI knee, 4a developed new clamps. Those clamps make contact over the full width of the bone core – in contradiction to the original ones that just contact the bones locally. Due to this, seating stress can be significantly reduced and much higher clamping forces can be achieved.

Figure 3 shows the two major parts as well as the final assemblies of the 4a bone core spare parts (see figure 3). The parts have the same attachment dimensions as the original parts and the same mass, they have a similar test performance, but they provide a better robustness and durability. However, especially the latter details needed to be proven by tests.

Figure 3: Final assembly of 4a femur bone core and 4a tibia bone core spare part, the PCB for a tibia as well as a tibia blank (from left to right) (photograph: 4a Engineering GmbH)

COMPARISON TESTS WITH THE NEW BONE CORES

During the development of the new bone cores, numerous tests had been conducted at BASt by BGS as well as by Bertrandt. The final tests confirming the usability were conducted by BGS. Besides the FlexPLI certification tests on component as well as on assembly level, the project partners decided to conduct tests against a test rig that was configured to represent a sedan-type vehicle. The test rig is a standard test rig that had been developed for validation purposes and was also used for other ACEA projects.

For the certification, quasi-static bending tests of the bone cores for sensor calibrate, certification tests of tibia, femur and knee assemblies as well as final certification tests of the complete legform impactor, have to be conducted. All tests were passed without issues using three different impactors. These three impactors were equipped with three different data acquisition systems. For the certification of the impactor, both tests configurations as foreseen in the UN R127 were conducted: the so-called pendulum testing as well as the so-called inverse testing.

Also, BGS conducted tests against the test rig that was designed to represent the typical load paths of a sedan-type passenger car (see figure 4). During these tests, no unexpected results were achieved and testing proceeded without any noticeable problems.

The test results from the certification tests and against the test rig are shown in annexes 1 to 3. Observed differences in elongation values of the knee are not influenced by long bones and are impactor specific since the knee section of the different impactors had not been modified.
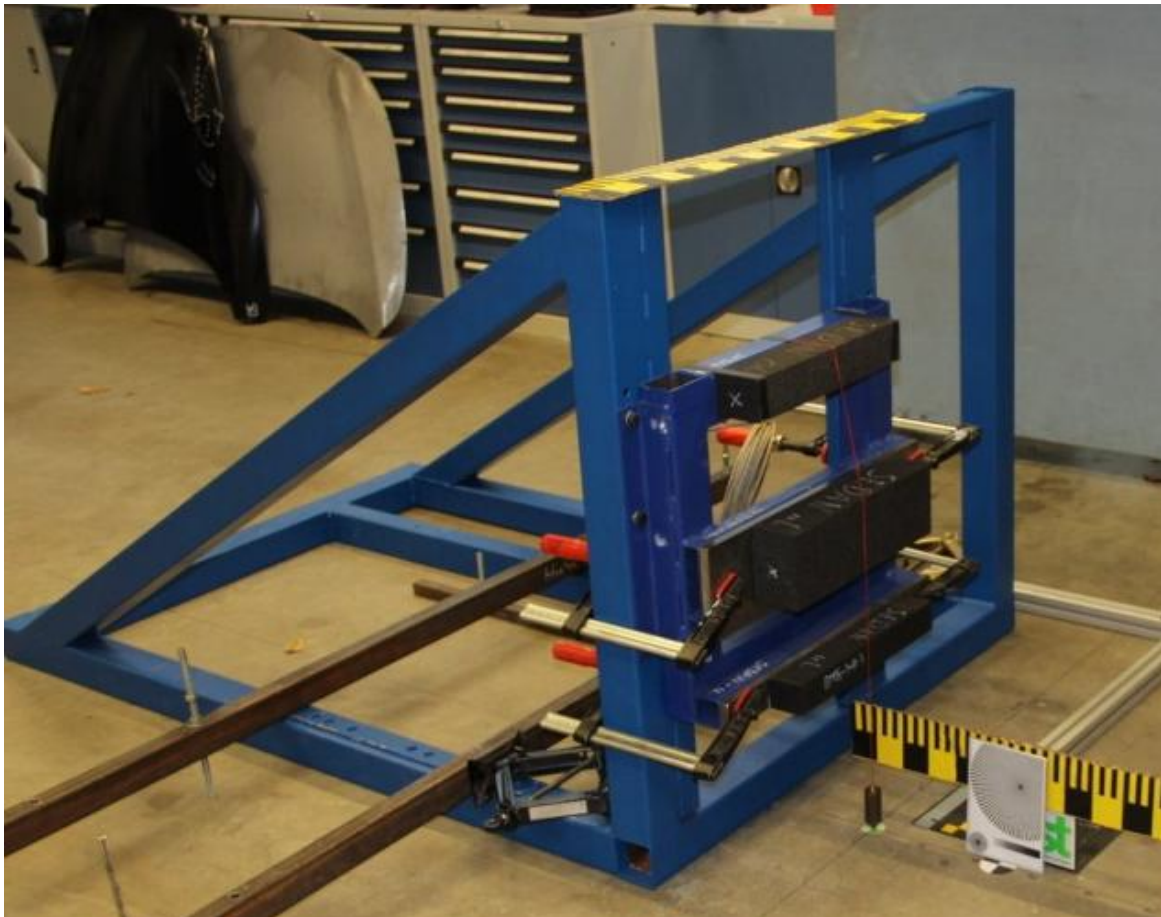
Figure 4: Test rig representing the typical load paths of a sedan-type passenger car
(photograph: BASt/BGS Boehme and Gehring GmbH)

After finalizing the tests described above, two further impactors have been equipped with the new 4a bone cores. In addition, these impactors work properly without any abnormalities. After evaluating the data generated in the tests, the project partners finally concluded that the new spare parts can be made available for industrial use.

REMAINING ISSUES

One major issue coming up during the activities described above were the connector plugs used for the data acquisition systems (including the wiring) of the different legforms. These plugs were observed to be not suitable for the usage in such an impactor and are subject to frequent failure (breakages of the plugs, breakage of the strain relief, disconnections during the acceleration of the impactor, etc.). In addition, these plugs are uncommon (at least in Europe) and acquiring spare parts turned out to be a serious challenge due to limited availability. Therefore, future users of the new 4a bone cores are recommended to also replace the connector plugs to ensure availability of the test tool for vehicle development. Substitution of the Wheatstone bridges may need additional efforts in the beginning but it ensures an uncomplicated and easy supply of spare parts afterwards.

In addition, the project partners noted that several further improvements to the FlexPLI may be possible, aiming at the improvement of the handling, the durability and the robustness of the whole impactor. It was therefore decided to further investigate possible improvements to the impactor in new projects.

Finally, further steps will be needed to develop the FE model of the FlexPLI. Currently, no validated model exists. As soon as this issue is solved, the new 4a bone cores will need to also be provided as supplements to this model. However, from the project team no further issues are expected with this.

CONCLUSIONS

In this joint project, ACEA together with 4a, BGS, Bertrandt as well as pdb developed universal spare parts for the FlexPLI bone cores. These parts can withstand higher bending loads than the original bone cores and have no influence on the certification output. They are available from stock and there is no need for legform-specific adaptations. In addition, the new parts are produced with higher accuracy so that no variation of their performance needs to be expected. Some further improvements to the electric equipment of the impactor as described above will allow the universal usage of the new bone cores.

ACKNOWLEDGEMENTS

Several experts have – actively or passively – supported this project. The authors would like to thank specifically BASt, Bertrandt with Mr. Jan-Christopher Kolb and his team, pdb with Mr. Klaus Bortenschlager and his team as well as the experts of the ACEA Task Force Pedestrians for their support, especially Mr. Benjamin Buenger.

FREQUENTLY USED ABBREVIATIONS

ACEA	European Automobile Manufacturers' Association
EEVC	European Enhanced Vehicle-Safety Committee [originally founded as European Experimental Vehicle Committee]
FE	finite element
ff.	and the following
FlexPLI	Flexible Pedestrian Legform Impactor
JAMA	Japan Automobile Manufacturers Association
JARI	Japan Automobile Research Institute
LFI	Legform Impactor
PCB	printed circuit boardUNECE United Nations Economic Commission for Europe

REFERENCES

Been u.a. 2008:
Been, Bernard; N.N. (JAMA); N.N. (JARI): First Technology Safety Systems / FLEX-PLI-GTR Development Prototypes. Add. 1 JAMA-JARI / Improvement of Durability of Bone Core; Add. 2 JAMA /JARI Development of A Dynamic Assembly Calibration Test Procedure for Flex-GTR using an FE Flex-GT-prototype model. Working document TEG-071 with annexes 1 and 2 for the 7th meeting of the FlexPLI Technical Evaluation Group, Bergisch Gladbach, 8 December 2008. – Available in internet: http://www.unece.org/trans/main/wp29/wp29wgs/wp29grsp/ pedestrian_flexpli.html (2015-02-27).

Humanetics 2011:
N.N. (Humanetics): FLEX PLI Upgrade Status / TEG Webex Meeting / May 11, 2011. Working document for the (planned) 13th meeting of the FlexPLI Technical Evaluation Group". – Not publically available since the meeting finally never took place. However, the document had been shared in advance with all experts involved in the TEG activities.

Humanetics 2015:
N.N. (Humanetics): Reviewed FlexPLI version GTR drawing package, Rev. 4 (final version status Feb. 2015). – Available in internet: https://www2.unece.org/wiki/display/trans/GTR9-2+9th+session (2015-02-27)

Kinsky 2011:
Kinsky, Thomas: FlexPLI Version GTR Prototype SN-02 – Durability Assessment. Working document GTR9-1-04c for the 1st meeting of the Informal Group on gtr No 9 –Phase 2 (IG GTR9-PH2), Geneva/Switzerland, 1 – 2 December 2011. – Available in internet: https://www2.unece.org/wiki/display/trans/GTR9-2+1st+session (2015-02-27).

Kinsky/Friesen/Buenger 2011:
Kinsky, Thomas; Friesen, Flavio; Buenger, Benjamin: The Flexible Pedestrian Legform Impactor and its Impact on Vehicle Design. Document 11-0328 for the 22nd ESV Conference, Washington D.C., 13 – 16 June 2011. – Available in internet: http://www.nhtsa.gov/ESV (2015-02-27).

Knotz 2004:
Knotz, Christoph: Comparison Tests Using a TRL Legform Impactor and a JARI Flexible Pedestrian Legform Impactor. Test Report Nr. 10160/FGS/01 Rev.2 of Concept Technologie GmbH under contract of the European Automobile Manufacturers' Association ACEA. – Gratkorn, 07.06.2004.

Mallory/Stammen/Legault 2005:
Mallory, Ann; Stammen, Jason; Legault, France: Component leg testing of vehicle front structures. Document 05-0194 for the 19th ESV-Konferenz, Washington D.C., 6 – 9 June 2005. – Available in internet: http://www.nhtsa.gov/ESV (2015-02-27).

UNECE 2015:
United Nations Economic Commission for Europe: Regulation No. 127 / 01 series of amendments to the Regulation – Date of entry into force: 22 January 2015 / Uniform provisions concerning the approval of motor vehicles with regard to their pedestrian safety performance. Document R127r1e of the addenda to UN Vehicle Regulations 1958 Agreement. – Available in Internet: http://www.unece.org/trans/main/wp29/wp29regs121-140.html (2015-02-27).

ANNEX 1 – TEST RESULTS PENDULUM CERTIFICATION

Test results for 3 different legforms with 3 repetitions each, the most right bar in each block represents the mean value.

Pendulum: Femur A3

Pendulum: MCL

Pendulum: Femur A2

Pendulum: Tibia A1

Pendulum: Femur A1

Pendulum: Tibia A2

Pendulum: ACL

Pendulum: Tibia A3

Pendulum: PCL

Pendulum: Tibia A4
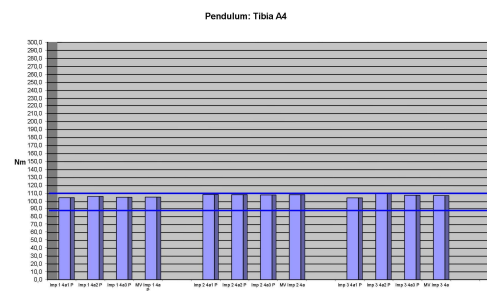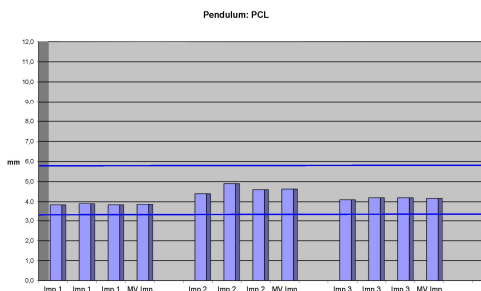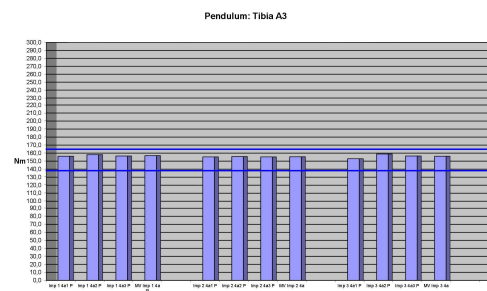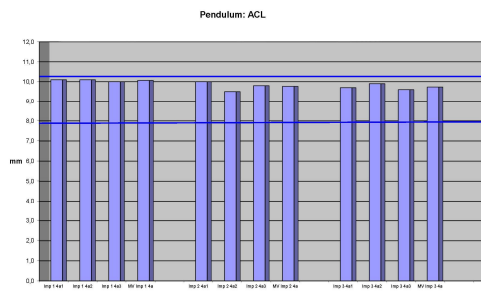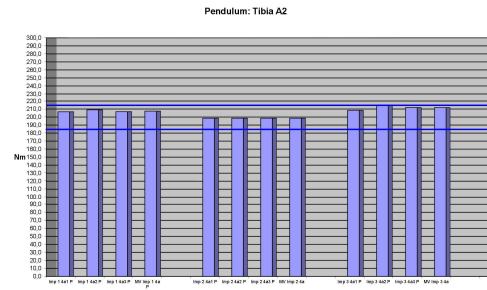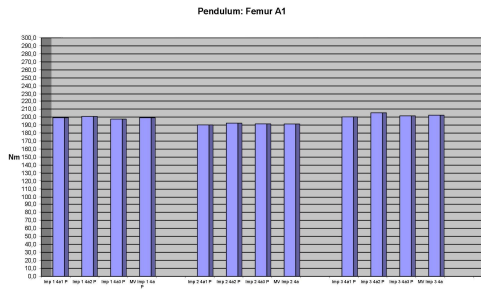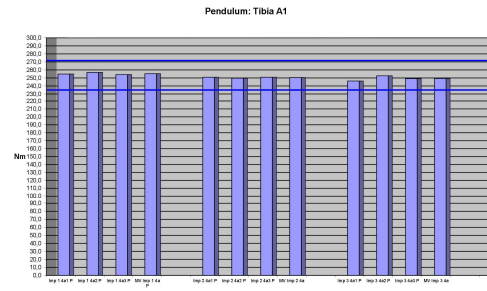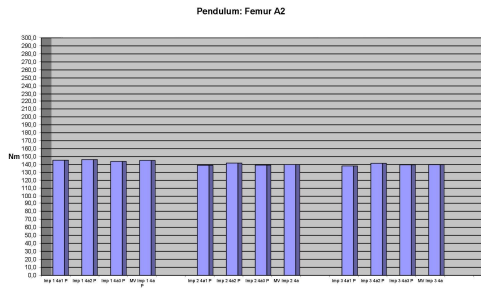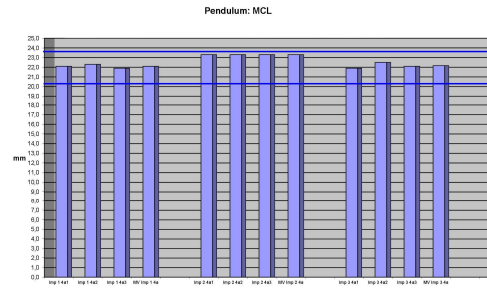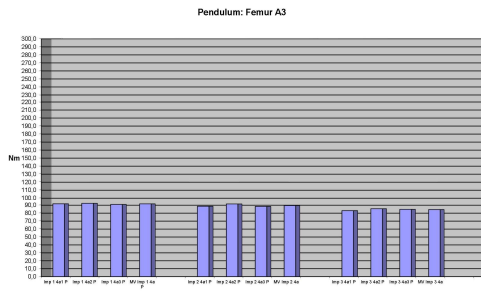
ANNEX 2 – TEST RESULTS INVERSE CERTIFICATION

Test results for 3 different legforms with 3 repetitions each, the most right bar in each block represents the mean value.

Invers: Femur A3

Invers: MCL

Invers: Femur A2

Invers: Tibia A1

Invers: Femur A1

Invers: Tibia A2

Invers: ACL

Invers: Tibia A3

Invers: PCL

Invers: Tibia A4
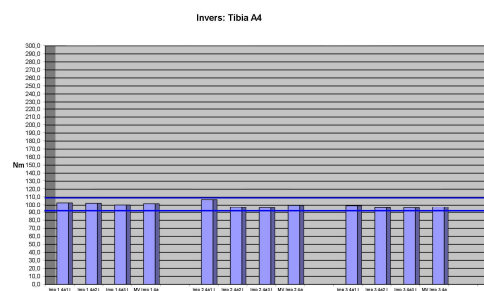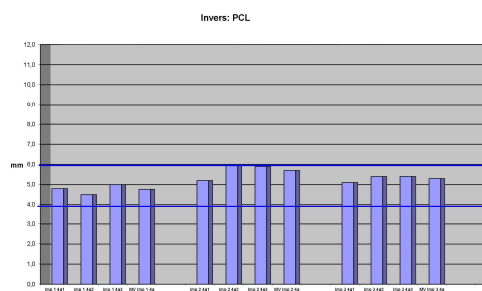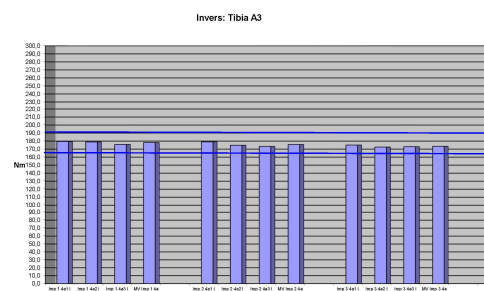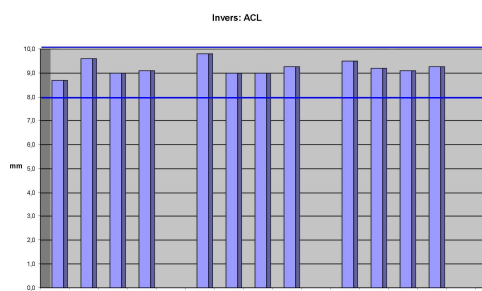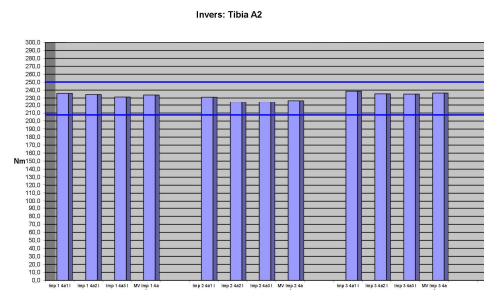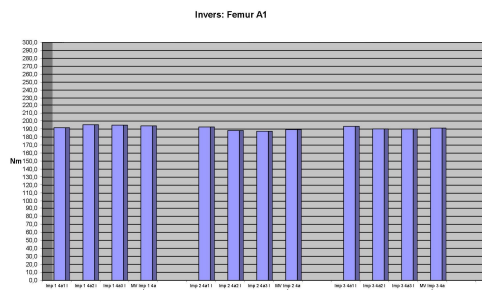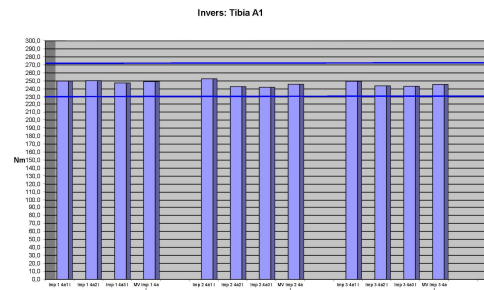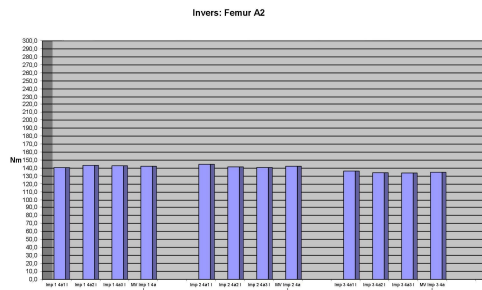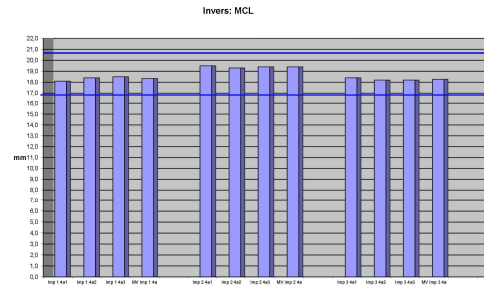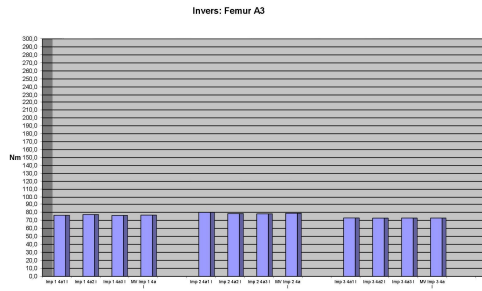
ANNEX 3 – TEST RESULTS SEDAN TEST FRAME

Test results for 3 different legforms equipped with 4 a bone cores with 3 repetitions each (left blocks in each diagram), in comparison with 3 legforms equipped with the original bone cores (right blocks). The most right bar in each block represents the mean value.

Sedan Test Frame: Femur A3

Sedan Test Frame: MCL

Sedan Test Frame: Femur A2

Sedan Test Frame: Tibia A1

Sedan Test Frame: Femur A1

Sedan Test Frame: Tibia A2

Sedan Test Frame: ACL

Sedan Test Frame: Tibia A3

Sedan Test Frame: PCL

Sedan Test Frame: Tibia A4
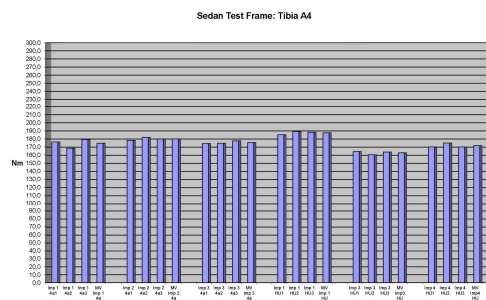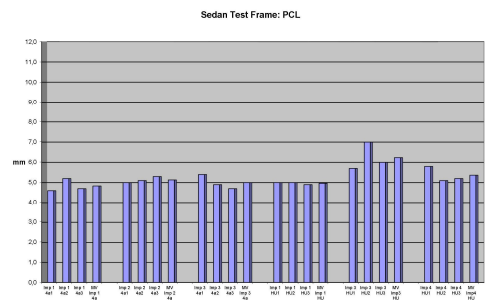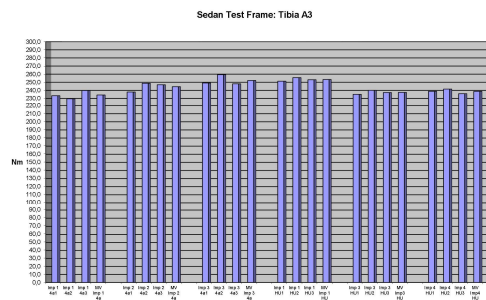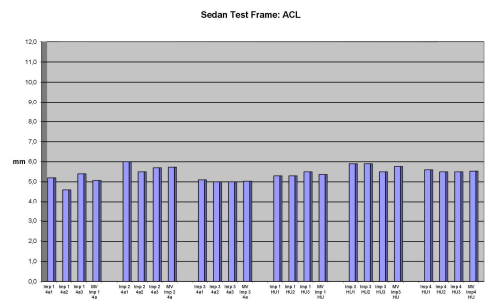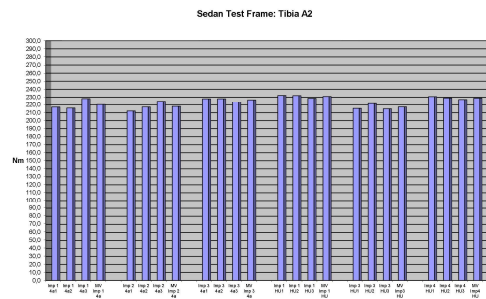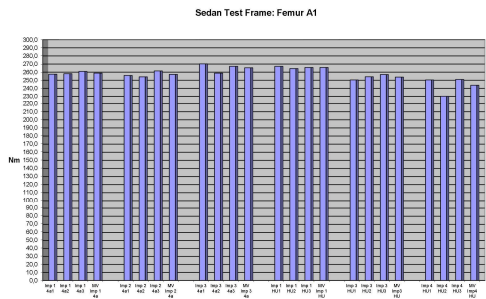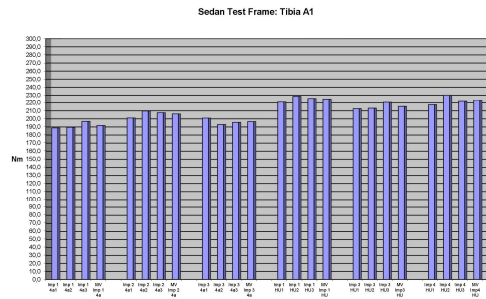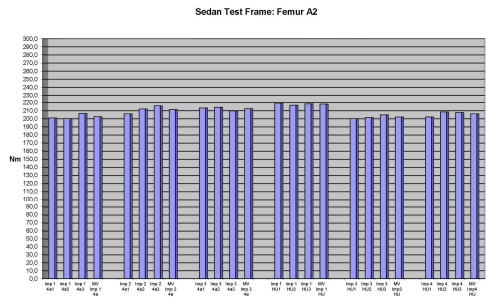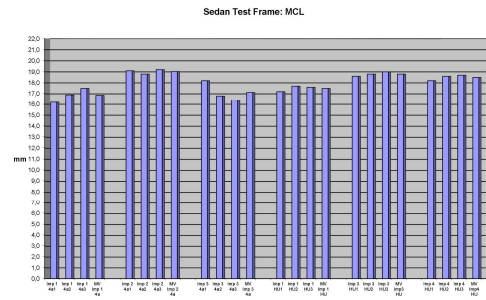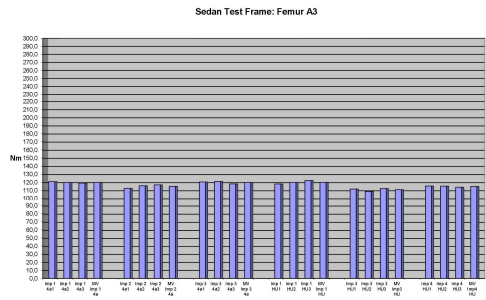
AN INVERSE MONTE-CARLO BASED METHOD TO ESTIMATE PRE-CRASH DISTRIBUTION FOR VRU SAFETY

Hariharan, Sankara Subramanian
Sudipto, Mukherjee
Anoop, Chawla
Indian Institute of Technology Delhi
India

Dietmar, Goehlich
Technical Universitaet Berlin
Germany

ABSTRACT

Current safety standards are based on maximum stiffness measures over a grid on the frontal surface of a vehicle. The safety of VRU is also influenced by the overall shape of the impacting vehicle. "Initial conditions" [IC] from the dominant crash scenarios are used for CAE simulations in Industrial practice to tweak designs. The IC's to design for are decided based on cluster analysis from reconstructions of crash data. Currently, CAE methods to predict the outcomes (final resting state of interacting elements) of a crash deterministically, given the initial conditions are available. But there are no established methods to do the inverse process, that is ascertain the conditions at the initiation of the crash given the final static state of the interacting elements. Recorded data being the final resting state of the interacting elements, the inverse problem is of significance, and is usually tackled by heuristics and iterations augmenting physical laws. While reconstructions of specific cases require detailed observation and experienced personnel, it is hypothesized that estimating a distribution of the pre-impact measures in crashes is more robust with respect to a distribution of the post impact observation than that of individual crashes.

Individual cases from crash reconstruction, approximated to a Gaussian "normal" probability density function, were assumed for the probability of occurrence of individual cases. Crash physics was captured using a multibody simulation in MADYMO solver. An inverse Monte Carlo [MC] simulation with MADYMO solver as the system under study was modelled in "FME" module in statistical software "R".

A set of post-crash data on head hit location [O1] was generated using forward MC simulation. The variable parameters were four different vehicle profiles, relative position of 50M along vehicle lateral axis [I2] and the relative orientation of with respect to vehicle. The pedestrian represented using one 50th percentile male [50M] pedestrian model was not varied.

Starting with the distribution of "O1" and an "I2" distribution perturbed by up to 20% in mean value as input, an I2 was computed using inverse MC. The "I2" distribution from inverse MC showed less than 10% deviation from the original v3 data set mean with randomized values of untracked variables.

During the inverse MC process, the quality of "fit" to a desired O1 distribution was tracked using the sum of root mean square of differences between normalized density coefficients and a "relaxation parameter" computed as squared logarithmic probability to a normal distribution. The stabilization of the tracking parameter indicated a robust solution.

INTRODUCTION

Vulnerable Road Users (VRU) is a term used to collectively refer to pedestrians, bicyclists and motorcyclists. Report by WHO (World Health Organisation 2013) shows bicyclists and pedestrians to constitute over a quarter (27%) of the total traffic related fatalities in the world. VRU safety in crash scenarios involving cars has remained an active area of research with safety tests put in place for pedestrian safety using body-form impact on the vehicle front to estimate the potential injury risk. One of the components of VRU – pedestrians - represent a majority of VRU exposed to traffic threats. Data from (World Health Organisation 2013) also indicate pedestrian fatalities to be 22% of total road fatalities. Pedestrian safety has been addressed by regulatory and rating tests like Euro-NCAP

(Hobbs and Mcdonough 1998) and by indirect indicators for threats to pedestrians from car fronts. These rating and regulatory tests have been modelled for estimating threats to target human populations and crash scenarios selected based on data in crash databases. Current safety standards are based on maximum stiffness measures over a grid on the frontal surface of a vehicle. It is however well understood that safety of VRU is also influenced by the overall shape of the impacting vehicle (Crandall et al. 2002).

Advancement in CAE has led to crash simulations being used as a method for virtually replicating crashes. In industrial practice, CAE simulations are used to model using "initial conditions" [IC] from the dominant crash scenario to tweak designs. The IC's to design for are decided based on cluster analysis from reconstructions of crash data. Lack of clear data from post-crash scenes limit the efficiency of replications of crashes through computer simulations. Crash reconstructions of specific cases require detailed observations of the crash scene and experienced personnel to apply heuristics and iterate on simulations. It is hypothesized that estimating a distribution of the pre-impact measures in crashes is more robust with respect to a distribution of the post impact observation than inferring the IC's of individual crashes through reconstructions. We also note that for design or standard setting purposes, it is the statistics as opposed to specific cases which is of relevance.

The authors (S subramanian et al. 2014) have proposed a method based on inverse Monte Carlo to estimate pre-crash variables using limited post-crash data. This work evaluates the robustness of the inverse Monte Carlo method using a synthetic randomized post-crash data to estimate pre-crash data.

METHODOLOGY

Crash simulation using computational techniques work on uni-directional physics of crash. The post-crash effects can be estimated using known pre-crash conditions. This work will discuss verification of previously proposed methodology to estimate pre-crash variables to model crash simulations. The first step of this study was to generate synthetically randomized crash data equivalent. Vehicle velocity (I1), vehicle category denoted by vehicle profile (I2), location of pedestrian in lateral plane of vehicle (I3) and orientation of pedestrian with respect to vehicle with pedestrian hit on left or right (I4) were selected for variation. The output of the crash simulation (O1) was captured. The present objective was to estimate most likely lateral position of pedestrian in front of vehicle (I3). An inverse Monte Carlo based on 'Mu' measure was executed with O1 distribution to estimate variable I3.

Crash simulation

Vehicle to pedestrian crash was simulated using multibody MADYMO solver with pedestrian represented by 50th percentile male pedestrian model. Vehicle was represented using multibody model for vehicle front and the crash scenario was similar to previous work by authors (S subramanian et al. 2014).

Generation of synthetic crash data

A synthetic randomized crash data was generated using forward Monte Carlo (FMC) simulation using sensitivity study module of OptiSlang (Dynardo Gmbh 2011) with 500 samples. The input variables I1 to I4 were classified as discrete and continuous variables with ranges of values shown in Table 1. I1 and I4 were discrete variables with three and four levels of values respectively. I2 and I3 were varied continuously in the range indicated. The input variable I2 was initialized with two values for every set of I1, I3 and I4. Two values of I2 was generated to simulate a "left" and "right" side impact of pedestrian with all other variables in same level for one iteration.

Table1.
Input variables to Monte Carlo simulations

	Unit	Variable Type	Range
Velocity (I1)	m/s	Discrete	30,40,50
Angle (I2)	Degrees	Continuous	-30 to +30
Location (I3)	m	Continuous	0.2 to 1.8
Category (I4)	No unit	Discrete	A, B, D or generic

The FMC study had an objective of data distribution generation of the head hit location of pedestrian (O1). An overview of the process is shown in Figure 1. The variables I1 to I4 form the input to vehicle-pedestrian crash

simulation in MADYMO. MADYMO solver output files were read back by OptiSlang for the estimated primary head hit point on the vehicle by tracking the head and vehicle front positions through the simulation.
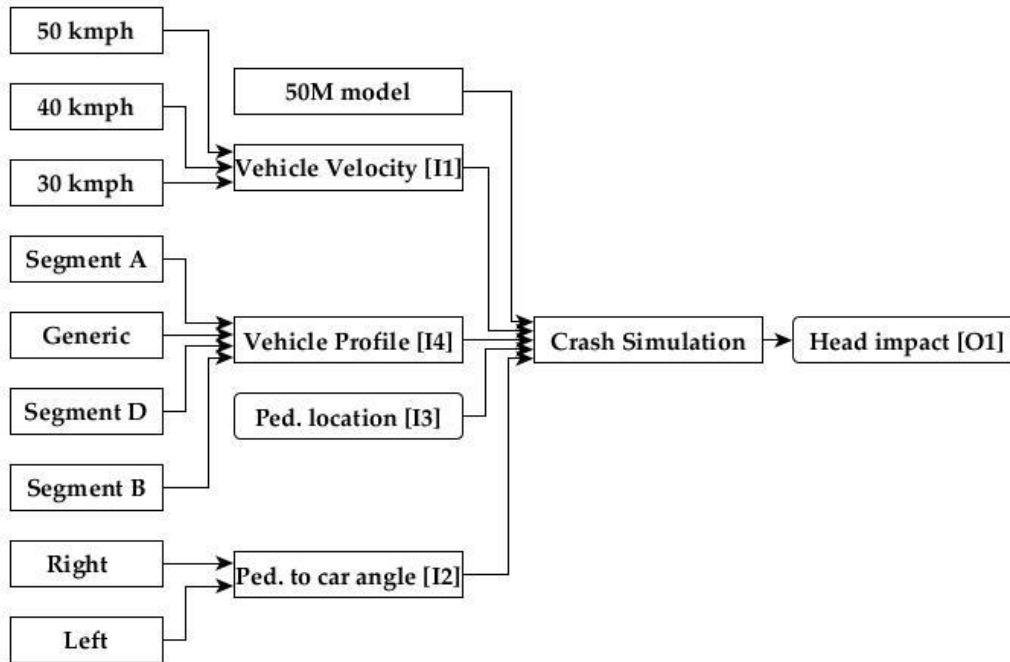
Figure1. Methodology for a synthetic data generation using Monte Carlo forward method

The data generated during FMC study of the I3 and O1 were exported from OptiSlang and a normal distribution was "fitted" to the data using modules in open source software R. The estimates of O1 distribution mean and variance obtained by the end of FMC would be used to provide an "expected" distribution of O1 for Inverse Monte Carlo method to estimate for I3 distribution. A normal distribution fitted to O1 had a mean of

Estimation of a pre-crash variable

Inverse Monte Carlo (IMC) based simulation was setup using FME module(Soetaert and Petzoldt 2010) in R language. The system under study was MADYMO solver with output being processed to provide O1 values. Most of the fine-tuning variables of FME were in default values. The number of iterations of this sample study was restricted to 500 iterations.

A 'µ' [Mu] measure was formulated based on the suggestions in FME documentations. µ was sum of RMS difference in density coefficients of present IMC iteration O1 values and similar values output from FMC along with a logarithmic normal probability of the I2 on expected normal probability function. The application µ in this work is shown in equation (1). A detailed discussion of µ can be found in (S subramanian et al. 2014).

Sample calculation of µ

µ = CF*RMS*100 +RP **(1)**

Where,

RMS - Root mean square difference in density coefficients between FMC and IMC
CF – Correction Factor
RP – Relaxation Parameter = -2 * log (Normal Probability)

For a specific I2 value of 145cm, the Normal distribution for RP has mean of 100cm and standard deviation of 45cm.

The normal probability of I2 = 4.9e-5

2*log (Normal probability) = RP = -8.6137

RMS calculated between FMC and IMC values of I2 were 0.015. The RMS values are multiplied by a factor of 100 in this case to make them significant in comparison to the RP.

μ = 0.015*100-8.6137 = 10.19
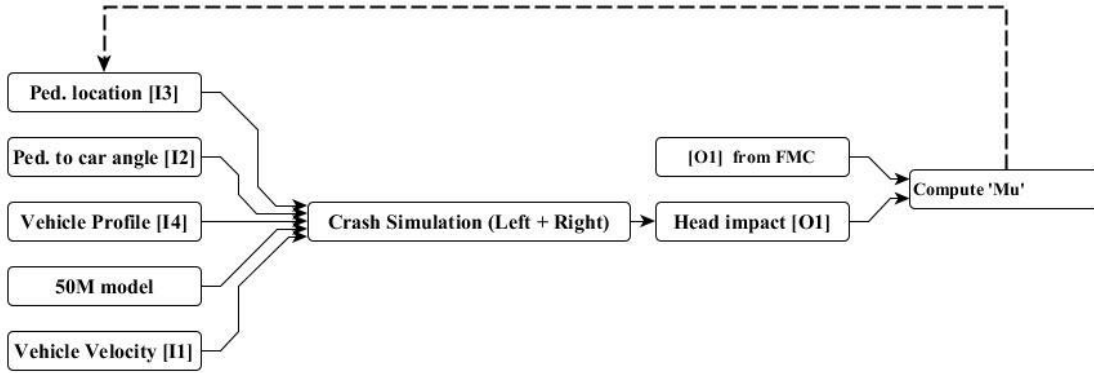
Figure2. Methodology to estimate pre-crash variable using inverse Monte Carlo method

RESULTS AND DISCUSSION

### Variation of μ

The parameter 'μ' is expressed as a sum of CF*RMS and RP. During IMC simulations, the best possible solution can be obtained when the value of 'μ' reduces to minimum. The variation of RMS is indicative of global variation of O1 from IMC with corresponding value from FMC. The variation in RMS is shown in Figure 3, which indicate the value to stabilize over 300 iterations.

The value of RP was controlled by the new data point generated by randomized number generator of Monte Carlo process. The variation of RP and μ (Mu) is shown in Figure 4. The variation of RP between 15 and 20 is the direct result of normal probability calculation. The influencing part, μ, was the global parameter CF*RMS which stabilized by 300 iterations and was relatively stable beyond that point. It was concluded that iterations beyond 600 may not be necessary.
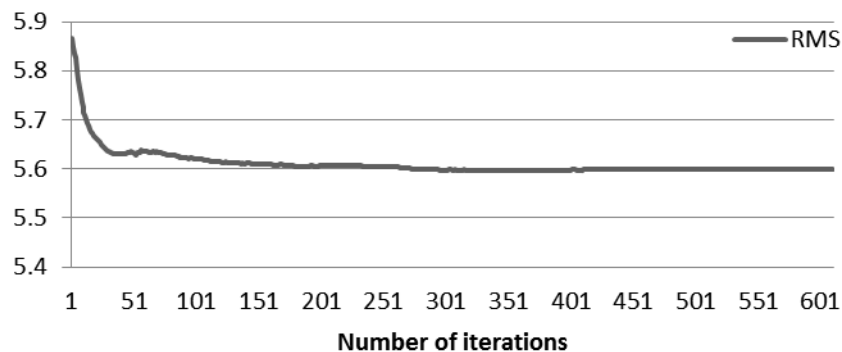

Figure3. Variation of RMS in IMC
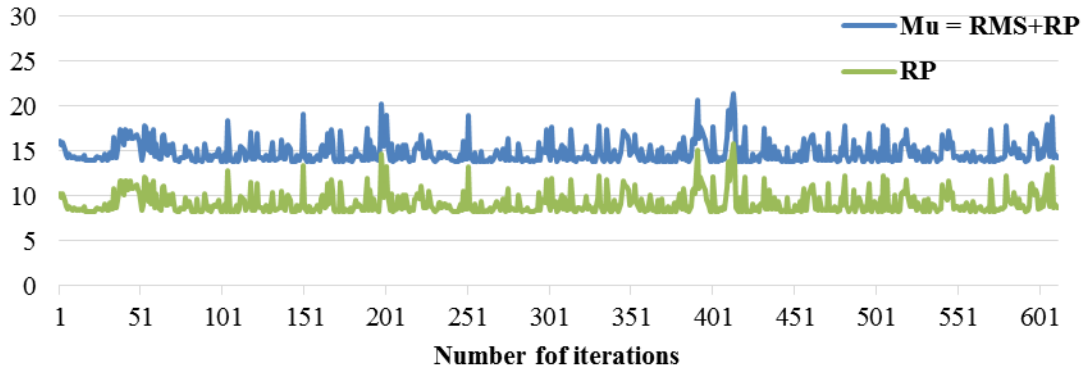
Figure4. Variation of 'μ' in IMC

Variation of O1

The objective of IMC simulation was to estimate the I2 distribution based on output distribution O1 processed from FMC simulations. In this study, a Gaussian normal probability function was assumed for all variables .Every head hit location (O1) was recorded and their density coefficient was obtained. The O1 density distribution obtained from FMC indicated a non-normal behavior as shown as dark shaded bars in Figure 5. The O1 distribution obtained from IMC process is indicated using lighter shades of bars in Figure 5, which show a mixed match with O1 from FMC. The O1 obtained from IMC process was generated with influence of normal probability which is evident with a peak near the middle of the O1 graph of density coefficients. The variation of the density coefficients of O1 distribution of FMC and IMC showed a Pearson coefficient of 0.83.
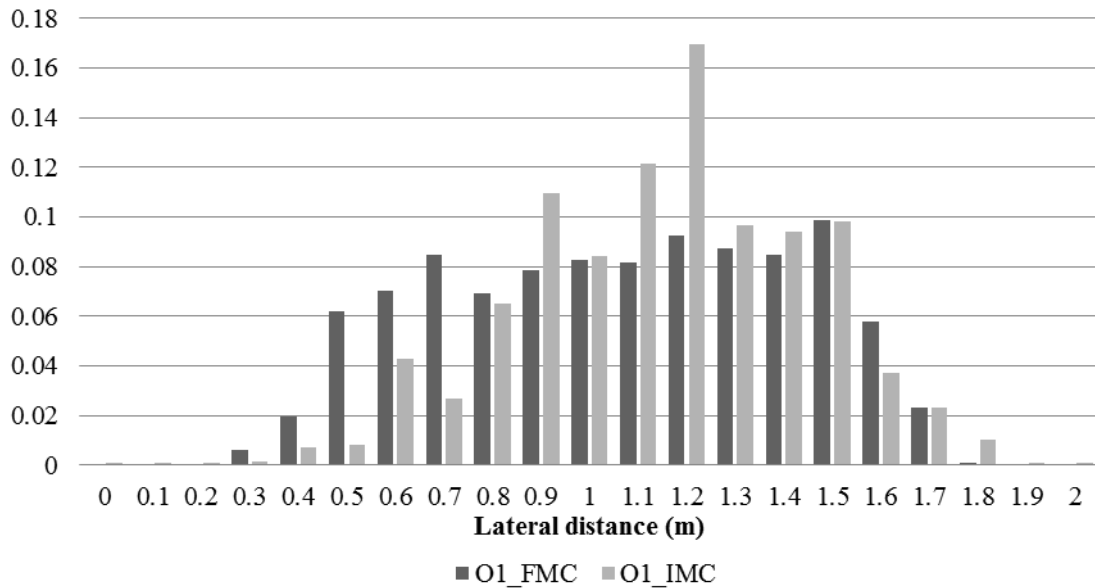
Figure5. Comparison density coefficients of O1 from FMC and IMC

The I2 variable was fitted to normal distributions by similar methods as O1 and their mean and variances were compared. Table 2 shows variable I2's normally distributed mean and standard deviation from FMC and IMC processes. Mean of I2 from IMC varies under 10% from the mean of I2 from FMC. The assumed normal distribution for comparison of I2 had mean at 1.10m and standard distribution of 0.25m. The initial value of I2 in IMC was assumed to be 1.45m. There was a significant shift in overall distribution towards FMC values.

5

Table2.
Comparison of I2 from FMC and IMC

	FMC	IMC
Mean I2 (m)	1.01	1.08
Variance I2 (m)	0.34	0.24

Limitations

A Gaussian normal distribution was assumed for all variables to estimate the probability. With clearer data available on specific variables, a better prediction probability function can be incorporated. The μ measure remains sensitive to the units of length used and appropriate correction factors need to be updated for better convergence. Sample runs of higher than 500 were not studied as the simulations trend was visible with shift in mean towards expected values.

The comparison was based on kinematic distributions, both at the input and output. The point of real concern is predicting trauma levels. An increased performance, when extended to HBM's applications (with significantly enhanced degrees of freedom) in conjunction with injury models has to be attempted.

CONCLUSIONS

During the inverse MC process, the quality of "fit" to a desired O1 distribution was tracked using the sum of root mean square of differences between normalized density coefficients and a "relaxation parameter" computed as squared logarithmic probability to a normal distribution. The stabilization of the tracking parameter indicated an optimal solution.

This methodology combined with advanced tools like FE human body model will improve injury prediction efficiency of CAE tools.

REFERENCES

[1] Crandall, J.R. et al. 2002. Designing road vehicles for pedestrian protection. *BMJ* (324), pp. 1145–1148.
[2] Dynardo Gmbh 2011. *Dynardo Gmbh OPTISLANG - The optimizing structural language v3.2.1*. Weimar, Luthergasse 1 D, Germany: Dynardo Gmbh.
[3] Hobbs, C.A. and Mcdonough, P.J. 1998. Development of the European New Car Assesment Programme (Euro NCAP). In: *ESV 98-S11-O-06*.
[4] S subramanian, H. et al. 2014. Methodology for estimation of probable location of VRU before impact using data from post-crash analysis. In: *IRCOBI conference 2014*.
[5] Soetaert, K. and Petzoldt, T. 2010. Inverse Modelling , Sensitivity and Monte Carlo Analysis in R Using Package FME. *Journal of statistical software* 33(3), pp. 1–28.
[6] World Health Organisation 2013. *Global status report on road safety 2013: supporting a decade of action*.